SERVIÇO PÚBLICO FEDERAL

MINISTÉRIO DA EDUCAÇÃO

UNIVERSIDADE FEDERAL DE UBERLÂNDIA

FACULDADE DE ODONTOLOGIA

PROGRAMA DE PÓS-GRADUAÇÃO EM ODONTOLOGIA

JÉSSICA AFONSO FERREIRA

Superfícies de implantes dentários e acetilação de Histona 3: efeitos na modulação óssea em condições de normalidade e osteoporose

Tese apresentada à Faculdade de Odontologia da Universidade Federal de Uberlândia, como requisito parcial para obtenção do Título de Doutor em Odontologia na Área de Concentração de Clínica Odontológica Integrada

Uberlândia, Dezembro de 2018

JÉSSICA AFONSO FERREIRA

Superfícies de implantes dentários e acetilação de Histona 3: efeitos na modulação óssea em condições de normalidade e osteoporose

Tese apresentada à Faculdade de Odontologia da Universidade Federal de Uberlândia, como requisito parcial para obtenção do Título de Doutor em Odontologia na Área de concentração de Clínica Odontológica Integrada.

Banca Examinadora:
Orientador: Prof. Dr. Denildo de Magalhães, UFU
Profª. Dra. Ana Paula Lima de Oliveira, UFU
Profª. Dra. Marina de Melo Naves, UFU
Prof. Dr. Gustavo Mendonça, UMICH
Prof. Dra. Luiz Duarte Meirelles, UMICH

Suplentes
Prof. Dr. Guilherme Pimentel Lopes de Oliveira, UFU
Prof. Dr. Marco Cicero Bottino, UMICH

Uberlândia, Dezembro de 2018

Ficha Catalográfica Online do Sistema de Bibliotecas da UFU
com dados informados pelo(a) próprio(a) autor(a).

F383 2018

Ferreira, Jéssica Afonso, 1991-
Superfícies de implantes dentários e acetilação de Histona 3: efeitos na modulação óssea em condições de normalidade e osteoporose [recurso eletrônico] / Jéssica Afonso Ferreira. - 2018.

Orientador: Denildo Magalhaes.
Coorientador: N/A N/A.
Tese (Doutorado) - Universidade Federal de Uberlândia, Pós-graduação em Odontologia.
Modo de acesso: Internet.
Disponível em: http://dx.doi.org/10.14393/ufu.te.2019.2024
Inclui bibliografia.
Inclui ilustrações.

1. Odontologia. I. Magalhaes, Denildo, 1960-, (Orient.). II. N/A, N/A, 0000-, (Coorient.). III. Universidade Federal de Uberlândia. Pós-graduação em Odontologia. IV. Título. CDU: 616314

Bibliotecários responsáveis pela estrutura de acordo com o AACR2:
Gizele Cristine Nunes do Couto - CRB6/2091
Nelson Marcos Ferreira - CRB6/3074

Uberlândia, Dezembro de 2018

DEDICATÓRIA

À *Deus*,

Agradeço por zelar de cada detalhe em minha vida, por ter me dado sabedoria e saúde para lutar por mais esta etapa da minha vida profissional. Sou grata pela família maravilhosa que me concedeu, pelo meu marido, pelos professores maravilhosos que foram colocadas em meu caminho e por todas as oportunidades que surgiram nessa etapa do Doutorado, de fato, me considero uma pessoa iluminada por Deus ter cuidado de exatamente tudo. Em especial, agradeço pelas graças recebidas em cada momento que precisei ter fé e sabedoria para não desistir. Agradeço por me ensinar a superar dificuldades e por acreditar que os sonhos são possíveis quando se tem perseverança.

Aos meus queridos pais Silvana e Fábio,

Obrigada mãe por ser meu esteio e por se doar inteiramente a mim, sendo minha fonte de força e amor. Obrigada pai, por ser meu primeiro herói, por lutar diariamente para oferecer o melhor para nossa família, o senhor é meu exemplo de humildade e caráter. Sem dúvidas, vocês são as pessoas a quem devo toda minha vida e formação. Vocês me ensinaram que a maior herança que poderiam me deixar em vida seria educação. Obrigada por sempre acreditarem em mim e, sobretudo, em meus sonhos. Vocês são minha luz. Amo vocês.

Ao meu amor Luiz Júnior,

Gratidão eterna por todo apoio, incentivo e pela trajetória que vivemos até aqui. Literalmente, você abriu mão de seus sonhos para que eu pudesse realizar os meus e no decorrer da caminhada sonhou junto comigo. Juntos com certeza foi mais fácil e gratificante, o sonho foi criando tamanho na medida que fomos realizando e hoje essa conquista não é somente minha. Sei que foram momentos difíceis, de angústia, ausência e, você sempre colaborou para tornar tudo mais fácil. Por isso, agradeço sua paciência, por me fazer feliz, por tudo que você proporciona para que a nossa vida seja mais leve e alegre. Você é meu descanso, meu companheiro e amigo, juntos ainda iremos realizar todos nossos

sonhos. Em especial, agradeço a sua família, meus cunhados Ana, Flávio, Mariana, Weber, meu sogro Luiz e principalmente, minha sogra Sirlene, por cuidar de mim como se fosse filha e por me ensinar o significado da palavra generosidade. Você sempre tão disposta e solícita nos mostra diariamente como é possível superar obstáculos.

As minhas queridas irmãs, Patrícia e Flaviane,

Por serem minhas primeiras amigas, por juntas acreditarmos desde a infância que tudo que se pode sonhar, também se pode realizar. Por serem minha inspiração profissional e por acreditarem tanto em meu potencial. Ainda iremos conquistar e celebrar conquistas, obrigada por estarem sempre tão perto de mim. Agradeço com carinho meu cunhado Marco, pelos momentos de descontração e alegria.

Aos meus familiares,

Agradeço de forma especial, minhas queridas vovós que são para mim, meus maiores exemplos de vida. Agradeço meus padrinhos, madrinhas, tios, tias, primas e primos por ser parte de mim, por me fazerem felizes e por todo amor que nossa família dispensa para cada momento de alegria ou dificuldade. Sou muito grata a Deus por me presentear com pessoas tão especiais para dividir toda a vida, vocês tornaram esta caminhada mais alegre mesmo distantes fisicamente. Obrigada por tudo!

Ao Fernando, João Luiz, Gabriel e Theodora,

Vocês, meus amados sobrinhos, são a esperança de um mundo melhor, me alegram com a doce existência de vocês. Obrigada por passar a ideia de que tudo pode ser mais simples se enxergado pelos olhos de vocês.

AGRADECIMENTOS ESPECIAIS

Ao professor **Dr. Denildo de Magalhães**, por ter me concedido a grande oportunidadede seguir seus passos e aprender cada dia mais com sua experiência e profissionalismo. Agradeço por ter acreditado em mim desde minha graduação, pelas inúmeras vezes que me aconselhou e me fez tornar um ser pensante. Obrigada pelos desafios e por confiar em meu trabalho. O senhor é o grande responsável pela minha formação profissional, serei eternamente grata a tudo que já me ensinou e por cada oportunidade que confiou em mim.

Ao professor **Dr. Gustavo Mendonça,** por ter sido essencial na trajetória do meu Doutorado. Serei eternamente grata por ter acreditado em mim e ter oferecido a oportunidade ao abrir as portas e me acolher para viver a experiência mais enriquecedora e única que já pude viver na minha vida profissional. Obrigada por não medir esforços para que eu pudesse evoluir e aprender cada dia mais com você. Sem dúvidas, um ser a frente do seu tempo e sua inteligência e conhecimento é admirável e inspirador. Obrigada por confiar em meu trabalho e por todo investimento nos trabalhos que executamos, agradeço sua seriedade e principalmente sua humildade como ser humano e professor. Você é um grande exemplo a ser seguido. Muito obrigada!

A **Profª. Dra. Daniela Mendonça,** agradeço com muito carinho por ter sido mentora e amiga desde o momento que nos conhecemos. Sou de fato uma pessoa muito iluminada por Deus por ter pessoas como você em minha trajetória. Competente, sábia, justa e sempre sorridente. Agradeço por tudo que me ensinou e pelas inúmeras oportunidades e conselhos que me ofereceu. Obrigada de forma especial por ter sempre estendido a mão com carinho e atenção, por nosso convívio ter ido além da relação entre professora e aluna, nos tornamos verdadeiras amigas. Ter vocês, Breno e Enzo em nossas vidas nos fez sentir verdadeiramente em casa. Muito obrigada.

Ao professor **Dr. Marco Bottino,** por ter me recebido em seu laboratório e confiado em meu trabalho. Agradeço pela oportunidade e por aprender diariamente com você. Admiro sua forma de conduzir os trabalhos científicos e seu interesse

incansável pela ciência nos motiva e nos faz querer ir além. Muito obrigada!

Ao professor **Dr. Rogerio Castilho**, agradeço pela disposição e ajuda em aperfeiçoar e executar metodologias pertinentes e essenciais para a condução de um dos objetivos deste trabalho, foi muito valido para meu desenvolvimento e aprendizado enquanto aluna. Muito obrigada.

A **Profª. Dra. Marina de Melo Naves**, minha co-orientadora desde a Iniciação Científica. Obrigada por todo apoio, independente do dia ou horário, sempre esteve disposta a me ajudar da melhor maneira possível. Nosso encontro na pesquisa me presentou com uma grande amiga, que desejo carregar em meu coração toda a vida, agradeço de forma especial todos os ensinamentos, conselhos, por me mostrar o melhor caminho e, principalmente por acreditar em mim. Meus sinceros agradecimentos por tudo que faz por mim, minha admiração por você é imensurável!

Ao **Prof. Ms. Helder Henrique Machado de Menezes,** sou grata por dividir comigo suas ideias e por acreditar na minha capacidade de colocá-las em prática. Obrigada por todas as oportunidades que já me proporcionou, pelo interesse em me formar especialista, pelos momentos de descontração e principalmente por incentivar minha capacidade de pensar. Sem dúvidas, seus ensinamentos foram essenciais para minha formação profissional. Muito obrigada!

A **Profª. Dra. Priscilla Barbosa Ferreira Soares**, por ter me despertado o gosto e amor pela pesquisa em 2010. Obrigada pelos ensinamentos e oportunidades que tive quando ainda conhecia tão pouco o universo científico, você é especial.

Aos professores da banca de qualificação, **Profª. Drª. Marina de Melo Naves, Profª. Drª. Ana Paula de Lima Oliveira, Prof. Dr. Denildo de Magalhaes,** por toda contribuição nas etapas desse trabalho.

Aos professores da banca de defesa, Profª. Drª. Marina de Melo Naves, Profª. Drª. Ana Paula de Lima Oliveira, Prof. Dr. Denildo de Magalhaes, Prof. Dr. Gustavo Mendonca, Prof. Dr. Luiz Meirelles. Agradecer também aos membros suplentes professores Dr. Marco Cicero Bottino e Dr. Guilherme Pimentel Lopes de Oliveira.

Aos professores da FOUFU, meus eternos e sábios mestres, pessoas a quem eu devo meus primeiros passos nesta jornada profissional, agradeço por cada momento compartilhado, pelas aulas, clínicas, experiências divididas na Graduação e Pós Graduação, em especial aos queridos: **Paulo Cesar Simamoto Junior, Carlos Jose Soares, Veridiana Resende Novais Simamoto, Adérito Soares da Mota, Alfredo Júlio Fernandes Neto, Luiz Carlos Gonçalves, Márcio Magno,Marlete Ribeiro da Silva, Rosana Ono, Márcio Teixeira, Paulo SérgioQuagliatto, Luís Henrique Araújo Raposo, Letícia Resende Davi, Paulo César, Flávio Domingues das Neves e Paulo Vinicius Soares**. Vocês despertaram em mim o amor pelo ensino e pela Odontologia.

A escola de pós-graduação, **HD Ensinos Odontológicos,** onde cursei minhas especializações em Periodontia e Implantodontia, por ser um lugar onde me sinto em casa e por ter sido fundamental em minha formação clínica. Agradeço aos professores, amigos de especialização e amizades que se formaram nesta escola.

Ao **Guilherme Faria Moura**, meu amigo, colega de graduação, mestrado, parceiro de clínica da especialização, e agora Doutorado Sanduiche, obrigada por todos os momentos que já dividimos durante tantos anos de amizade. Você é especial, espero comemorar muitas vitórias ao seu lado, conte sempre comigo.

As minhas amadas amigas **Laura, Jéssica e Marina**, por serem presentes de Deus em minha vida, por estarem comigo independente da situação e por tornar esta caminhada mais alegre. Obrigada por todos os momentos que já passamos juntas e pela certeza que teremos sempre o carinho e amor uma das outras. Amo vocês!

A minha amiga **Marcela Gonçalves Borges**, como foi bom ter você ao meu lado, durante todo este tempo, dividindo sonhos, inseguranças e também vitórias. São muitos anos de amizade e em todo tempo estivemos juntas em busca de nossos ideais. Obrigada por estar sempre ao meu lado, ainda temos muito que conquistar e evoluir.

As amigas **Francielle, Nayara, Ludmilla, Thauana, Flávia, Edilene e Thais** pelos momentos felizes e preciosos que já dividimos juntas. Vocês são especiais.

Aos coelgas de de doutorado, em especial, **Camila Lopes, Pedro, Frederick, Camila Silva**, que entre seminários, e dificuldades, aprendemos uns com os ostros, nos ajudamos, tornamos amigos e tenho certeza que todos nós iremos colher muitos frutos desta linda jornada. Sucesso a todos!

Aos amigos que fiz durante o Doutorado Sanduiche, **Rafael, Fábio, Lidia, Elisa, Liana, Joe, Zeynep, Nilesh, Jinping, Arwa, Luiz, Mariane, Erika e Thamara.** Vocês tornaram essa caminhada mais fácil e alegre, obrigada pela amizade e ajuda na condução dos trabalhos.

À **Faculdade de Odontologia da Universidade Federal de Uberlândia,** por possibilitar a concretização desta etapa. Tenho orgulho de ter me formado nesta casa e ter usufruído de todas as oportunidades que já foram oferecidas enquanto aluno de graduação e pós-graduação.

As secretárias do PPGO, **Brenda e Graça,** por serem competentes e sempre dispostas a ajudarem no que for preciso, além de excelentes profissionais e amigas.

A **CAPES e CNPq** pela bolsa de mestrado e pelo apoio financeiro no desenvolvimento deste trabalho.

E a todas as pessoas que, de alguma forma, contribuíram para que essa etapa fosse vencida!

EPÍGRAFE

"Meu sonho não tem fim, e eu tenho muita vida pela frente."

Ayrton Senna, 1991

SUMÁRIO

RESUMO

RESUMO

O número de pacientes idosos em busca de tratamento com implante dentário aumentou nos últimos anos. Ao mesmo tempo, espera-se que um número maior desses pacientes sofra de uma ou mais doenças metabólicas crônicas, como a osteoporose, que afetam a cicatrização óssea e podem levar a mais falhas nos implantes. Este trabalho tem como objetivo geral caracterizar a modulação óssea e expressão gênica em relação a diferentes superfícies de implantes dentais e acetilação de Histona 3 através do uso farmacológico de Vorinostat (HDACi) em condições de normalidade e submetidos a osteoporose. Este estudo foi dividido em três objetivos específicos; **Objetivo específico 1:** avaliar o efeito de uma superfície de tratamento hidrofílico na diferenciação de osteoblastos e seus efeitos na osseointegração. **Objetivo específico 2:** determinar o padrão de formação óssea e expressão gênica em duas superfícies diferentes de implantes de titânio (hidrofóbica e hidrofílica) em um modelo osteoporótico. **Objetivo específico 3:** investigar modificações globais na cromatina presente no núcleo celular mediadas por nano superfície de titânio e influência farmacológica da acetilação de histonas influencia na diferenciação de células-tronco mesenquimais, especialmente em condições de osteoporose. Devido ao aumento da expressão de genes relacionados à diferenciação osteogênica e à quantidade significativa de cálcio e volume ósseo formado diretamente sobre a superfície de implantes dentários SAE-HD, a escolha da superfície hidrofílica em situações de osteoporose pode ser significativamente considerada a fim de melhorar processo de osseointegração. Superfícies hidrofílicas e em nanoescala, assim como Vorinostat mediados pela histona, podem desempenhar um papel fundamental na diferenciação das células-tronco mesenquimais em osteoblastos, especialmente nas condições de osteoporose. Isso ocorre devido propriedades osteocondutoras e possibilidade de melhorar eventos biológicos que ocorrem na interface osso/implante.

ABSTRACT

ABSTRACT

The number of elderly patients seeking dental implant treatment has increased in recent years. At the same time, more of these patients are expected to suffer from one or more chronic metabolic diseases, such as osteoporosis, that affect bone healing and may lead to more implant failures. This study aimed to characterize bone modulation and gene expression in relation to different surfaces of dental implants and Histone 3 acetylation through the pharmacological use of Vorinostat (HDACi) in conditions of normality and submitted to osteoporosis. This study was divided into three specific objectives; **Specific objective 1:** to evaluate the effect of a hydrophilic treatment surface on osteoblast differentiation and its effects on osseointegration. ***Specific objective 2:*** to determine the pattern of bone formation and gene expression on two different surfaces of titanium implants (hydrophobic and hydrophilic) in an osteoporotic model. ***Specific objective 3***: to investigate global modifications in chromatin present in the cell nucleus mediated by titanium nano surface and pharmacological influence of histone acetylation influences the differentiation of mesenchymal stem cells, especially under conditions of osteoporosis. Due to the increased expression of genes related to osteogenic differentiation and to the significant amount of calcium and bone volume directly formed on the surface of SAE-HD dental implants, the choice of hydrophilic surface in osteoporotic situations can be significantly considered in order to improve process of osseointegration. Hydrophilic and nanoscale surfaces, as well as histone-mediated Vorinostat, may play a key role in the differentiation of mesenchymal stem cells into osteoblasts, especially under osteoporotic conditions. This is due to osteoconductive properties and the possibility of improving biological events occurring at the bone/implant interface.

INTRODUÇÃO E REFERENCIAL TEÓRICO

1. INTRODUÇÃO E REFERENCIAL TEÓRICO

O número de pacientes idosos em busca de tratamento com implante dentário aumentou nos últimos anos. Ao mesmo tempo, espera-se que um número maior desses pacientes sofra de uma ou mais doenças metabólicas crônicas, como a osteoporose, que afetam a cicatrização óssea e podem levar a mais falhas nos implantes (Gaetti-Jardim et al., 2011; Giro G et al., 2015). A osteoporose é definida como uma desordem esquelética caracterizada por uma redução na massa óssea e deterioração microarquitetural do tecido ósseo que aumenta o risco de fratura. Tanto a etiologia quanto a terapia da osteoporose (estrógenos, vitamina D e bifosfonatos) podem interferir no processo de cicatrização de uma ferida óssea e osseointegração (Highlights NIH, 2011; Sanfilippo et al., 2003; Fini et al., 2004; Erdogan et al., 2007; Tsolaki et al., 2009).

Brånemark e seus colegas descobriram acidentalmente um mecanismo de adesão do titânio ao osso quando estudavam a microcirculação na tíbia de coelho (Lemus et al., 2009). Esse fenômeno ficou conhecido como osseointegração (Melo et al., 2006). Em 1981, Adell et al. relataram que aproximadamente 90% dos implantes colocados na região anterior da mandíbula tiveram sucesso entre 5 a 12 anos após a instalação; entretanto, taxas mais baixas foram observadas para implantes na maxila anterior (Adell et al., 1981). Noack et al. (1999) relataram que os implantes mandibulares tiveram uma taxa de sucesso maior que na maxila, com uma taxa de perda protética total de 1,9%, enquanto 4,3% dos implantes foram perdidos após o tratamento protético. Segundo Saab et al. (2007) observaram que o problema se deve ao padrão de perda óssea, que não pode ser previsto com precisão na região dos dentes maxilares anteriores. A maxila pode apresentar quantidade insuficiente de osso para inserção dos implantes, sendo um grande desafio cirúrgico-protético devido à redução da qualidade óssea e baixa densidade trabecular (Capelli et al., 2007).

Após o posicionamento do implante e sua carga inicial, o osso da crista sofre um processo de remodelação e reabsorção (Danza et al., 2010). Esse processo de remodelamento no osso peri-implantar pode ser influenciado pela direção, repetição e magnitude da carga biomecânica (Hasan et al., 2011). Os fatores que podem afetar a magnitude das forças nas zonas peri-implantares do

osso são geometria, posição e número de implantes (Sahin et al., 2002). A aplicação de forças funcionais induz cargas e tensões no conjunto prótese-implante, afetando o processo de remodelação óssea ao redor dos implantes (Bidez et al., 1992). Entretanto, os limites de tolerância fisiológica das mandíbulas humanas não são conhecidos e algumas falhas nos implantes podem estar relacionadas à magnitude das tensões desfavoráveis (Sahin et al., 2002).

Pesquisas envolvendo o titânio e suas ligas, a fim de atender e auxiliar na saúde geral do paciente, vêm sendo progressivamente utilizadas na fabricação de implantes ortopédicos e odontológicos. Isso se deve à presença de excelente biocompatibilidade (Wang et al., 2018), alta resistência mecânica, alta resistência à corrosão e baixa densidade desse material (Hotchkiss et al., 2016). É importante notar que o desenvolvimento de biomateriais compatíveis com tecidos é necessário para manter a viabilidade celular e induzir proliferação e diferenciação em linhagens específicas. Muitos tipos de tratamentos de superfície de implante foram realizados para este fim (Kapoor et al., 2010). E podem ser classificados em cinco grupos**:** usinados, macrotexturizados, microtexturizados, nanotexturados ou biomiméticos (Ahn et al., 2010). Os tratamentos de superfície de implantes dentários têm mostrado resultados positivos na redução do tempo de osseointegração e constantemente novos tratamentos de superfície são desenvolvidos para reduzir o processo de cicatrização do osso ao redor dos implantes (Wang et al., 2018).

Devido aos vários tipos de tratamentos de superfície de implante, é possível obter várias formas de caracterização da superfície, auxiliando na compreensão da formação óssea e do comportamento celular. A modificação química das superfícies de titânio pode resultar em uma superfície hidrofílica que pode alterar o comportamento das células e melhorar a osseointegração (Buser et al., 2004; Bosshardt et al., 2011). Estudos anteriores mostraram que o aumento da rugosidade superficial e molhabilidade de uma superfície de Ti pode melhorar a osseointegração (Wennerberg et al., 2009). A topografia e a molhabilidade da superfície podem afetar a diferenciação das células de diferentes maneiras, mas há uma falta de compreensão do mecanismo molecular que regula a osteogênese nessas superfícies.

Estudos in vitro e pré-clínicos em animais ovariectomizados relataram que a

baixa densidade óssea poderia retardar a cicatrização de fraturas do fêmur (Namkung-Matthai et al., 2001), defeitos cranianos de tamanho crítico após enxerto com substitutos ósseos aloplásticos (Kim et al., 2004), soquetes pós-extração10,11 e a osseointegração de implantes dentários de titânio (Fini et al. 2004; Tsolaki et al., 2009). A modificação da superfície do implante de titânio, e pela deposição de revestimentos inorgânicos / orgânicos, foi tentada antes para melhorar a resposta implante-osso em comparação com condições osteoporóticas vs. Saudáveis (Gao et al., 2009; Vidigal et al., 2009; Mardas et al., 2011; Qi et al., 2012; Yang et al., 2012; Alghamdi et al., 2013). Embora estudos experimentais tenham demonstrado que os revestimentos osteogênicos são efetivos no aumento do contato implante-osso, sua relevância clínica requer mais investigações Ghanem et al., 2017. Por outro lado, a superfície hidrofílica tem sido usada para reduzir o tempo de cicatrização e também para promover uma osseointegração mais segura em pacientes com doenças sistêmicas, como diabetes e osteoporose.

Estudos experimentais com Células-Tronco Mesenquimais (MSC) fornecem evidências de que a formação óssea poderia ser promovida por modificações na superfície do implante, dependendo das alterações da topografia e rugosidade da superfície (Palmquist A et al., 2010), embora o processo biológico não seja bem compreendido. A diferenciação celular é influenciada por mudanças no interior da célula (Mosser DM et al., 2008), implicando assim um papel para diferentes topografias em relação a osseointegração. A nanotopografia pode contribuir para o mimetismo de ambientes celulares naturais que promovem a acumulação óssea rápida (Stanford CM et al., 2010). A topografia em nanoescala tem efeitos diretos e indiretos no comportamento celular. Ele imita o ambiente celular favorecendo a adsorção de proteínas, modulando interações célula/superfície e destino celular (Masuda et al., 1997; Stanford et al., 2010).

Sabe-se que a regulação epigenética é um modulador importante na diferenciação de células-tronco e um fator chave na diferenciação de osteoblastos relacionados à topografia do implante (Ezhkova et al., 2009; Lian et al., 2006). A acetilação das histonas desempenha um papel na transcrição do DNA mesmo sem modificação da sequência de DNA. Histonas são proteínas que auxiliam no empacotamento do DNA e podem sofrer modificações pós-

traducionais, como acetilação ou desacetilação. Essas modificações resultam na transcrição do gene através do desenrolamento da cromatina ou silenciamento do gene através da compactação do DNA (Warburton et al., 2005; Cooper et al., 1998; Dike LE et al., 1999; Mendonca, et al., 2009). Em geral, as modificações das histonas modulam uma gama diversa de processos biológicos, incluindo regulação gênica, reparo de DNA, diferenciação via remodelamento cromossômico (Mendonca et al., 2009).

A modificação pós-traducional das histonas influencia dinamicamente a expressão gênica independente de alterações na seqüência do DNA. Estes mecanismos são frequentemente mediados por ligantes de histonas, associadas ao recrutamento de proteínas de ligação ao DNA, proteínas que interagem com HDAC I e II, ativadores da transcrição, coativadores ou compressores centrais. Portanto, as histonas são marcadores moleculares de alterações epigenéticas (Yang J et al., 2014). Evidências iniciais sugeriram que as histonas e seus modificadores estão envolvidos em processos sofisticados que modulam os tecidos normais e o comportamento de tecidos tumorais junto com o fenótipo celular. Apesar de todas as pesquisas realizadas neste campo, ainda há uma falta de conhecimento sobre como os sinais de topografia em nanoescala são integrados dentro da célula e controlam a diferenciação celular. Diante disso, torna-se viável estudar os efeitos de superfície de titânio de maneira que otimize a modulação óssea a fim de promover rápida osseointegração em situações de baixa qualidade óssea, prevenir e minimizar os danos causados pela osteoporose de tal maneira que contribua com a melhora da qualidade de vida de pacientes.

Diante de toda relevância clínica, sabe se que no Brasil, cerca de 800 mil implantes são instalados por ano no país, segundo levantamento da Associação Brasileira da Indústria Médica, Odontológico e Hospitalar (Abimo). Com isso estabelece-se um horizonte que é de pacientes vivendo mais e muitos deles com reabilitações dentais associadas a implantes. Pensar então em doenças que interagem com a vida adulta ou terceira idade e que tenha impacto na longevidade de implantes dentais é um horizonte importante para a pesquisa científica e deve ser entendida como real problema de saúde pública.

A produção intelectual da Odontologia brasileira ocupa hoje a segunda posição mundial e tem se destacado tanto por indicadores quantitativos e

qualitativos (Scariot et al., 2011; Scimago SJR, 2014). Porém os clínicos brasileiros que atuam, por exemplo, na área de periodontia e implantodontia não acompanham na mesma intensidade a divulgação de conhecimento com evidência científica em periódicos publicados em língua inglesa e livremente disponíveis no Brasil apenas para instituições com acesso ao Portal de Periódicos da CAPES. Por outro lado, os eventos científicos nacionais têm se tornado cada vez mais foco de divulgação mercantil de novos implantes que surgem a cada dia, produzidos muitas vezes por empresas com credibilidade duvidosa. Revistas nacionais, publicadas na língua portuguesa, de ampla tiragem que cheguem aos consultórios odontológicos deve ser um horizonte para que de forma complementar possa divulgar os principais achados científicos em área tão relevante econômica e socialmente como o foco deste estudo produzido no interior de uma Universidade Pública Brasileira.

Desta forma, parece pertinente utilizar associação de metodologias não destrutivas de análise microtomografia computadorizada aliado a testes minuciosos, como análise de expressão genica, imunohistoquímica, fosfatase alcalina, para analisar de maneira integrada e progressiva os diferentes fatores envolvidos no processo de osseointegração de implantes dentais e diferenciação óssea, tanto em situações de normalidade quanto em casos mais críticos, como casos de osteoporose. Gerando com isso artigos a serem submetidos aos periódicos de alto fator de impacto da odontologia mundial e ao mesmo tempo gerar síntese destes achados articulado em uma visão de educação continuada e popularização da ciência a ser submetido na forma de artigo de comunicação aos clínicos brasileiros cumprindo a função social da geração do conhecimento.

OBJETIVOS

2. OBJETIVOS

Objetivo Geral

Caracterizar a modulação óssea e expressão gênica em relação a diferentes superfícies de implantes dentais e acetilação de Histona 3 através do uso farmacológico de Vorinostat (HDACi) em condições de normalidade e submetidos a osteoporose em condições de normalidade e quando submetido à osteoporose.

Objetivos específicos

Objetivo específico 1

Capítulo 1 - ***Analysis in vivo of bone modulation in hydrophilic titanium surfaces***

O objetivo deste estudo foi avaliar o efeito de uma superfície de tratamento hidrofílico na diferenciação de osteoblastos e seus efeitos na osseointegração.

Objetivo específico 2

Capítulo 2 - ***Gene expression of hydrophilic titanium surface in osteoporotic model***

O objetivo deste estudo foi determinar o padrão de formação óssea e expressão gênica em duas superfícies diferentes de implantes de titânio (hidrofóbica e hidrofílica) em um modelo osteoporótico.

Objetivo específico 3

Capítulo 3 – *Hypoacetylation of acetyl-histone H3 (H3K9ac) as marker of bone modulation in titanium implants with nanoscale surface*

O objetivo desse estudo foi investigar modificações globais da cromatina presente em núcleos celulares mediadas por nano superfície de titânio e como a indução farmacológica da acetilação de histonas influencia na diferenciação de células-tronco mesenquimais, especialmente em condições de osteoporose.

CAPÍTULOS

3. CAPÍTULOS

3.1 CAPÍTULO 1

Artigo a ser enviado ao periódico Clinical Oral Implant Research

---

Analysis *in vivo* of bone modulation in hydrophilic titanium surfaces

Jessica Afonso Ferreira[1,2], MSc., PhD.

Elisa Matias Sartori[3], MSc., PhD.

Fábio Antônio Piola Rizzante[4], MSc., PhD.

Daniela Baccelli Silveira Mendonça[1], MSc., PhD.

Denildo de Magalhães[2], PhD.

Gustavo Mendonça[1*], MSc., PhD.

[1]Department of Biological and Material Sciences, Division of Prosthodontics, University of Michigan School of Dentistry, Ann Arbor, MI, USA.

[2]Department of Periodontology and Implant Dentistry, School of Dentistry, Federal University of Uberlandia, Uberlândia, MG, Brazil.

[3]Department of Clinical Propaedeutics, School of Dentistry, Brazil University, Fernandopolis, SP, Brazil.

[4]Department of Comprehensive Care, School of Dental Medicine, Case Western Reserve University, Cleveland, OH, USA.

***Correspondence to: Gustavo Mendonça**

Clinical Associate Professor

University of Michigan School of Dentistry

Biologic & Materials Sciences, Division of Prosthodontics

1011 N University Ave, Rm 1027

Email mgustavo@umich.edu

ABSTRACT

Advancements in bioengineering and biotechnology with the development of novel biomaterials has allowed to improvement and new approaches in oral rehabilitation with dental implants. Novel implant surfaces have been developed and they help improving the biological response by guiding the differentiation of stem cells into osteoblast to allow for proper bone support around the implants. The use of modified-etched hydrophilic titanium to enhance endosseous implant surfaces may improve the clinical control of interfacial osteoblast biology. **Purpose**: To evaluate the effect a hydrophilic treatment surface on osteoblast differentiation and its effects on osseointegration. **Methods and Materials**: Two types of wire implants (Neodent, Curitiba, Brazil), with same macrogeometry but different surface technology (i) dual acid-etched surface (SAE) treatment with hydrochloric and sulfuric acid followed by insertion in isotonic saline solution to increase hydrophilicity (SAE-HD) (test, n = 16); (ii) dual SAE (control, n = 16) were installed bilaterally in the each femur of thirty-two Osterix-cherry male mice of 3 month old. After different periods of euthanasia based on the methodology used, biological tests were performed in the femur and implant: scanning electron microscopy (SEM) and energy-dispersive x-ray spectroscopy (EDS), to evaluate and quantify the presence of calcium on the implant surface. The femurs were analyzed for BIC and bone volume (BV) by μCT scanning followed by histology. Fresh bone marrow was harvested from mice from each group at sacrifice and Real-time polymerase chain reaction (PCR) was used to measure levels of several gene profiles (osterix, sialo-bovine protein, SOST, IL-1a and IL-10). Additionally, the characterization of implants included surface roughness analysis with interferometer. Data were analyzed using two-way ANOVA followed by Tukey's test ($p < 0.05$). **Results:** The amount of calcium deposited on the surface due to the mineralization process was higher for SAE-HD after 7 days. Nano CT assessment revealed significantly more bone volume (BV) around the implant in the SAE-HD group treatment compared to SAE group. Histological assessment showed increased bone-to-implant contact (BIC) in the test group in comparison to control group. Consistently, in our gene expression studies, hydrophilic treatment surface showed increase levels of expression analysis in showed that genes involved in the bone morphogenetic protein signaling, such as ALP, BSP, SOST and SP7, were significantly activated in the SAE-HD. **Conclusions:** Both surfaces were able to modulate bone responses toward

osteoblast differentiation; however, hydrophilic treatment surface presented a better response when compared to the control group. Due to increased expression of genes related to the process of osteogenic differentiation, percentages of BIC and BV increased with time as well significant amount of calcium content was observed, one can suggest the choice of the hydrophilic surface in order to improve osseointegration process.

Keywords: bone-to-implant contact, oral implants, implant surfaces, osseointegration

INTRODUCTION

Brånemark and colleagues accidentally discovered a mechanism of adhesion of titanium to the bone when studying microcirculation in rabbit tibia (Lemus et al., 2009). This phenomenon was known as osseointegration (Melo et al., 2006). In 1981, Adell et al. reported that approximately 90% of the implants placed in the anterior region of the mandible were successful between 5 to 12 years after the installation; however, lower rates were observed for implants in the anterior maxilla (Adell et al., 1981). Noack et al. (1999) reported that mandibular implants had a higher success rate than on maxilla, with an overall prosthetic loss rate of 1.9% while 4.3% of implants were lost after prosthetic treatment. According to Saab et al. (2007) the problem is due to the pattern of bone loss, which cannot be precisely predicted in the region of the anterior maxillary teeth. The maxilla may have an insufficient amount of bone for insertion of implants, being a great surgical-prosthetic challenge due to reduced bone quality and low trabecular density (Capelli et al., 2007).

After the positioning of the implant and its initial load, the bone of the crest undergoes a process of remodeling and resorption (Danza et al., 2010). This process of remodeling in the peri-implantar bone can be influenced by the direction, repetition and magnitude of the biomechanical load (Hasan et al., 2011). The factors that may affect the magnitude of the forces in the peri-implant zones of the bone are the geometry, position and number of implants (Sahin et al., 2002). The application of functional forces induces loads and stresses in the prosthesis-implant assembly, affecting the process of bone remodeling around the implants (Bidez et al., 1992). However, the limits of physiological tolerance of human jaws are not known and some implant failures may be related to the magnitude of unfavorable stresses (Sahin et al., 2002).

Research involving titanium and its alloys in order to meet and assist in the general health of the patient has been making its progressive use in the manufacture of implants, both orthopedic and dental. This is due to the presence of excellent biocompatibility (Wang et al, 2018), high mechanical strength, high corrosion resistance and low density of this material (Hotchkiss et al 2016). It is important to note that the development of biomaterials that are compatible to tissues is necessary in order to maintain cell viability and induce proliferation and differentiation in specific

strains. Many types of implant surface treatments have been performed for this purpose (Kapoor et al., 2010). And they can be classified into five groups, machined, macrotexturized, microtexturized, nanotexturized or biomimetic (Ahn et al., 2010). The surface treatments of dental implants have shown positive results in reducing the time of osseointegration and constantly new surface treatments are developed to reduce the healing process of the bone around the implants (Wang et al 2018).

Due to the various types of implant surface treatments it is possible to obtain various forms of surface characterization, aiding in the understanding of bone formation and cell behavior. Chemical modification of titanium surfaces can result in a hydrophilic surface that can change cell behavior and improve osseointegration (Buser et al, 2004; Bosshardt et al, 2011). Previous studies shown that the increase in surface roughness and wettability of a Ti surface can improve osseointegration (Wennerberg ET AL 2009). Surface topography and wettability can affect the differentiation of cells in different ways but there is a lack of understanding the molecular mechanism that regulates osteogenesis on these surfaces. Thus, the aim of this study was to examine osteoblast differentiation effect and bone formation on a hydrophilic and hydrophobic surface.

MATERIALS AND METHODS

Surface Characterization

Confocal laser scanning microscopy

Confocal laser microscope (LEXT-OLS4100 Olympus, Waltham, MA) was used to investigate micro-scale topography of each surface. Four samples of each surface group were imaged using a 20X objective and 100 nm pitch. The characterization of surface topography consisted of three components: shape, waviness and roughness, where filters were necessary to isolate each of these components for analysis. This microscope has LEXT-OLS4100 Olympus software, that was used for this purpose, which also permitted 2D and 3D images based on numerical description of the parameters for surface roughness. The numerical description of surface roughness at the different regions used five height parameters (Sa, Sq, Ssk, Sku, Sz), one spacing spatial parameter (Sdr) and one horizontal with texture aspect (Str). Sa and Sq, also referred to as mean roughness, is the arithmetic mean height of the asperities. Sz is related to the height distribution curve, Ssk and

Sku are related to the direction of de roughness, where Ssk is a measure of asymmetry of surface deviations about the mean plane and Sku is a measure of the peakedness or sharpness of the surface height distribution. Str is the texture aspect ratio of the surface, used to identify uniformity of texture aspect.

In vivo procedures

Experimental animal model

The research protocol was approved by The Institutional Animal Use & Care Committee (IACUC), University of Michigan. This research was conducted incompliance with University guidelines, State and Federal regulations and the standards of the “Guide for the Care and Use of Laboratory Animals.

Thirty-two, male, Tg (Sp7/mCherry)2Pmay/J (OSX-Cherry), 3 months old, weighting between 23 and 30 g, with no injuries or congenital defects were used in the study. They were developed by Dr. Peter Maye (University of Connecticut). This strain is now on C57BL/6 (B6) background and available from Jackson laboratories. OSX-Cherry mouse contains one copy of the Osterix (SP7) gene tagged with cherry fluorescent protein. This animal allows for visualization of osteoblast differentiation at the early stages of bone formation. Before each surgical session, the animals were anaesthetized via inhalation isoflurane (Piramal, Pennsylvania, USA) (4-5%) for induction and maintained with isoflurane (1-3%) as necessary to maintain surgical anesthesia using a calibrated vaporizer. Level of anesthesia was monitored by toe pinch and eye reflex. Local anesthesia with Lidocaine was administered. Ophthalmic ointment was used to protect the eyes of the animals during surgery. Alcohol-soaked gauze sponges were alternated with iodophor-soaked gauze sponges or Q-tips to disinfect the surgical site. The wound area was shaved gently. The surgical field was cleaned with povidone iodine solution (3 alternating scrubs of povidone iodine/chlorhexidine with normal saline/alcohol/sterile water). For post-operative pain management Carprofen (Piramal, Pennsylvania, USA) was provided preemptively, for 48 hours postoperatively and then as needed. Signs of complications related to surgery were monitored daily. Surgery records were kept and also included the records regarding the frequency of using of post-operative analgesics.

Experimental implant surgical procedure

The same experimental surgical procedure was performed in all animals (both test and control group). The surgery region was shaved and disinfected with iodine solution (Betadine 10%, Meda). The incision was made in the medial parapatellar region with displacement and remoteness of the muscle complex and the implants were placed in the long axis of the femur through of a medial parapatellar arthrotomy, filling the entire medullary canal. A sequence from 30 gauge needle to 21 gauge needle were used manually to perform the proximal epiphysis and to access the intramedullary canal. Implants in the control group were only sandblasted and dual acid-etched (SAE; n = 16). In the test group, after sandblasting and dual acid-etching, implants received proprietary technology treatment, including microwave treatment and insertion in isotonic saline solution resulting insignificantly increased hydrophilicity (SAE-HD; n = 16). Neodent® (Curitiba, PR, Brazil) supplied all implants (Fig 1a, b). Each femur received a different surface, for standardization, rights femurs received SAE implants and lefts SAE-HD implants. The tissues were repositioned through 5-0 Vicryl® wire suture (Ethicon, San Angelo, TX, USA). The animals were medicated with anti-inflammatory and analgesic drugs (5mg/kg Carprofen®base, Pfizer) subcutaneously for 48 hours post-surgery and were kept in cages in groups of five, housed at 21^{o}C ambient temperature and maintained in a light/dark cycle of 12/12h. The animals were euthanized with an overdose of carbon dioxide at different times after the experimental surgical procedure. For PCR assay, tissues were collected at 1, 3 and 7 days following surgery. For scanning electron microscopy (SEM) and energy-dispersive x-ray spectroscopy (EDS), samples were collected at 7 days. The femurs were collected at 14 and 21 days and analyzed for (Bone Implant Contact) BIC and (Bone Volume) BV by Nano CT scanning followed by histology.

Scanning Electron Microscopy and EDS Analysis

Animals were euthanized at 7 days for this analysis. The implants were examined by high-resolution scanning electron microscopy (Philips XL30 FEG, SEM, Philips, Eindhoven, Netherlands and the chemical analysis by energy-dispersive x-ray spectroscopy (EDS), is an analysis performed by an equipment coupled to the scanning electron microscope, which allows a qualitative and semiquantitative evaluation from the emission of characteristic x-rays. This tool allows the indication of the presence of chemical elements in several types of sample components, whether mineral or organic. The calcium content was measured at the surface of each implant

in 6 different areas. The results are expressed by the mean value of the 6 measurements randomly taken.

Nano CT Analysis

Animals were euthanized at 14 and 21 days post-implant (n=5 animals). Muscle tissue and epiphyses were removed and bone/implant was fixed with 4% paraformaldehyde (Z Fix). Non-destructive analysis of the neoformed bone at the implant interface was performed using the Nano CT (Nanotom-S, phoenix|x-ray, GE; Germany), located at the University of Michigan, Orthopedic Research Laboratories, Ann Arbor, MI. The samples were scanned with pieces rotation in 360º, using monochromatic x-rays with 80 kV, 320µA., 120ms exposure time, 3 frame averaging, 6 µm voxel size. The software NRecon and Dataviewer were used for the image reconstruction. A region of interest (ROI) around the implant were defined, where the bone volume (BV) could be calculated. Outcome variables were BV, being the percentage of bone that is present in the region around the implant and bone-implant contact (BIC), being the area percentage of the total implant surface that is covered by bone.

Histological processing

Immediately following the Nano CT analysis samples were prepared for histological assessments of non-demineralized samples. Fixation of samples was performed in 10% formaldehyde for a week followed by gradual dehydration using a series of alcohol solutions ranging 70 to 100% ethanol. Specimen were processed using a Leica ASP300 tissue processor and then placed in a series of methyl methacrylate and dibutyl phthalate with progressively higher concentrations of benzoyl peroxide. Samples were manually embedded in partially polymerized poly methyl methacrylate (PMMA) and allowed to cure at room temperature for up to ten days. Blocks were then hardened in a 37°C oven overnight. The tissues were sliced (~300 µm in thickness) through the center of the implant along its long axis with an Isomet 2000 precision diamond saw (Buehler Ltd., Lake Bluff, Illinois, United States), glued to acrylic plates with an acrylate-based cement Technovit 7000 VCL (Külzer, Wehrheim, Hesse, Germany), and allowed to set for 24 h prior to grinding and polishing. The sections were then reduced to a final thickness of ~30 µm by grinding/polishing using a series of abrasive papers EXACT 310 CP series (400, 1200,

55 and 15) (EXACT Apparatebau, Norderstedt, Schleswig-Holstein, Germany) under water irrigation. The unstained sections were analyzed by polarized light microscopy Axioplan 2 (Zeiss, Jena, Thuringia, Germany); the sections were then stained with toluidine blue and submitted to an optical microscopy evaluation Olympus BX51 Microscope (Olympus).

Histomorphometric analysis

In each histological slice, eight non-superimposing fields, corresponding to the implant/bone interface (four fields on each side of the implant), were captured by scanning at a 20x magnification, and digital image analysis software (Image J®v.1.45; National Institutes of Health, Bethesda, MD, USA) was used to measure the bone-to-implant contact (BIC). The regions of bone-to-implant contact along the implant perimeter were subtracted from the total implant perimeter, and calculations were performed to determine the BIC. Results were reported as percentages.

RNA isolation and analysis

The data points were analyzed at 1,3 and 7 days after surgery (n=5, each time point). Implants were removed from femur and placed in 1ml Trizol lysis reagent (Invitrogen, Carlsbad, CA, USA). The samples were kept frozen at -80°C for at least 24 hours. Total RNA in the cell lysates was isolated according to the manufacturer's protocol and collected by ethanol precipitation. Total RNA concentration was quantified using a NanoDrop 2000 spectrophotometer (NanoDrop products, Wilmington, DE, USA). The extracted RNA was reverse transcribed following a conventional protocol to synthesize complementary DNA (cDNA). cDNA synthesis was performed using 500ng of RNA following the manufacturer's recommendations (SuperScript VILO cDNA Synthesis, Invitrogen). The cDNA was used as a template in real-time PCR. All primers for quantitative PCR (qPCR) were obtained from Qiagen (Qiagen Sciences, Germantown, MD, USA). The reactions were prepared using SYBR Green Real-Time PCR Master Mix (Qiagen) according to the manufacturer's protocol. Thermal cycling was performed on an ABI 7900HT (Applied Biosystems, Foster City, CA, USA) according to recommended protocol. The relative mRNA expression was determined by $2^{-\Delta\Delta Ct}$ method and reported as fold induction. Samples of SAE group at day 1 were set as control; 1.0-fold expression level. All cDNAs were

subjected to polymerase chain reaction (PCR) for Glyceraldehyde-3-phosphate dehydrogenase (GAPDH) as a test of RNA integrity and cDNA synthesis. Subsequently, equal volumes of cDNA were used to program real-time PCR reactions specific for mRNAs encoding the early osteogenic markers: *SP7*; late osteogenic marker: *Bsp*; osteocyte differentiation marker: *Sost*; pro-inflammatory marker: *Il-1a* and anti-inflammatory marker *Il-10*. GAPDH was used as house-keeping gene control.

Statistical analysis

Real time PCR results were shown as Fold Change by the $2^{-\Delta\Delta Ct}$ method, in baseline 2, with SAE at day 1 being used as the control. The test - t was used as statistical test for comparison between the day 1 SAE and the other groups. For the other tests, two-way ANOVA was used followed by the Tukey test when necessary. The software used for statistical analysis was Prism 6 (Graphpad Software INC, La Jolla, CA, USA). For all statistical analyzes, the level of significance was set at $p < 0.05$.

RESULTS

Surface Characterization

Confocal laser scanning microscopy

The S_a parameter provides a good overview of the values of the height of the irregularities on the surface. Based on the mean values obtained for Group SAE (1.74 µm±0.03) and Group SAE-HD (1.60 µm±0.10), it can be said that the two have a similar surface roughness, but only with this parameter, it is not possible to describe the surface as a whole. The S_z parameter indicates the average distance between the highest peak and the deepest valley. In this case, due to the process of obtaining the topography by the same method, the S_z value doesn't change considerably (SAE: 33.28µm±0.38and SAE-HD: 34.31µm±0.47). S_{dr} is the parameter that indicates the surface area enlargement. We can say that the surface area enlargement of group SAE (mean value 0.015%) is similar to the implant surface of Group SAE-HD (mean value 0.01%) due to the fact that the process of obtaining the topography is the same in both cases. S_{sk} is the parameter associated with height distribution of surface irregularities, also related with asymmetry of the height distribution curve, where curves with approximately normal distribution present S_{sk} values close to 0. S_{ku} is associated with the flatness of the height distribution curve, where curves with approximately normal distribution have S_{ku} values close to 3. All implant regions of

SAE-HD and SAE showed S_{sk} values close to 0 (Table 1). The S_{sk} values for all implants showed no significant changes (Table 1). To quantify the texture strength, i.e., the uniformity of surface texture, the parameter S_{tr} was used, which evaluates the texture aspect ratio of the surfaces. Values of S_{tr}> 0.5 indicate a uniform texture in all directions, i.e., the surface is topographically isotropic; whereas S_{tr}<0.3 indicate strong directionality of the texture (anisotropy) [Stout KJ et al. 1993]. Therefore, the results of S_{tr} (Table 1) are indicating anisotropy for both surfaces of this study.

In vivo evaluation

Scanning Electron Microscopy and EDS Analysis

Figure 2 shows representative images of the implants after removal from the bone (Fig. 4A-F). Although the images are very similar qualitatively in both conditions, it is possible to observe more uniform bone formation and apposition on the SAE-HD surface (Fig. 4D-F). The results of the amount of calcium content measured by EDS on the surface of the implant are presented in Figure 3. Two-way ANOVA showed the amount of deposition statistically higher for hydrophilic surface after 7 days.

Nano CT Analysis

3D reconstruction of the new bone formation around the implant in different surfaces are shown in Figure 4. Specifically, the area of new bone tissue present and the entire trabecular bone around implant are represented by yellow and green, respectively. At 14 days after implantation, it was not possible to identify substantial differences between SAE and SAE-HD surfaces (Fig. 4A), however, in 21 days (Fig. 4B) it is evident the greater presence of BV and BIC. Additionally, SAE-HD showed a wide increase of BV (P=0.0081) and BIC (P=0.0042) compared with SAE surface at 21 days post-implantation (Fig. 4C-D).

Histological analysis

Both groups presented peri-implant bone regeneration. In the cortical region of both groups at 14 days post-implantation, the complete adaptation of cortical bone with the apical region of the implant was observed, which ensured initial stability. Generally, both groups presented new bone formation around the implants in a time-dependent fashion.

After 14 days, the SAE group showed areas with little new bone formation (Fig. 5A, C, E and G). The SAE-HD group showed more new bone formation compared with

the SAE group (Fig. 5B, D F and H). The SAE-HD surface exhibited a rapid increase of bone formation with more compact trabecular bone (Fig. 5A–B) than did the SAE surface at day 14. At 21 days, the SAE group showed trabecular bone more structured than it had at 14 days, with discrete regions of BIC (Fig. 6C–G). In contrast, the SAE-HD group was surrounded by more continuous bone, which seemed to be the trabecular extending from the cortical layer. Additionally, the hydrophilic group showed intimate contact between the new bone and the implant surface (Fig. 6F–H).

Histomorphometric results

The values of BIC obtained in the Histomorphometric analysis presented a normal distribution by D'Agostino–Pearson test. Two-way analysis of variance (ANOVA) with Tukey's post hoc test was used to determine differences between experimental time points of the same implant group. The values (in percentages) of the SAE and SAE-HD implants at all experimental time points are illustrated in Fig. 6.

After 14 days, the SAE-HD group presented a higher BIC than did the SAE group ($P = 0.0009$) (Fig. 6). At day 21, the SAE-HD group had enhanced BIC rates compared with SAE at day 14, whereas the SAE-HD group showed a 'jump' of BIC that was almost twofold greater than day 14. SAE-HD had higher BIC values than did SAE ($P = 0.0002$) (Fig. 6). After 21 days, both the hydrophilic and hydrophobic groups showed increased BIC values compared with those observed on day 14.

Gene expression analysis

The results show the relative levels of expression in relation to the SAE day 1 as control group (Method $2^{-\Delta\Delta Ct}$) n = 5 for each time point. Early osteoblast differentiation gene (SP7 - Osterix) had higher expression on hydrophilic surfaces (Fig. 7A). SP7 (figure 7B) also an osteoblast key transcription factor for differentiation, showed up-regulation at day 1 on the SAE-HD with values close to the baseline reaching maximum peak at day 3, presenting expression almost 5 times higher than the baseline, showing on this day statistical differences in relation to the control group. The expression of the osteogenic late gene is represented by bone sialoprotein (*Bsp)* (Fig. 7B) showed values above the baseline, for both surfaces, presented 3-fold upregulated starting at day 3 for the hydrophobic surface and in the same period for hydrophilic surface, presented 5-fold upregulated. At day 7 there is an increase in this gene expression for SAE surface, showing a 6-fold change. *Bsp* did not change

significantly after day 3. Esclerotin (*Sost*) as a marker of osteocyte differentiation, might indicate maturation of osteoblasts. Sost showed upregulated on SAE-HD surface at day 3 and 7 (Fig. 7C), while SAE presented only minor up-regulation. Higher gene expression was also observed at day 7 on which hydrophilic surface comparing to hydrophobic surface, fold change 3 and 1, respectively for Sost. The patterns of gene expression for the inflammatory genes are showed in the figures 8A and B. At day 1, pro inflammatory gene *Il-1a* (fig. 8A) showed low levels of gene expression for both surfaces. At day 3 there is an increase in this gene expression for SAE surface, with a 5-fold upregulation. For this time point SAE-HD exhibited low expression, close to the baseline levels. At day 7 the levels of *Il1a* for the two surfaces increased and showed 12-fold upregulated for the SAE-HD surface and 31-fold upregulated for the SAE surface. Anti-inflammatory gene, *Il-10* (Fig. 8B) showed under the baseline at day 1 for hydrophilic surface compared to the control group. At day 3, this gene showed overexpressed on SAE-HD surface at day 3 presented 5-fold regulated, while SAE presented 2-fold regulated, higher genic expression was also observed at day 7 on which hydrophilic surface comparing to hydrophobic surface, fold change 3 and -1, respectively.

DISCUSSION

The present investigation followed the sequence of events during the early osseointegration of two different titanium implant surfaces that were placed in femurs of mice. Results have shown that implants with a sandblasted and dual SAE, specifically treated to increase its hydrophilicity (SAE-HD), not only achieved higher amounts of BIC but also promoted more amount of Ca on the surface and expression of genes related to osteogenesis as only sandblasted and dual acid-etched implants (SAE), during initial stages of healing. This result agrees with previously published preclinical in vivo studies evaluating hydrophilic implant surfaces (Sartoretto et al. 2016; Buser et al. 2004; Bornstein et al. 2008; Rossi et al. 2014; Mainetti et al. 2015) and humans (Bosshardt et al. 2011; Lang et al. 2011). Morphology and surface roughness evaluation, which were performed by confocal laser scanning microscopy indicated no remarkable differences between the groups.

As previously shown, hydrophilic surface modification may accelerate blood contact on the implant surface, increase clot formation, adhesion and differentiation of osteogenic cells (Jesus el al. 2017; Buser et al. 2004; Masaki et al. 2005; Zhao et

al. 2005; Schwarz et al. 2007; Mamalis & Silvestros 2011), upregulate expression of various genes related to bone formation, e.g. BSP, ALP (An et al. 2010; Raines et al. 2010), and modulate pro-inflammatory cytokine genes (Hamlet et al. 2012). In this context, our findings corroborate to achieve rapid coverage of the implant surface, by proving that the amount of Calcium is greater around the hydrophilic surface at 7 days post-implantation and it is known from previous studies that Ca^{2+} and $(PO_4)^{3-}$ ions stimulate cellular and intracellular signaling and favor osteoblastic cell activity in the process of bone formation (Chai YC et al. 2012; Barradas A et al. 2012). Further, Ca^{2+} ions might increase osteogenic cell chemotaxis and migration toward the coated surface via the activation of calcium signaling. Ca^{2+} and $(PO_4)^{3-}$ ions also play an essential role in bone mineralization and can facilitate the precipitation of bone-like apatite on the implant surface (Cochran DL et al. 1998; Kokubo T et al. 2006).

Investigation of BIC and BV are long established measures for osseointegration in scientific literature (Buser D et al. 2004; Wennerberg A et al., 2009; Xavier SP et al. 2010; Park IP et al. 2011; Dagher M et al. 2014; Wennerberg A et al. 2014; Eriksson C et al. 2004; Rupp F et al. 2011; Yeo IS et al. 2014). BIC shows new bone formation in contact with implant surface, which has been related to osteogenesis contact. However, the ideal interface or surface between an implant and the host tissue is influenced by surgical, biomechanical, implant design, manufacturing, site of implantation and commercial related factors (Soares PBF et al. 2015, Walsh WR et al. 2015). Similarly for the current study, in a recent study in sheep, similar commercial implants (Acqua; Neodent, Curitiba, Brazil) manufactured by an almost identical technique as the SAE-HD herein was shown to possess a significantly higher hydrophilicity comparing to a commercially available implant with surface technology identical with the SAE implant (Neoporos; Neodent, Curitiba, Brazil) (contact angle 0° vs. $>$103.3°, respectively), Acqua group presented superhydrophilic behavior and showed complete wetting of the surface (Sartoretto et al. 2017). Furthermore, “hydrophilic” implants placed in the tibia of the sheep achieved 1.3 times more BIC compared with the “hydrophobic” ones after 28 days of healing (Sartoretto et al. 2017). Consistently, these results were similar to our data and also support that hydrophilic topographical features made an effective contribution to osseointegration. In this context, this theory can be proved by our results obtained by Nano CT. Nanotomography showed better results with statistical differences for the SAE-HD surface at 21 days compared to SAE and SAE-HD at day 14, evidencing a progressive

increase of the bone neoformed in this surface, an important process for establishment of osseointegration and implant maintenance.

Histology has been used as an important tool to evaluate bone neoformation at the bone / implant interface in nanoscale surface implants (Karazisis et al. 2016; Karazisis et al. 2017; Fabbro et al. 2017). Our study allowed a more complete and visual analysis of the bone neoformation at the interface of the implant. Once again, histology showed bests results with statistical differences for the SAE-HD surface at 14 and 21 days compared to SAE at day 14. Besides that, we observed that, at day 21, SAE-HD showed almost 2 times more than SAE at day 14, which in the osseointegration process is extremely desirable, since implants clinical success is related to rapid osseointegration (Le Guehenec et al. 2007).

Evidence suggests that hydrophilic surfaces can attract selective proteins that exert the specific regulation of genes expressed by adjacent progenitor cells, thus favoring the early mineralization of the matrix cells (Wall et al. 2009). In addition, hydrophilic surfaces demonstrated anti-inflammatory properties by modulating the inflammatory response in adherent macrophages. This may facilitate improved bone healing and osseointegration (Hamlet et al. 2012). Inflammatory, early and late osteogenic genes are related to each stage of differentiation of the bone cell line, and the intensity of each marker can indicate how active is the cell, which ideally could determine the ability of these cells in to form bone at implant surface (Meirelles, 2010). The relative gene expression of SP7, BSP and SOST had prominently increased on the SAE-HD surface compared with the control group (SAE Day 1) (Fig 8). This pattern of expression could be noticed on titanium micro and nano surfaces that had been studied with osteoprogenitor cells as well (Chakravorty N et al. 2012; Mendonça G et al. 2010; Mendonça G et al. 2009; Kato RB et al. 2014). The overexpression of these osteo-related genes indicates that these changes could be attributed to the nanoscale surface used in this study. BSP is related to the binding of basic elements in the extra-cellular bone matrix and bone mineralization (Belibasakis GN et al. 2012) and its presence could improve bone repair around dental implants (Campos JM et al. 2015). BSP (bone sialoprotein) is the largest structural protein in the bone matrix and fully differentiated osteoblasts express this gene, being the first to be detected in differentiated osteoblasts forming bone (Tang et al. 2011). Additionally, the molecular data support the histomorphometric evidences of progressive bone healing, since SOST (sclerostin), a marker of advanced osteoblastic differentiation and osteocyte

markers, shows upregulated at this time period (Bonewald LF et al. 2011; Dallas SL et al. 2013).

After implant surgery the modulation of the inflammatory process during the early stages of healing provides a key element for implant fixation. (Thalji et al. 2013). Once implanted, surgical implants adsorb proteins and simultaneously incite an inflammatory foreign body response that begins with an acute response and develops as a chronic fibrotic response representing the first step in tissue repair (Anderson et al. 2008; Ma et al. 2014). Macrophages are the first to recognize the foreign body and secrete inflammatory mediators to initiate inflammation (Jones et al. 2007). M1 macrophages secrete key proinflammatory cytokines such as IL-1a, NOS2 and TNF-α that promote inflammation, neutrophil recruitment, osteogenic differentiation of MSCs as well as bone remodeling. While M2 macrophages produce anti-inflammatory mediators such as IL-10 that promote inflammation resolution and tissue regeneration (Ma et al. 2014). The rapid physiological resolution of inflammation is necessary for bone healing, thus it is desirable that the increase of the gene expression of the pro-inflammatory genes be only in the early stages of implantation and anti-inflammatory genes in the final stages, since the presence of pro and anti-inflammatory cytokines expressed at the same time contribute to a poorly balanced environment for proper wound healing to occur (Eming et al. 2010). In our study, we observed this pattern of behavior for both pro and anti-inflammatory genes in both SAE and SAE-HD surface. According, Il-1a showed an increase in expression as a function of time and the progressive decrease in IL-10 expression, prolongs the inflammatory phase, slows healing (Eming et al. 2010), disrupting collagen synthesis and preventing bone formation (Ma et al. 2014). These aspects suggest the increase of osteogenesis and consequently greater bone formation (Thalji and Cooper 2014). Preclinical and clinical studies support our findings that the early healing phase, was enhanced for hydrophilic surface implants compared with hydrophobic surface implants (Lang et al. 2011).

CONCLUSION

In summary, the results of the present study revealed that both hydrophobic and hydrophilic implant surface contributed to a favorable biological response. However, the superior osseointegration from 21 days post-operation of the hydrophilic surface SAE-HD group presented greater advantages within the first month of wound healing.

In addition, our data suggest that the hydrophilic surface can enable a reduction

in the healing period post-implant placement through increased bone apposition *in vivo* compared with the conventional hydrophobic surface.

CONFLICT OF INTEREST

No conflict of interest.

ACKNOWLEDGMENTS

The authors are grateful to Neodent for full donation of the implants used in this study and CAPES by scholarship concession for PhD.

REFERENCES

1. Lemus, LM.; Almagro, Z.; León, C. Origen y evolución de los implantes dentales. Rev. Hab. Cienc. Méd., v.8, n.4, out-nov, 2009.
2. Melo, MD.; Shafle, H.; Obeid, G. Implant survival rates for oral and maxillofacial surgery residents: a retrospective clinical review with analysis of resident level of training on implant survival. J. Oral Maxillofac. Surg., v.64, n.8, p.1185-1189, ago, 2006.
3. Adell, R.; Lekholm, U.; Rockler, B.; Brånemark, PI. A 15-year study of osseointegrated implants in the treatment of the edentulous jaw. Int. J. Oral Surg., v.10, n.6, p.387-416, Dez, 1981.
4. Noack, N.; Willer, J.; Hoffmann, J. Long-term results after placement of dental implants: Longitudinal study of 1,964 implants over 16 years. Int. J. Oral Maxillofac. Implants, v.14, n.5, p.784–755, set-oct, 1999.
5. Saab, XE.; Griggs, JA.; Powers, JM.; Engelmeier, RL. Effect of abutment angulation on the strain on the bone around an implant in the anterior maxilla: a finite element study. J. Prosthet. Dent., v.97, n.2, p.85-92, fev, 2007.
6. Capelli, M; Zuffeti, F.; Del Fabbro, M.; Testori, T. Immediate rehabilitation of the completely edentulous jaw with fixed prostheses supported by either upright or tilted implants: a multicenter clinical study. Int. J. Oral Maxillofac. Implants, v.22, n.4, p.639-644, jul-ago, 2007.
7. Danza, M.; Quaranta, A.; Carinci, F.; Paracchini, L.; Pompa, G.; Vozza, I. Biomechanical evaluation of dental implants in D1 and D4 bone by Finite Element

Analysis. Minerva Stomatol., v.59, n.6, p.305-313, jun, 2010.

8. Hasan, I.; Bourauel, C.; Keilig, L.; Reimann, S.; Heinemann, F. The influence of implant number and abutment design on the biomechanical behavior of bone for an implant-supported fixed prosthesis: a finite element study in the upper anterior region. Comput. Methods Biomech. Biomed. Engin., v.14, n.12, p.1113-1116, dez, 2011.
9. Sahin, S.; Cehreli, M.C.; Yalçin, E. The influence of functional forces on the biomechanics of implant-supported prostheses--a review. J. Dent., v.30, n.7- 8, p.271-282, set-nov, 2002.
10. Bidez, M.W.; Misch, C.E. Force transfer in implant dentistry: basic concepts and principles. J. Oral Implantol., v.18, n.3, p.264-274, 1992.
11. Wang, J.; Meng, F.; Song, W.; Jin, J.; Ma, Q.; Fei, D.; Fang, L; et al. Nanostructured titanium regulates osseointegration via influencing macrophage polarization in the osteogenic environment. Int. J. of Nanomedicine, v.13, p.4029-4043, 2018.
12. Hotchkiss, K.M.; Reddy, G.B.; Hyzy, S.L.; Boyan, B.D.; Olivares-Navarrete R. Titanium surface characteristics, including topography and wettability, alter macrophage activation. Acta Biomater., v.31, p.425-434, 2016.
13. Kapoor, R. et al. Comparative assessment of structural and biological properties of biomimetically coated hydroxyapatite on alumina (alpha-Al2O3) and titanium (Ti-6Al- 4V) alloy substrates. J. Biomed. Mater. Res. A., v.94, n.3, p.913-26, Sep. 2010.
14. Ahn SJ; Leesungbok, R; Lee, SW. Histomorphometric Analysis and Removal Torque of Small Diameter Implants with Alternative Surface Treatments and Different Designs. J. O. Impl., v. 16, n. 4, p.263-272. 2010.
15. Buser D, Broggini N, Wieland M, Schenk RK, Denzer AJ, Cochran DL, et al. Enhanced bone apposition to a chemically modified SLA titanium surface. J. Dent. Res., v.83, p.529–33, 2004.
16. Bosshardt DD, Salvi Ge, Huynh-Ba G, Ivanovski S, Donos N, Lang NP. The role of bone debris in early healing adjacent to hydrophilic and hydrophobic implant surfaces in man. Clin. Oral Implants Res., v.22, p.357–64, 2011.
17. Wennerberg A, Albrektsson T. Effects of titanium surface topography on bone integration: a systematic review. Clinical Oral Implants Research, v.20 (Suppl 4):172–84, 2009

18. Stout K J, Sullivan P J, Dong W P, Mainsah E, Luo N, Mathia T and Zahouani H 1993 The Development of Methods for the Characterisation of Roughness in 3 Dimensions (Brussels: ECSC-EEC-EAEC).
19. Sartoretto SC, Uzeda MJ, Miguel FB, Nascimento JR, Ascoli F, Calasans-Maia MD. Sheep as an experimental model for biomaterial implant evaluation. Acta Ortop Bras. 2016.
20. Rossi, L., Lang, N.P., De Santis, E., Morelli, F., Favero, G. & Botticelli, D. (2014) Bone-healing pattern at the surface of titanium implants: an experimental study in the dog. Clinical Oral Implants Research 25: 124–131.
21. Mainetti, T., Lang, N.P., Bengazi, F., Sbricoli, L., Soto Cantero, L. & Botticelli, D. (2015) Immedi- ate loading of implants installed in a healed alveolar bony ridge or immediately after tooth extraction: an experimental study in dogs. Clinical Oral Implants Research 26: 435–241.
22. Bosshardt, D.D., Salvi, G.E., Huynh-Ha, G., Iva- novski, S., Donos, N. & Lang, N.P. (2011) The hole of bone debris in early healing adjacent to hydrophilic and hydrophobic implant surfaces in man. Clinical Oral Implants Research 22: 357–364.
23. Lang, N.P., Salvi, G.E., Huynh-Ba, G., Ivanovski, S., Donos, N. & Bosshardt, D.D. (2011) Early osseointegration to hydrophilic and hydrophobic implant surfaces in humans. Clinical Oral Implants Research 22: 349–356.
24. de Jesus RNR, Stavropoulos A, Oliveira MTF, Soares PBF, Moura CCG, Zanetta-Barbosa D. Histomorphometric evaluation of a dual acid-etched vs. a chemically modifted hydrophilic dual acid-etched implant surface. An experimental study in dogs. Clin. Oral Impl. Res. 28, 2017, 551–557.
25. Masaki, C., Schneider, G.B., Zaharias, R., Seabold, D. & Stanford, C. (2005) Effects of implant sur- face microtopography on osteoblast gene expression. Clinical Oral Implants Research 16: 650– 656.
26. Zhao, G., Schwartz, Z., Wieland, M., Rupp, F., Geis-Gerstorfer, J., Cochran, D.L. & Boyan, B.D. (2005) High surface energy enhances cell response to titanium substrate microstructure. Journal of Biomedical Materials Research Part A 74: 49–58.
27. Schwarz, F., Ferrari, D., Herten, M., Mihatovic, I., Wieland, M., Sager, M. & Becker, J. (2007) Effects of surface hydrophilicity and microtopography on early stages of soft and hard tissue integration at non-submerged titanium implants:

an immuno- histochemical study in dogs. Journal of Periodontology 78: 2171–2184.

28. Mamalis, A.A. & Silvestros, S.S. (2011) Analysis of osteoblastic gene expression in the early human mesenchymal cell response to a chemically modified implant surface: an in vitro study. Clinical Oral Implants Research 22: 530–537.
29. An, N., Schedle, A., Wieland, M., Andrukhov, O., Matejka, M. & Rausch-Fan, X. (2010) Proliferation, behavior, and cytokine gene expression of human umbili-cal vascular endothelial cells in response to different titanium surfaces. Journal of Biomedical Materials Research Part A 93: 364– 372.
30. Raines, A.L., Olivares-Navarrete, R., Wieland, M., Cochran, D.L., Schwartz, Z. & Boyan, B.D. (2010) Regulation of angiogenesis during osseointegration by titanium surface microstructure and energy. Biomaterials 31: 4909–4917.
31. Hamlet, S., Alfarsi, M., George, R. & Ivanovski, S. (2012) The effect of hydrophilic titanium surface modification on macrophage inflammatory cytokine gene expression. Clinical Oral Implants Research 23: 584–590.
32. Chai YC, Carlier A, Bolander J, Roberts SJ, Geris L, Schrooten J, et al. Current views on calcium phosphate osteogenicity and the translation into effective bone regeneration strategies. Acta Biomater 2012;8:3876e87.
33. Barradas A, Fernandes HAM, Groen N, Chai YC, Schrooten J, van de Peppel J, et al. A calcium-induced signaling cascade leading to osteogenic differentiation of human bone marrow-derived mesenchymal stromal cells. Biomaterials 2012;33:3205e15.
34. Cochran DL, Schenk RK, Lussi A, Higginbottom FL, Buser D. Bone response to unloaded and loaded titanium implants with a sandblasted and acid-etched surface: a histometric study in the canine mandible. JBiomed Mater Res 1998;40:1-11.
35. Kokubo T, Takadama H. How useful is SBF in predicting in vivo bone bioactivity? Biomaterials 2006;27:2907e15.
36. Buser D, Broggini N, Wieland M, Schenk RK, Denzer AJ, Cochran DL, et al. Enhanced bone apposition to a chemically modified SLA titanium surface. J Dent Res 2004;83:529-533.
37. Wennerberg A, Albrektsson T. Effects of titanium surface topography on bone integration: a systematic review. Clin Oral Implants Res 2009;20:172-184.

38. Xavier SP, Ikuno KE, Tavares MG. Enhanced bone apposition to Brazilian microrough titanium surfaces. Braz Dent J 2010;21:18-23.
39. Park IP, Kim SK, Lee SJ, Lee JH. The relationship between initial implant stabilit quotient values and bone-to-implant contact ratio in the rabbit tibia. J Adv Prosthodont 2011;3:76-80.
40. Dagher M, Mokbel N, Jabbour G, Naaman N. Resonance frequency analysis, insertion torque, and bone to implant contact of 4 implant surfaces: comparison and correlation study in sheep. Implant Dent 2014;23:672-678.
41. Wennerberg A, Jimbo R, Stübinger S, Obrecht M, Dard M,. Berner S Nanostructures and hydrophilicity influence osseointegration: a biomechanical study in the rabbit tibia. Clin Oral Implants Res 2014;25:1041-1050.
42. Eriksson C, Nygren H, Ohlson K. Implantation of hydrophilic and hydrophobic titanium discs in rat tibia: cellular reactions on the surfaces during the first 3 weeks in bone. Biomaterials 2004;25:4759-4766.
43. Rupp F, Scheideler L, Eichler M. Geis-Gerstorfer J Wetting behavior of dental implants. Int J Oral Maxillofac Implants 2011;26:1256-1266.
44. Yeo IS. Reality of dental implant surface modification: a short literature review. Open Biomed Eng J 2014;8:114-119.
45. Soares PB, Moura CC, Claudino M, Carvalho VF, Rocha FS, Zanetta-Barbosa D. Influence of Implant Surfaces on Osseointegration: A Histomorphometric and Implant Stability Study in Rabbits. Braz Dent J. 2015 Oct;26(5):451-7.
46. Walsh WR, Bertollo N, Christou C, Schaffner D, Mobbs RJ. Plasma-sprayed titanium coating to polyetheretherketone improves the bone-implant interface. Spine J. 2015 May 1;15(5):1041-9.
47. Sartoretto SC, Calasans-Maia JA, Costa YOD, Louro RS, Granjeiro JM, Calasans-Maia MD. Accelerated Healing Period with Hydrophilic Implant Placed in Sheep Tibia. Braz Dent J. 2017 Sep-Oct;28(5):559-565.
48. Karazisis D, Ballo AM, Petronis S, Agheli H, Emanuelsson L, Thomsen P , Omar O. 2016. The role of well defined nanotopography of titanium implants on osseointegration: cellular and molecular events in vivo. Int J Nanomedicine. 11:1367-82.
49. Karazisis D, Petronis S, Agheli H, Emanuelsson L, Norlindh B , Johansson A, Rasmusson L, Thomsen P, Omar O. 2017. The influence of controlled surface

nanotopography on the early biological events of osseointegration. Acta Biomater.53:559-571.

50. Fabbro MD, Taschieri S, Canciani E, Addis A, Musto F, Weinstein R, Dellavia C.2017. Osseointegration of Titanium Implants With Different Rough Surfaces: A histologic and histomorphometric study in an adult minipig model. Implant Dent.(3):357-366.
51. Le Gue´hennec L, Soueidan A, Layrolle P, Amouriq Y.2007. Surface treatments of titanium dental implants for rapid osseointegration. Dent Mater.23(7):844-54.
52. Wall I, Donos N, Carlqvist K, Jones F, Brett P. Modified titanium surfaces promote accelerated osteogenic differentiation of mesenchymal stromal cells in vitro. Bone. 2009 Jul;45(1):17-26.
53. Hamlet S, Alfarsi M, George R, Ivanovski S. The effect of hydrophilic titanium surface modification on macrophage inflammatory cytokine gene expression. Clin Oral Implants Res. 2012 May;23(5):584-90.
54. Meirelles L. Nanoestruturas e a resposta óssea.Uma alternativa segura para a reabilitação com implantes osseointegráveis. 2010.Revista Implant News. 7(2): 169-72.
55. Chakravorty N, Ivanovski S, Prasadam I, Crawford R, Oloyede A, Xiao Y.2012.The microRNA expression signature on modified titanium implant surfaces influences genetic mechanisms leading to osteogenic differentiation. Acta Biomater. 8(9):3516-23.
56. Mendonça G, Mendonça DB, Aragão FJ,Cooper LF.2010. The combination of micron and nanotopography by H2SO4/H2O2 treatment and its effects on osteoblast-specific gene expression of hMSCs. J Biomed Mater Res A. 94(1):169-79.
57. Mendonça G, Mendonça DB, Aragão FJ, Cooper LF. The combi- nation of micron and nanotopography by H(2)SO(4)/H(2)O(2) treatment and its effects on osteoblast-specific gene expression of hMSCs. J Biomed Mater Res Part A 2010;94:169–179.
58. Belibasakis GN, Bostanci N. The RANKL-OPG system in clinical periodontology. J Clin Periodontol 2012;39:239–248.
59. Campos JM, Prati AJ, Cirano FR, et al. Smoking modulates gene expression of type I collagen, bone sialoprotein, and osteocalcin in human alveolar bone. J Oral Maxillofac Surg 2015;73:2123–2131.

60. Tang W, Li Y, Osimiri L, Zhang C.2011. Osteoblast-specific transcription factor Osterix (Osx) is an upstream regulator of Satb2 during bone formation. J Biol Chem. 286(38):32995- 3002.
61. Bonewald LF. The amazing osteocyte. Journal of bone and mineral research: the official journal of the American Society for Bone and Mineral Research. 2011;26(2):229–38. Epub 2011/01/22. pmid:21254230; PubMed Central PMCID: PMC3179345.
62. Dallas SL, Prideaux M, Bonewald LF. The Osteocyte: An Endocrine Cell and More. Endocrine reviews. 2013. Epub 2013/04/25.
63. Thalji G, Cooper LF. Molecular assessment of osseointegration in vivo: a review of the current literature. Int J Oral Maxillofac Implants. 2013 Nov-Dec;28(6):e521-34.
64. Anderson JM, Rodriguez A, Chang DT.2008. Foreign body reaction to biomaterials. Semin Immunol .20(2):86-100.Ma QL, Zhao LZ, Liu RR, Jin BQ, Song W, Wang Y. 2014 Improved implant osseointegration of a nanostructured titanium surface via mediation of macrophage polarization. Biomaterials. 35(37):9853-9867.Jones 2007
65. Eming SA, Koch M, Krieger A, Brachvogel B, Kreft S, Bruckner-Tuderman L, Krieg T, Shannon JD, Fox JW. Differential proteomic analysis distinguishes tissue repair biomarker signatures in wound exudates obtained from normal healing and chronic wounds. J Proteome Res. 2010 Sep 3;9(9):4758-66.
66. Thalji G, Cooper LF. Molecular assessment of osseointegration in vitro: a review of current literature. Int J Oral Maxillofac Implants. 2014. 29(2):e171-99.

FIGURES AND LEGEND

Figure 1

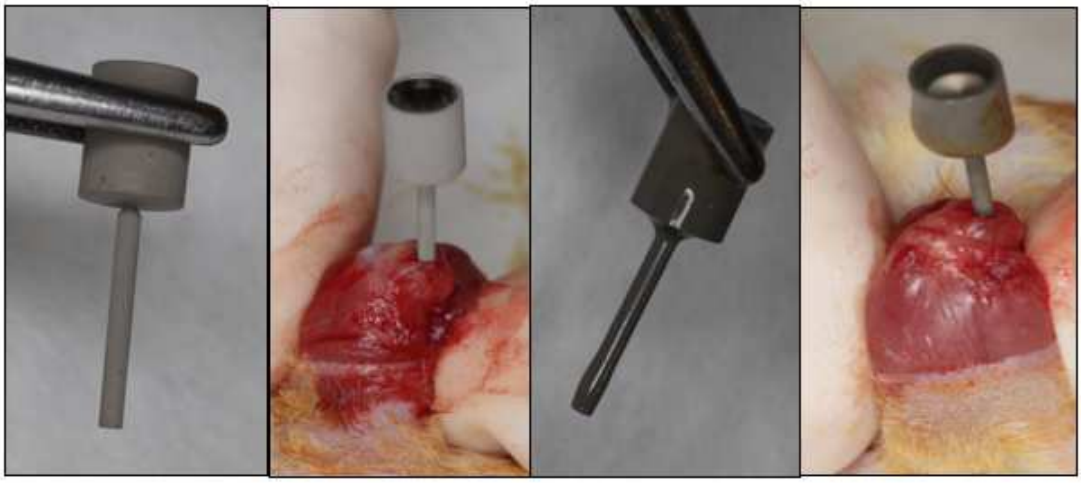

Figure 1. One pair of cpTi grade IV wire (diameter 0.7 mm and length 8mm) prepared with a hydrophobic (SAE) (left) and hydrophilic (SAE-HD) (right) surface was placed in each femur.

Figure 2

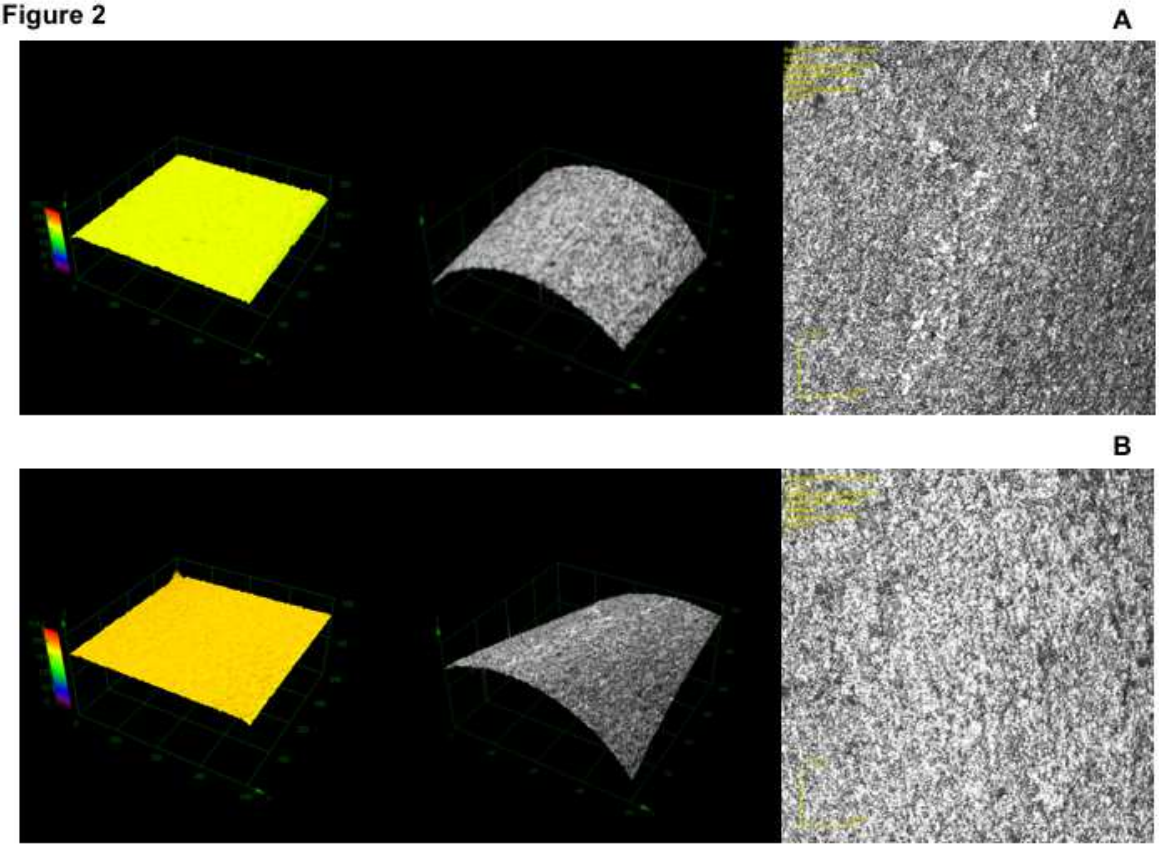

Figure 2. A. Bone volume fraction (%) of the two different surface at day 14 and 21 obtained from analysis of the Micro-CT. The results are expressed as the mean±SD; * represents a signifcant diference (P<0.05). B. Neoformed bone volume (mm) of the two different surface at day 14 and 21 obtained from analysis of the Micro-CT. The results are expressed as the mean±SD; * represents a signifcant diference (P<0.05)

Surface	Sample	Sa [µm]	Sq [µm]	Ssk	Sz [µm]	Str
SAE	1	1.787	2.722	0.274	96.399	0.036
	2	1.738	2.481	-1.220	53.554	0.039
	3	1.703	2.390	-1.247	32.629	0.041
	4	1.756	2.463	-1.331	33.573	0.037
	Mean	1.746	2.514	-0.881	54.039	0.038
	SD	0.030	0.125	0.668	25.845	0.002
SAE-HD	1	1.663	2.603	0.619	67.751	0.041
	2	1.599	2.873	0.127	54.897	0.036
	3	1.512	2.233	-1.691	47.813	0.044
	4	1.634	2.747	0.752	49.788	0.032
	Mean	1.602	2.614	-0.048	55.062	0.038
	SD	0.057	0.240	0.977	7.769	0.005

Table 1 – Topographic analysis of the implant surface roughness, values obtained from confocal microscopy.

Figure 3

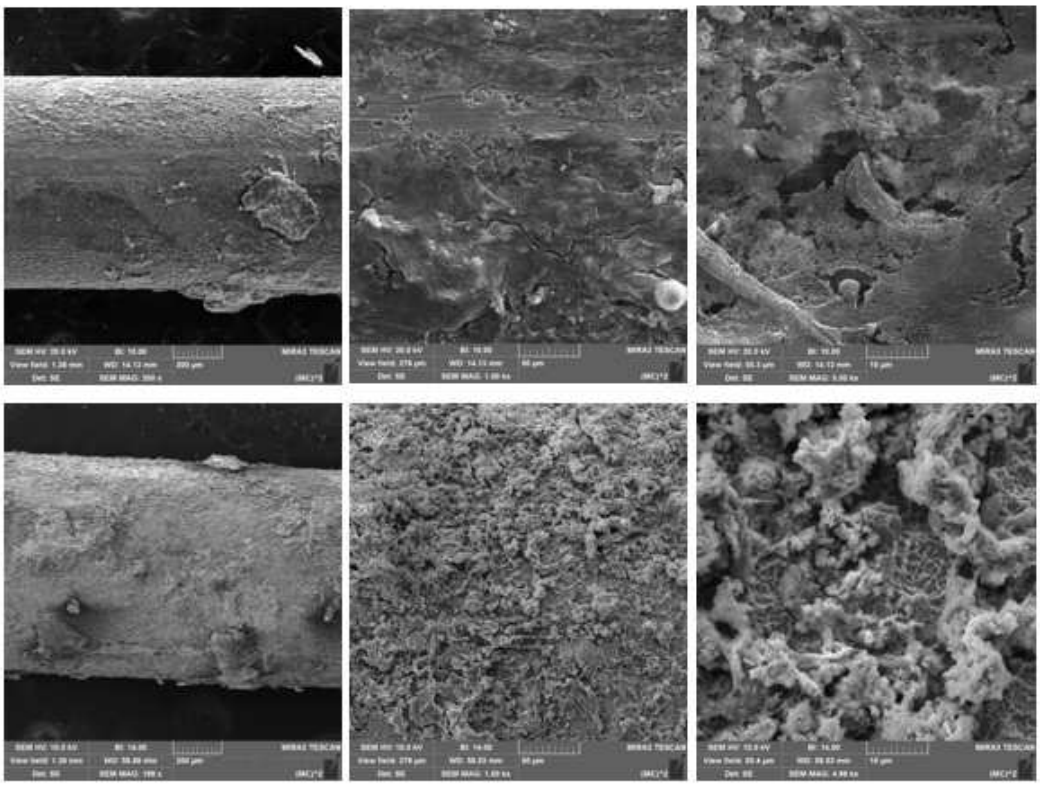

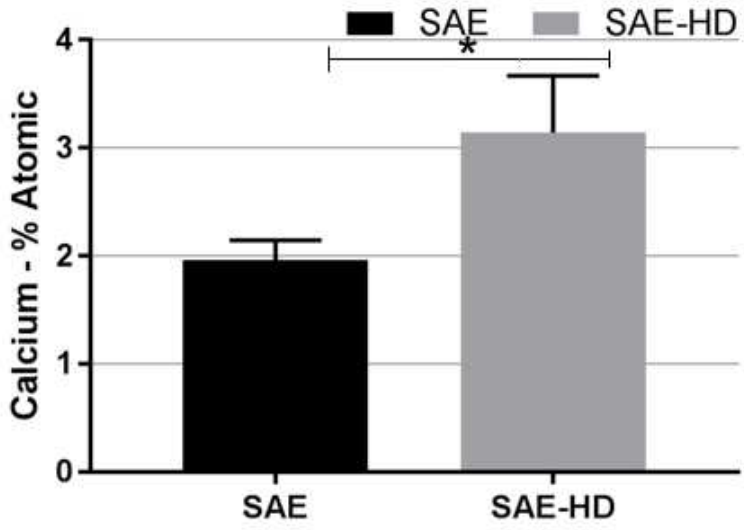

Figure 3. A. Bone volume fraction (%) of the two different surface at day 14 and 21 obtained from analysis of the Micro-CT. The results are expressed as the mean±SD; * represents a signifcant diference (P<0.05). **B.** Neoformed bone volume (mm) of the two different surface at day 14 and 21 obtained from analysis of the Micro-CT. The results are expressed as the mean±SD; * represents a signifcant diference (P<0.05).

Figure 4

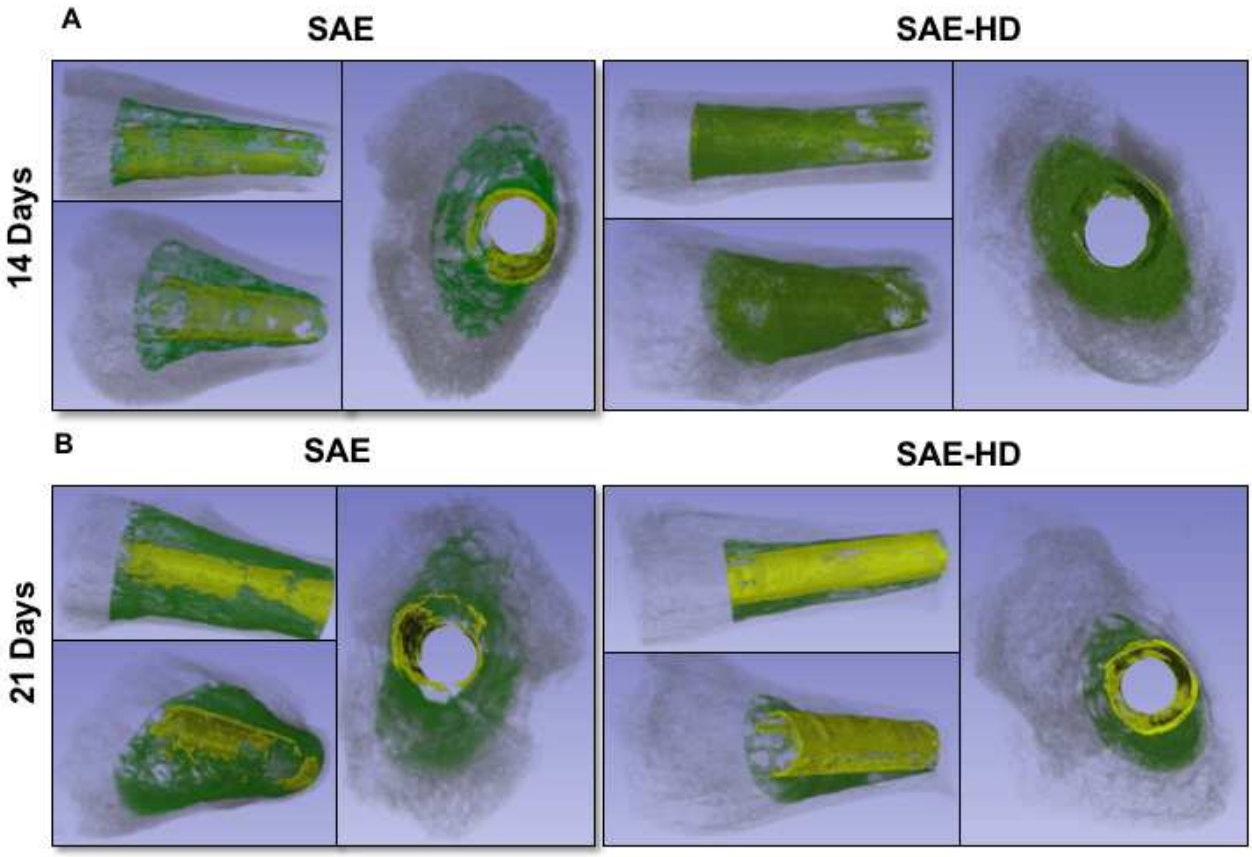

Figure 4. Representative Micro-CT 3D Reconstruction of the area of new bone tissue present and the entire trabecular bone around implant are represented by yellow and green, respectively. Hydrophilic SAE-HD and etched SAE implants at 14 days (upper row) and 21 days (lower row) post-implantation.

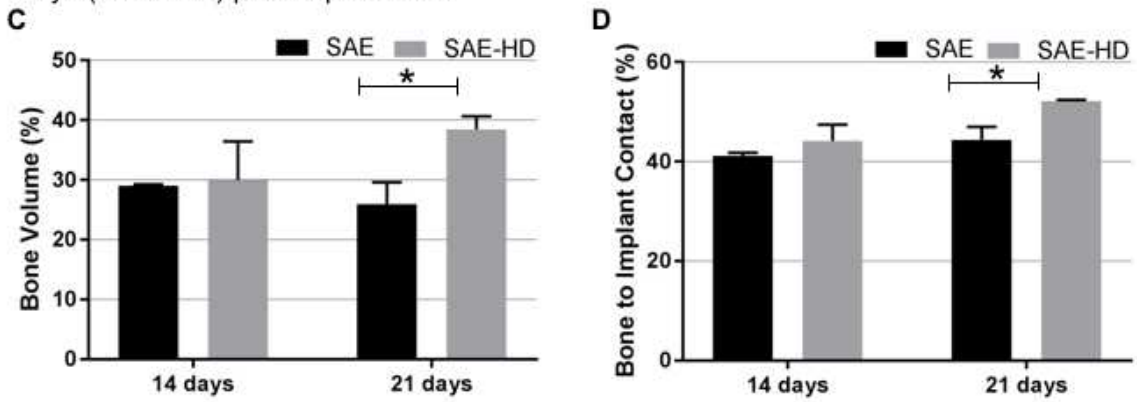

Figure 4.C and D. Bone volume fraction (BV) and bone-implant contact (BIC), respectively, of micro-computed tomography analyses calculated as a percentage of the total implant perimeter. Results are shown as mean percentages ± standard deviation in the SAE and SAE-HD groups, 14 and 21 days post-implantation. Statistically significant differences are indicated by an asterisk, BV: * p=0.0081; BIC: * p=0.0042.

Figure 5

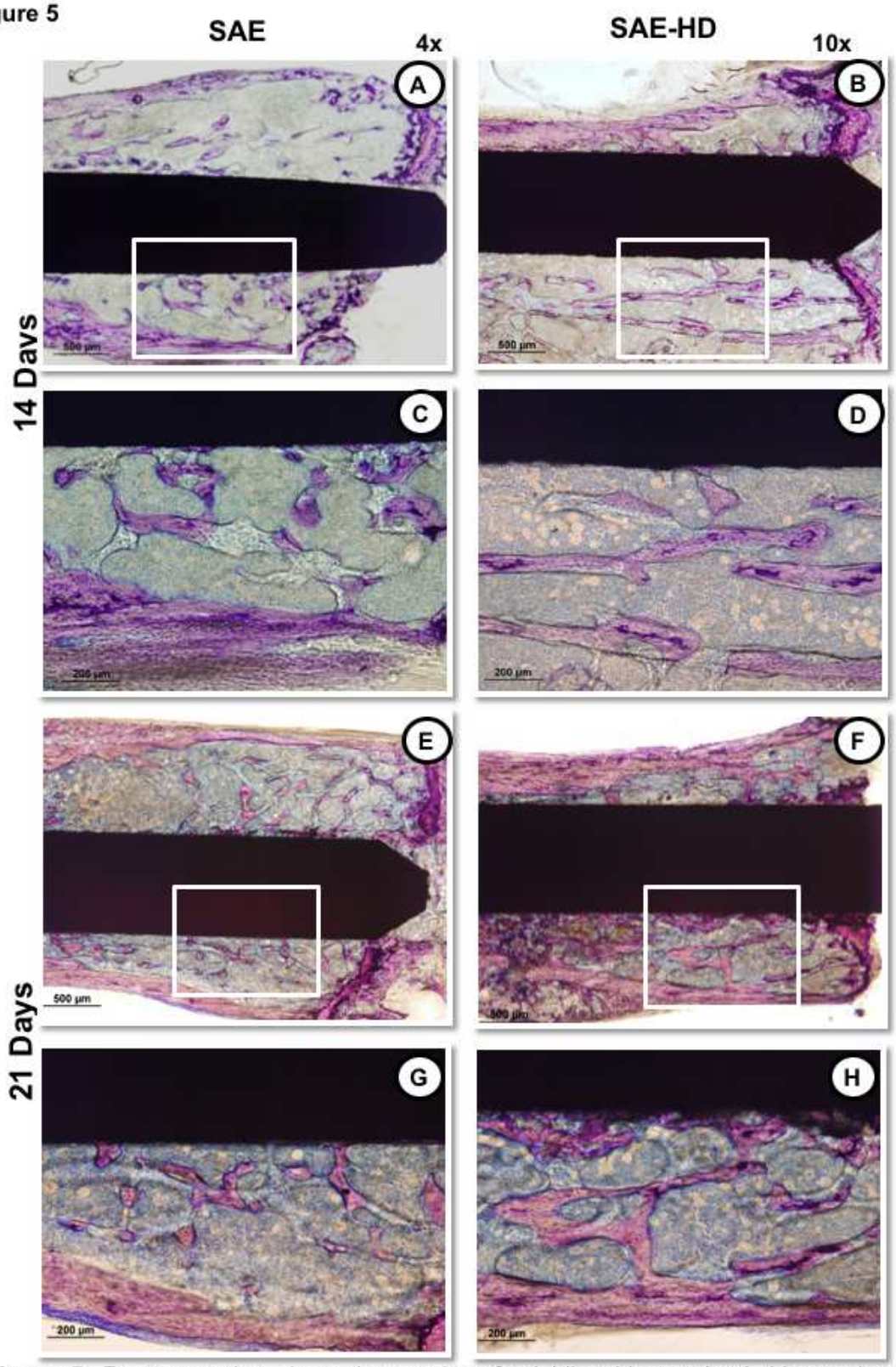

Figure 5. Representative photomicrographs of toluidine blue stained thin sections (original magnification at x4 and x10) in bright field of Hydrophilic SAE-HD (a, c, e & g) and etched SAE implants (b, d, f & h) at 14 days (upper two rows) and 21 days (lower two rows). Observe the presence of new bone formation and the contact between bone and both implant groups. In Group SAE-HD at 21 days, see the presence of trabecular bone more compact and in a greater number than Group SAE at the same period, suggesting the acceleration of osseointegration.

A

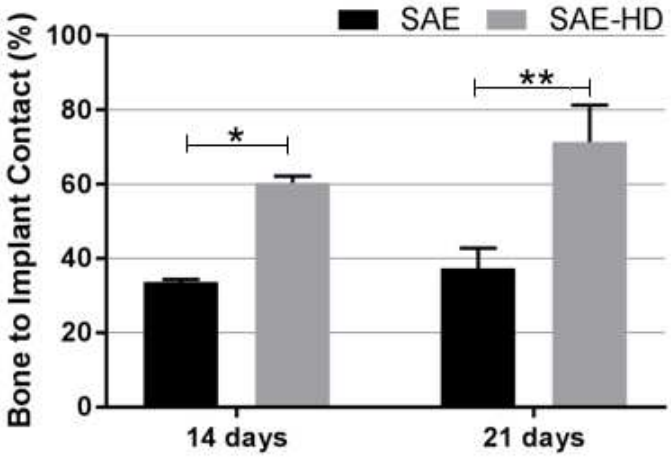

Figure 6. Histomorphometric analysis of bone-to-implant contact (BIC), calculated as a percentage of the total implant perimeter. Results are shown as mean percentages ± standard deviation in the SAE and SAE-HD groups, 14 and 21 days post-implantation. Statistically significant differences are indicated by an asterisk, * p=0.0009; ** p=0.0002.

Figure 7

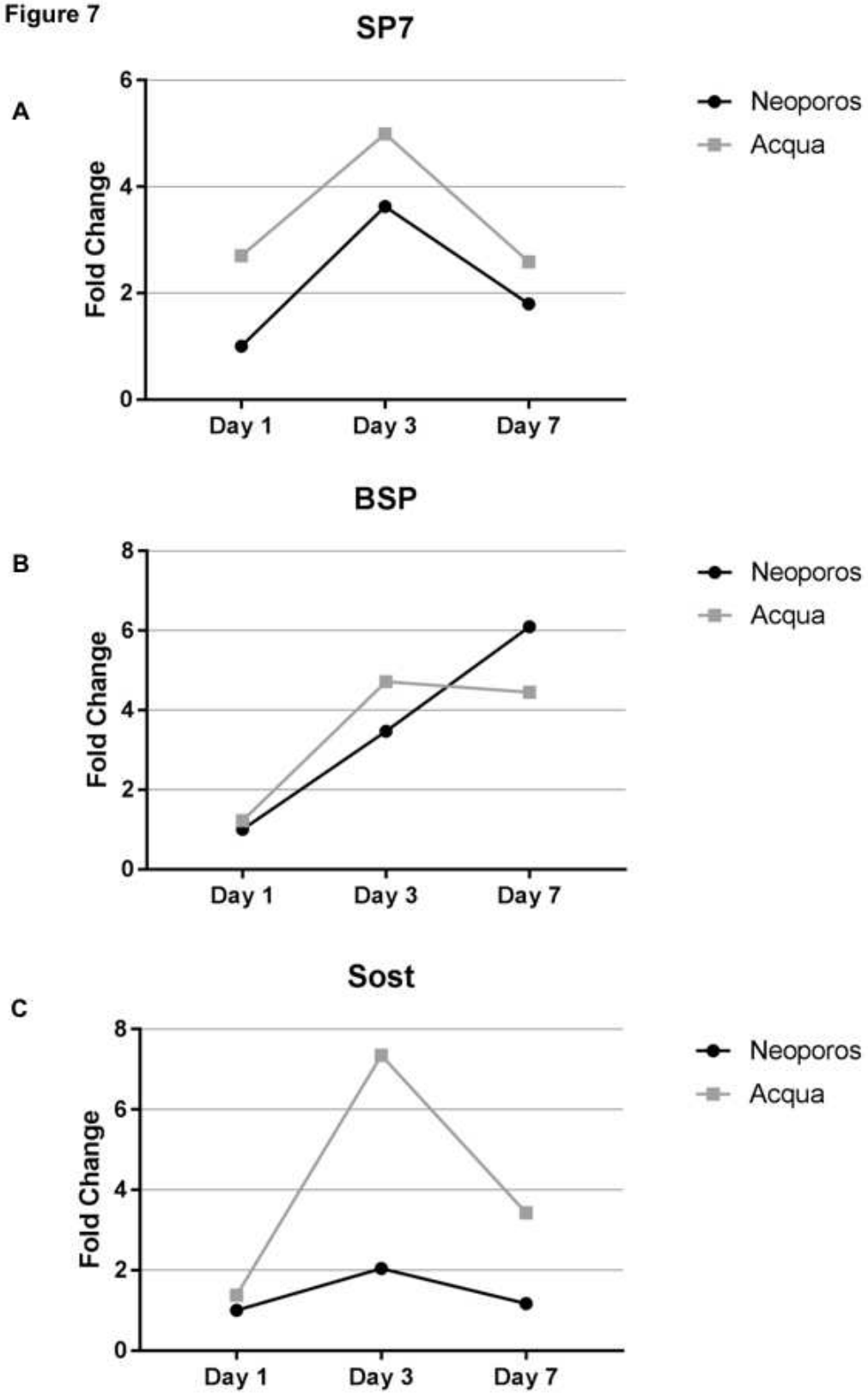

Figure 7 (A,B,C). Relative gene expression level for early and late osteogenic genes. Total RNA was isolated on days 1,3 and 7 days. The results are shown in the relative expression for the Neoporos Day 1 (Method 2-ΔΔCt) n = 5 control group. (A) SP7; (B) BSP; (C) Sost.* Statistical differences p(P<0.05) when compared to the SAE day 1.

Figure 8

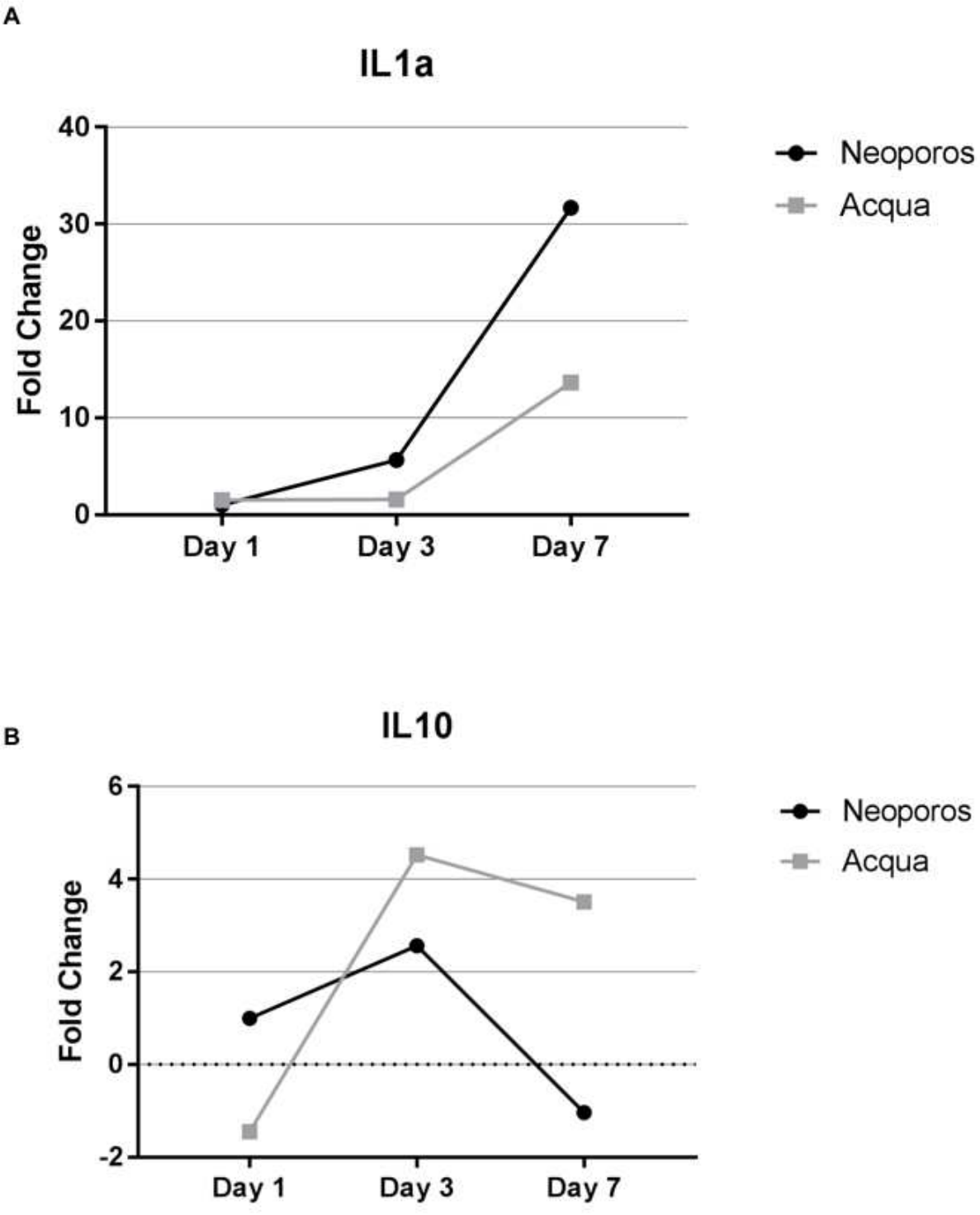

Figure 8 (A,B). Relative gene expression level for pro-inflammatory and anti-inflammatory genes. Total RNA was isolated on days 1,3 and 7 days. The results are shown in the relative expression for the SAE Day 1 (Method 2-ΔΔCt) n = 5 control group. (A) IL1a; (B) IL10.* Statistical differences $p < 0.05$ when compared to the SAE day 1.

CAPÍTULOS

3.2 CAPÍTULO 2

Artigo a ser enviado ao periódico Journal of Dental Research

Gene expression of hydrophilic titanium surface in osteoporotic model

Jessica Afonso Ferreira[1,2], DDS, MSc.

Rafael Amorim Siqueira[3], DDS, MSc.

Fábio Antônio Piola Rizzante[4], DDS, MSc., PhD.

Daniela Baccelli Silveira Mendonça[1], DDS, MSc., PhD.

Denildo de Magalhães[2], DDS, PhD.

Renata Cimoes[5], DDS, MSc., PhD.

Gustavo Mendonça[1*], DDS, MSc., PhD.

[1]Department of Biological and Material Sciences, Division of Prosthodontics, University of Michigan School of Dentistry, Ann Arbor, MI, USA.

[2]Department of Periodontology and Implant Dentistry, School of Dentistry, Federal University of Uberlandia, Uberlândia, MG, Brazil.

[3] Department of Periodontics and Oral Medicine, School of Dentistry, University of Michigan, Ann Arbor, MI, USA.

[4]Department of Comprehensive Care, School of Dental Medicine, Case Western Reserve University, Cleveland, OH, USA.

[5]Department of Prosthesis and Maxillofacial Surgery, Federal University of Pernambuco, Recife, Pernambuco, Brazil.

***Correspondence to: Gustavo Mendonça**

Clinical Associate Professor

Biologic & Materials Sciences, Division of Prosthodontics

1011 N University Ave, Rm 1027

Email mgustavo@umich.edu

ABSTRACT

The number of elderly patients seeking treatment with dental implants and affected by conditions that lead to more implant failures has been increasing in the recent years. The literature remains deficient in indication protocols for dental implants in patients with osteoporosis. **Purpose:** Using a mouse osteoporotic model this study aimed to determine the influence of titanium surfaces (hydrophobic and hydrophilic) on gene expression and bone formation during the osseointegration process. **Material and Methods:** Thirty, female, 3-month old mice were included in the study. Osteoporosis was induced by ovariectomy (OVX) and 7 weeks of calcium and phosphorus deficient diet in 15 mice, test group (OVX). The other 15 mice were sham operated, only had their ovaries identified and surgically exposed, and free access to regular food and water, control group (Sham). Seven weeks following the ovaries surgical procedures, 1 implant specially made (0.7 x 8 mm) of each surface was placed in each femur for both groups, in a way that each animal received 2 different implants. One implant had a hydrophobic surface (SAE) and the other one had a hydrophilic treatment surface (SAE-HD). Calcium content was measured by Energy-dispersive x-ray spectroscopy (EDS) on the surface of the implant after 7 days. Additionally, after 3 and 7 days implants were removed, and cells were collected around the implant to access gene expression profile of key osteogenic and inflammatory genes (Runx2, ALP, BSP, SOST, OCN, Il1b, Il10, TNF and NOS2) by PCR assay. Statistical analyses were performed by ANOVA and paired *t*-test with significance at $p < 0.05$. **Results:** The amount of calcium deposited on the surface due to the mineralization process was higher for SAE-HD surface compared to SAE on the intra-group analysis, after 7 days. Analysis in OVX group showed that genes involved in the bone morphogenetic protein signaling, such as ALP, BSP, SOST and OCN, were significantly activated in the hydrophilic treatment surface. **Conclusion:** Based in our results, due to the increased expression of genes related to osteogenic differentiation and significant amount of calcium content, the choice of the hydrophilic surface in situations of osteoporosis could be considered to improve osseointegration process.

Key-words: osseointegration, surface treatment, dental implant, osteoporosis.

1. INTRODUCTION

The number of elderly patients seeking treatment with dental implant has increased in recent years. At the same time, an increased number of these patients are expected to suffer from one or more of chronic metabolic diseases, like osteoporosis, which affect bone healing and can lead to more implant failures[1,2]. Osteoporosis is defined as a skeletal disorder characterized by a reduction in bone mass and microarchitectural deterioration of the bone tissue that increases the risk of fracture. Both etiology and therapy of osteoporosis (estrogens, vitamin D and bisphosphonates) may interfere the healing process of a bone wound and osseointegration[3-7].

In vitro and preclinical studies in ovariectomized animals reported that low bone density might delay the healing of femoral fractures[8], critical-sized cranial defects following grafting with alloplastic bone substitutes[9], post extraction sockets[10,11] and the osseointegration of titanium dental implants[5,7]. The modification of the titanium implant surface, e.g. by the deposition of inorganic/ organic coatings, has been tried before to improve the implant-bone response compared in osteoporotic vs. healthy conditions[12-17]. Although experimental studies have shown that osteogenic coatings are effective in enhancing BIC, their clinical relevance requires further investigations[18]. In the other hand, hydrophilic surface has been used to reduce the healing time and also to promote a safer osseointegration in patients with systemic diseases, like diabetes and osteoporosis.

The mechanisms that control osseointegration are only partially understood and in situations of poor bone quality and impaired healing it requires more studies. Activation and de-activation of key regulatory genes is crucial to the process of differentiation of osteoprogenitor cells and it is also affected by cell-surface interactions[19]. Based on the previous evidence, it is logical to assume that osteoporotic bone has a different potential for bone regeneration, and therefore, a modification of the current treatment protocols and materials for dental implant therapy may be necessary when treating osteoporotic patients. The present study aims to determine the pattern of bone formation on two different titanium implant surfaces (hydrophobic and hydrophilic) in an osteoporotic model defining surface

influence in osseointegration.

2. MATERIAL AND METHODS

2.1. Experimental animal model

The research protocol was approved by The Institutional Animal Use & Care Committee (IACUC), University of Michigan. This research was conducted in compliance with University guidelines, State and Federal regulations and the standards of the “Guide for the Care and Use of Laboratory Animals.

Seventy-two, female, osterix-cherry (OSX-cherry) reporter mice, 3 months old, weighting between 23 and 30 g, with no injuries or congenital defects were used in the study. Before each surgical session, the animals were anaesthetized via inhalation isoflurane (Piramal, Pennsylvania, USA) (4-5%) for induction and maintained with isoflurane (1-3%) as necessary to maintain surgical anesthesia using a calibrated vaporizer. Level of anesthesia was monitored by toe pinch and eye reflex. Local anesthesia with Lidocaine was administered. Ophthalmic ointment was used to protect the eyes of the animals during surgery. Alcohol-soaked gauze sponges was alternated with iodophor-soaked gauze sponges or Q-tips to disinfect the surgical site. The wound area was shaved gently. The surgical field was cleaned with povidone iodine solution (3 alternating scrubs of povidone iodine/chlorhexidine with normal saline/alcohol/sterile water). %). For post-operative pain management Carprofen (Piramal, Pennsylvania, USA) was provided preemptively, for 48 hours postoperatively and then as needed. Signs of complications related to surgery was monitored daily. Surgery records were kept and also included the records regarding the frequency of using of post-operative analgesics.

2.2. Induction of osteoporosis-like conditions

Experimental osteoporosis was induced by ovariectomy (OVX) and calcium and phosphorus deficient diet using a method previously described[10]. In all the animals, the ovaries were identified and displayed bilaterally, following a longitudinal incision in the region below the last rib and next to the kidney. In 15

OVX animals (OVX group), hemostasis was secured by suturing the top of the fallopian tube (Vicryl 4-0; Ethicon, Somerville, NJ, USA) and the ovaries together with the oviduct and a small portion of the uterus were excised. The remaining 15 control mice were sham operated (Sham group) by only having their ovaries identified and surgically exposed, and free access to regular food and water. The muscles and skin were then sutured in layers in all animals (Vicryl 4-0; Ethicon) and wound clips were used to final closure.

The ovariectomized mice were fed with calcium and phosphorus deficient diet (0.1% calcium and phosphorus 0.77%; Lab diet, St. Louis, MO, USA) and water ad libitum throughout the whole experimental period. At 7 weeks following the ovaries surgical procedure, one implant with hydrophobic and one with hydrophilic surface were installed in each animal of both OVX and Sham group.

2.3. Experimental implant surgical procedure

The same experimental surgical procedure was performed in all animals (both test and control group). The distal femur was accessed through a medial parapatellar arthrotomy. After locating the femoral intercondylar notch, the femoral intramedullary canal was manually reamed with a sequence from a 30 gauge needle to a 21 gauge needle (Fig 1). A cpTi grade IV wire (diameter 0.7 mm and length 8mm) prepared with a hydrophobic and hydrophilic surface were placed (Neodent, Curitiba, Brazil) (Fig 2a, b). Each femur received a different surface. The soft tissues were repositioned, and the overlying muscles and periosteum were sutured with simple interrupted sutures (Vicryl 5-0; Ethicon). The animals were euthanized with an overdose of carbon dioxide at different times after the experimental surgical procedure. For PCR assay, tissues were collected at 3 and 7 days following surgery. For scanning electron microscopy (SEM) samples were collected at 7 days.

2.4. Scanning Electron Microscopy and EDS Analysis

The chemical analysis by energy-dispersive x-ray spectroscopy (EDS), is an analysis performed by an equipment coupled to the scanning electron microscope,

which allows a qualitative and semiquantitative evaluation from the emission of characteristic x-rays. This tool allows the indication of the presence of chemical elements in several types of sample components, whether mineral or organic.

Five animals for each group were euthanized at 7 days for this analysis. The implants were examined by high-resolution scanning electron microscopy (Hitachi S-4700, Tokyo, Japan) and atomic force microscopy (Nanoscope IIIA, Digital Instruments, Santa Barbara, CA). The calcium content was measured at the surface of each implant in 6 different areas. The results are expressed by the mean value of the 6 measurements randomly taken.

2.5. Nano CT Analysis

Animals were euthanized at 21 and 28 days post-implant (n=5 animals). Muscle tissue and epiphyses were removed, and bone/implant was fixed with 4% paraformaldehyde (Z Fix). Non-destructive analysis of the neoformed bone at the implant interface was performed using the Nano CT (Nanotom-S, phoenix|x-ray, GE; Germany), located at the University of Michigan, Orthopedic Research Laboratories, Ann Arbor, MI. The samples were scanned with pieces rotation in 360º, using monochromatic x-rays with 80 kV, 320µA., 120ms exposure time, 3 frame averaging, 6 µm voxel size. The software NRecon and Dataviewer were used for the image reconstruction. A region of interest (ROI) around the implant were defined, where the bone volume (BV) could be calculated. Outcome variables were BV, being the percentage of bone that is present in the region around the implant and bone-implant contact (BIC), being the area percentage of the total implant surface that is covered by bone.

2.6. RNA isolation, complementary DNA (cDNA) synthesis, and quantitative real time PCR

Five animals for each group were euthanized at 3 and 7 days. Immediately thereafter, the femurs sites were isolated, and the implant site was exposed using sterile technique and the entire femurs were harvested. Implants were explanted by fracture of the femurs. For evaluation of genes expression in cells adherent to explanted endosseous implant surfaces, the implants were rinsed in cold PBS

(Gibco—Life Technologies, Grand Island, NY, USA) immediately following retrieval and then placed into 1mL of Trizol reagent (Invitrogen Life Technologies, Carlsbad, CA, USA). Total RNA was isolated from the lysates using manufacturer's protocol and processed as to evaluate RUNX2, OSX, ALP, OCN, Sost, BSP, IL1b, IL10, NOS2 and TNF. (SABioscience, Frederick, MD) expression.

Total RNA concentration was quantified using a NanoDrop 2000 spectrophotometer (NanoDrop products, Wilmington, DE, USA). The extracted RNA was reverse transcribed following a conventional protocol to synthesize complementary DNA (cDNA). cDNA synthesis was performed using 500ng of RNA following the manufacturer's recommendations (SuperScript VILO cDNA Synthesis, Invitrogen). The cDNA was used as a template in real-time PCR.

All primers for quantitative PCR (qPCR) were obtained from Qiagen (Qiagen Sciences, Germantown, MD, USA). The reactions were prepared using SYBR Green Real-Time PCR Master Mix (Qiagen) according to the manufacturer's protocol. Thermal cycling was performed on an ABI 7900HT (Applied Biosystems, Foster City, CA, USA) according to recommended protocol. The relative mRNA expression was determined by $2^{-\Delta\Delta Ct}$ method and expressed as a relative expression level. Sham SAE 3 days implants in healthy conditions were set as control; 1.0-fold expression level. Osteoblastic cell differentiation was monitored by the expression of runt-related transcription factor-2 (Runx-2), osteoblast-specific transcription factor osterix (OSX), alkaline phosphatase (ALP), osteocalcin (OC), bone sialoprotein (BSP), and sclerostin (Sost) and inflammatory related genes (IL1b, IL10, TNF and NOS2). Glyceraldehyde-3-phosphate dehydrogenase (GAPDH) was used as house-keeping gene control.

3. Statistical Analysis

Real-time PCR data were analyzed using the $2^{-\Delta\Delta Ct}$ method and results reported as fold change[20,21]. T-test was performed for comparison gene expression levels compared to GAPDH at day 3 and 7 days. The results of calcium content were subjected to analysis of variance (ANOVA). For all tests, results were

considered significant if $p \leq 0.05$. The control group is characterized by Sham SAE 3 days implants in healthy conditions.

4. RESULTS

4.1. Surface Analysis by EDS

The amount of calcium deposited on the surface due to the mineralization process was higher for hydrophilic surface compared to the hydrophobic surface in the same group in both time points. Calcium content was also significantly different between the OVX and control group (Fig 3).

4.2. Nano CT Analysis

3D reconstruction of the new bone formation around the implant in different surfaces are shown in Figure 2. Specifically, the area of new bone tissue present and the entire trabecular bone around implant are represented by yellow and green, respectively. At 21and 28 days (Fig. 4A) it is evident the greater presence of BV and BIC. Additionally, SAE-HD showed a wide increase of BV (P=0.0120) and BIC (P=0.0026) compared with SAE surface at 21 days post-implantation (Fig. 4B), however, in 28 days after implantation, it was not possible to identify substantial differences between SAE healthy and osteoporotic conditions (Fig. 4A). Another interesting finding was that the SAE-HD surface considerably improved BIC results comparing SHAM and OVX (***** P< 0.0132).

4.3. Osteogenic Differentiation and Gene Expression

For the early stages of osteogenic expression there was a 2- and 2.5-fold increase for ALP gene at 3 and 7 days, respectively, in the OVX SAE-HD group compared to control (Sham SAE 3 days = 1). A great increase of OSX expression was observed at 7 days for both Sham SAE and Sham SAE-HD, 3.6-fold and 2.4-fold, respectively. There was no difference between OVX SAE and OVX SAE-HD

compared to the control group, with 7 days for OSX expression. At 7 days there was a 2.4-fold increase for Runx2 in the OVX SAE-HD group compared to the control group, and the difference was slightly higher when compared to the OVX SAE group with 7 days (Fig 4).

The analysis of the late stages osteogenic markers showed a 2-fold increase for Sost at 3 days for the Sham SAE-HD group compared to the control group, while in all other time points and groups Sost expression was constant and slightly smaller than the control group. OCN presented higher levels of expression at 7 days for all groups compared to the control group. Comparing the osteoporotic like conditions groups, there was a 1.2- and 1.6-fold increase for the OVX SAE and OVX SAE-HD, respectively. There was an increase of 2.8-fold for BSP levels at 7 days for the Sham groups and a 1.5- and 2.4-fold SAE-HD (Fig 5).

When evaluating the inflammatory markers, higher values of IL1b were expressed for the OVX groups compared to the Sham groups at the same time points. IL10 had a 1.7-fold increase for the Sham SAE-HD at 3 days while all other groups and time points showed reduced IL10 expression compared to the control group. TNF expression had a 0.5-fold reduction for the OVX SAE-HD at 7 days and NOS2 was constant showing slightly smaller values compared to the control group, despite the 2-fold increase at 3 days for the Sham SAE-HD (Fig 6).

5. DISCUSSION

In the present study, two different implant titanium surfaces were used in an approach to enhance bone-implant integration for osteoporotic and control groups. Interestingly, by EDS and quantitative real time PCR, a significant increase in Calcium and expression of genes related to osteogenesis was observed in association with the use of a hydrophilic surface compared to the hydrophobic surface, in both osteoporotic and healthy conditions. Clinically bone-implant osseointegration is achieved by direct bone formation and bonding at the implant surface, which is clinically relevant for high success rates of dental implants[22].

An increase in the differentiation of mesenquimal stem cells and their production of osteogenic and angiogenic microenvironment has been shown to

occur with increased roughness and wettability of a Ti surface[23]. Histological studies have also demonstrated optimization of the osseointegration process with the increase in the wettability of implants with a titanium surface in comparison to implants submitted to sandblasting and acid etching[24,25]. In the present study, experimental osteoporosis was induced in adult female mice by bilateral OVX and the administration of a calcium-deficient diet. Successful induction of osteoporosis in rodents have been reported in previous studies where a similar experimental model was used for the evaluation of bone healing in osteoporotic conditions[26]. In this study, it has been proved that the amount of Calcium is greater around the hydrophilic surface and it is known from previous studies that Ca^{2+} and $(PO_4)^{3-}$ ions stimulate cellular and intracellular signaling and favor osteoblastic cell activity in the process of bone formation[27,28]. Further, Ca^{2+} ions might increase osteogenic cell chemotaxis and migration toward the coated surface via the activation of calcium signaling. Ca^{2+} and $(PO_4)^{3-}$ ions also play an essential role in bone mineralization and can facilitate the precipitation of bone-like apatite on the implant surface[29,30].

Several preclinical studies reported lower osseointegration rates in ovariectomized animals when different types of root form implants were inserted in extraoral locations[5,7]. In addition, clinical reports suggested that implant osseointegration may be delayed and biomaterial failures may be increased in osteoporotic patients[5,6]. Real-time PCR analysis at 3 and 7 days revealed different effects of the experimental surfaces on gene expression levels involved in periimplant osteogenesis. The hydrophilic surface often presented superior levels of osteogenic markers and these present findings might play an important role in the osseointegration process due to the fact that biological response requires early recruitment, attachment, and proliferation of bone cells to the implant surface, which can be improved by surface modifications[27]. The over expression of the osteo-related genes could be attributed to the hydrophilic surface used in this study. ALP is described as a marker of primary osteogenic activity and calcification regulator[31] and their presence proves the osteoblasts differentiation[32]. Runx2 and OSX are transcription factors essential for osteoblast differentiation and their increase are an indicative of osteoinductive and osteoblast differentiation[33]. Consistently, in our gene expression studies, hydrophilic treatment surface showed increase levels of

gene expression related to bone formation.

Activation of the immune system controls the initial response to the implanted material and affects its long-term survival and integration. Continued immune system activation can lead to chronic inflammation that can result in the breakdown of healthy tissue surrounding the implant[34]. However, a lack of inflammatory response will leave the debris from implantation to remain and affect the integration of the material and generation of new tissue[35]. The ability of a material surface to control the reaction of these cells will influence the host's initial response to the device, and ultimately decide the integration of the material[36].

Greater levels of pro-inflammatory (IL1b and TNFα) factors were present in comparison to anti-inflammatory factors. TNFα was higher in the OVX group after 3 days for the hydrophilic surface and reduced after 7 days. Before osteoblasts can arrive and begin forming bone, the inflammatory response must be resolved, and the lower levels of TNFα after 7 days could indicate that the initial inflammatory response is about to resolve, and more anti-inflammatory responses are activated at this time, which may corroborate with the findings of the present study, since levels of anti-inflammatory cytokines (IL10) remained constant or slightly increased after 7 days.

Successful implant integration relies on a balance of classically activated (M1) macrophages to clear the wound site coupled with anti-inflammatory (M2) activated macrophages to promote wound healing and regeneration. A consistently high M1 response will recruit additional immune cells to the site, and this chronic inflammation can lead to fibrous encapsulation instead of successful tissue integration[36]. The control ratio of pro-inflammatory and anti-inflammatory response revealed in this study at the host-biomaterial interface will allow damaged tissue to be removed without a prolonged immune response that can lead to the creation of foreign body giant cells and inhibition of healing and integration.

6. CONCLUSION

Based in our results, due to the increased expression of genes related to osteogenic differentiation and significant amount of calcium content, the choice of the

hydrophilic surface in situations of osteoporosis could be considered to improve osseointegration process.

CONFLICT OF INTEREST

No conflict of interest.

ACKNOWLEDGMENTS

The authors are grateful to Neodent for full donation of the implants used in this study and CAPES by scholarship concession for PhD.

REFERENCES

1. Gaetti-Jardim EC, Santiago-Junior JF, Goiato MC, Pellizer EP, Magro-Filho O, Jardim Junior EG. Dental implants in patients with osteoporosis: a clinical reality? J Craniofac Surg. 2011;22(3):1111-3.

2. Giro G, Chambrone L, Goldstein A, Rodrigues JA, Zenóbio E, Feres M, Figueiredo LC, Cassoni A, Shibli JÁ. Impact of osteoporosis in dental implants: A systematic review. World J Orthop. 2015;18:6(2):311–315.

3. NIH consensus development panel on osteoporosis prevention, diagnosis, and therapy, March 7–29, 2000: Highlights of the conference. South Med J. 2001;94: 569–573.

4. Sanfilippo F, Bianchi AE. Osteoporosis: the effect on maxillary bone resorption and therapeutic possibilities by means of implant prostheses: a literature review and clinical considerations. Int J Periodont Rest Dent 2003;23:447e57.

5. Fini M, Giavaresi G, Greggi T, et al. Biological assessment of the bone-screw interface after insertion of uncoated and hydroxyapatite-coated pedicular screws in the osteopenic sheep. J Biomed Mater Res Part A. 2004;66:176–183.

6. Erdogan O, Shafer DM, Taxel P, Freilich MA. A review of the association between osteoporosis and alveolar ridge augmentation. Oral Surg Oral Med Oral Pathol Oral Radiol Endod. 2007;104(6):738.e1-13.

7. Tsolaki IN, Madianos PN, Vrotsos JA. Outcomes of dental implants in osteoporotic patients. A literature review. Journal of Prosthodontics 2009;18:309–323.

8. Namkung-Matthai, H, Appleyard R, Jansen J, Hao Lin J, Maastricht S, Swain M, Mason RS, Murrell GA, Diwan AD, Diamond T. Osteoporosis influences the early period of fracture healing in a rat osteoporotic model. Bone 2001;28: 80–86.

9. Kim SY, Kim SG, Lim SC, Bae CS. Effects on bone formation in ovariectomized rats after implantation of tooth ash and plaster of Paris mixture. J Oral Maxillofac Surg 2004;62: 852–857.

10. Shimizu M, Furuyam R, Kawawam T, Sasaki T.Bone wound healing after maxillary molar extraction in ovariectomized aged rats: quantitative backscattered electron image analysis. Anatomical Records 2000;259: 76–85.

11. Teofilo JM, Brentegani LG, Lamano-Carvalho TL. Bone healing in osteoporotic female rats following intra-alveolar grafting of bioactive glass. Archives of Oral Biology 2004;49: 755–762.

12. Gao Y, Zou S, Liu X, Bao C, Hu J. The effect of surface immobilized bisphosphonates on the fixation of hydroxyapatite-coated titanium implants in ovariectomized rats. Biomaterials 2009;30:1790e6.

13. Vidigal Jr GM, Groisman M, Gregorio LH, Soares Gde A. Osseointegration of titanium alloy and HA-coated implants in healthy and ovariectomized animals: a histomorphometric study. Clin Oral Impl Res 2009;20:1272e7.

14. Mardas N, Schwarz F, Petrie A, Hakimi A-R, Donos N. The effect of SLActive surface in guided bone formation in osteoporotic-like conditions. Clin Oral Impl Res 22, 2011; 406–415.

15. Qi M, Hu J, Li J, et al. Effect of zoledronate acid treatment on osseointegration and fixation of implants in autologous iliac bone grafts in ovariectomized rabbits. Bone. 2012;50: 119–127.

16. Yang G, Song L, Guo C, Zhao S, Liu L, He F. Bone Responses to Simvastatin-Loaded Porous Implant Surfaces in an Ovariectomized Model. Int J Oral Maxillofac Implants 2012;27:369–374.

17. Alghamdi HS,Bosco R, van den Beucken JJJP, Walboomers XF, Jansenet JA. Osteogenicity of titanium implants coated with calcium phosphate or collagen type-I in osteoporotic rats. Biomaterials 2013;34:3747-3757.

18. Ghanem A, Kellesarian SV, Abduljabbar T, Al-Hamoudi N, Vohra F, Javed F. Role of Osteogenic Coatings on Implant Surfaces in Promoting Bone-To-Implant Contact in Experimental Osteoporosis: A Systematic Review and Meta-Analysis. Implant Dent 2017;26:770–777.

19. Jiang P, Liang J, Song R, Zhang Y, Ren L, Zhang L,, Tang P. Effect of Octacalcium-Phosphate-Modified Micro/NanostructuredTitania Surfaces on Osteoblast Response. ACS Appl Mater Interfaces 2015, 7, 14384−14396.

20. Yuan JS, Reed A, Chen F, Stewart CN Jr. Statistical analysisof real-time PCR data. BMC Bioinformatics 2006;7:85.

21. Wescott DC, Pinkerton MN, Gaffey BJ, Beggs KT, Milne TJ,Meikle MC. Osteogenic gene expression by human periodontalligament cells under cyclic tension. J Dent Res 2007;86:1212–1216.

22. Puelo D, Nanci A. Understanding and controlling the bone implant interface. Biomaterials 1999;20:2311e21.

23. Wennerberg A, Albrektsson T. Effects of titanium surface topography on bone integration: a systematic review. Clin Oral Impl Res 2009;20(Suppl 4):172–84.

24. Lang NP, Salvi GE, Huynh-Ba G, Ivanovski S, Donos N, Bosshardt DD. Early osseointegration to hydrophilic and hydrophobic implant surfaces in humans. Clin Oral Impl Res 2011;22:349-356.

25. Saroretto SC, Alves AT, Resende RF, Calasans-Maia J, Granjeiro JM, Calasans-Maia MD. Early osseointegration driven by the surface chemistry and wettability of dental implants. J Appl Oral Sci 2015;23(3):279-287.

26. Mardas N, Busetti J, de Figueiredo JAP, Mezzomo LA, Scarparo RK, Donos N. Guided bone regeneration in osteoporotic conditions following treatment with zoledronic acid. Clin Oral Impl Res 28, 2017, 362–371.

27. Chai YC, Carlier A, Bolander J, Roberts SJ, Geris L, Schrooten J, et al. Current views on calcium phosphate osteogenicity and the translation into effective bone regeneration strategies. Acta Biomater 2012;8:3876e87.

28. Barradas A, Fernandes HAM, Groen N, Chai YC, Schrooten J, van de Peppel J, et al. A calcium-induced signaling cascade leading to osteogenic differentiation of human bone marrow-derived mesenchymal stromal cells. Biomaterials 2012;33:3205e15.

29. Cochran DL, Schenk RK, Lussi A, Higginbottom FL, Buser D. Bone response to unloaded and loaded titanium implants with a sandblasted and acid-etched surface: a histometric study in the canine mandible. JBiomed Mater Res 1998;40:1-11.

30. Kokubo T, Takadama H. How useful is SBF in predicting in vivo bone bioactivity? Biomaterials 2006;27:2907e15.

31. Peng F, Yu X, Wei M. In vitro cell performance on hydroxyapatite particles/poly (L- lactic acid) nanofibrous scaffolds with an excellent particle along nanofiber orientation. Acta Biomater 2011;7:2585-2592.

32. Gardin C, Ferroni L, Bressan E, et al. Adult stem cells properties in terms of commitment, aging and biological safety of grit-blasted and acid-etched ti dental implants surfaces. Int J Mol Cell Med2014;3:225-236

33. Mendonca DB, Miguez PA, Mendonca G, Yamauchi M, Aragao FJ, Cooper LF. Titanium surface topography affects collagen biosynthesis of adherent cells. Bone 2011;49:463-472.

34. Mavrogenis AF, Dimitriou R, Parvizi J, Babis GC. Biology of implant osseointegration. J Musculoskelet Neuronal Interac 2009;9:61–71

35. Bosshardt DD, Salvi GE, Huynh-Ba G, Ivanovski S, Donos N, Lang NP. The role of bone debris in early healing adjacent to hydrophilic and hydrophobic implant surfaces in man. Clin Oral Impl Res 2011;22:357–64.

36. Hotchkiss KM, Reddy GB, Hyzy SL, Schwartz Z, Boyan BD, Navarretea RO. Titanium Surface Characteristics, Including Topography and Wettability, Alter Macrophage Activation. Acta Biomater. 2016 Feb; 31: 425–434.

FIGURES AND LEGEND

Figure 1

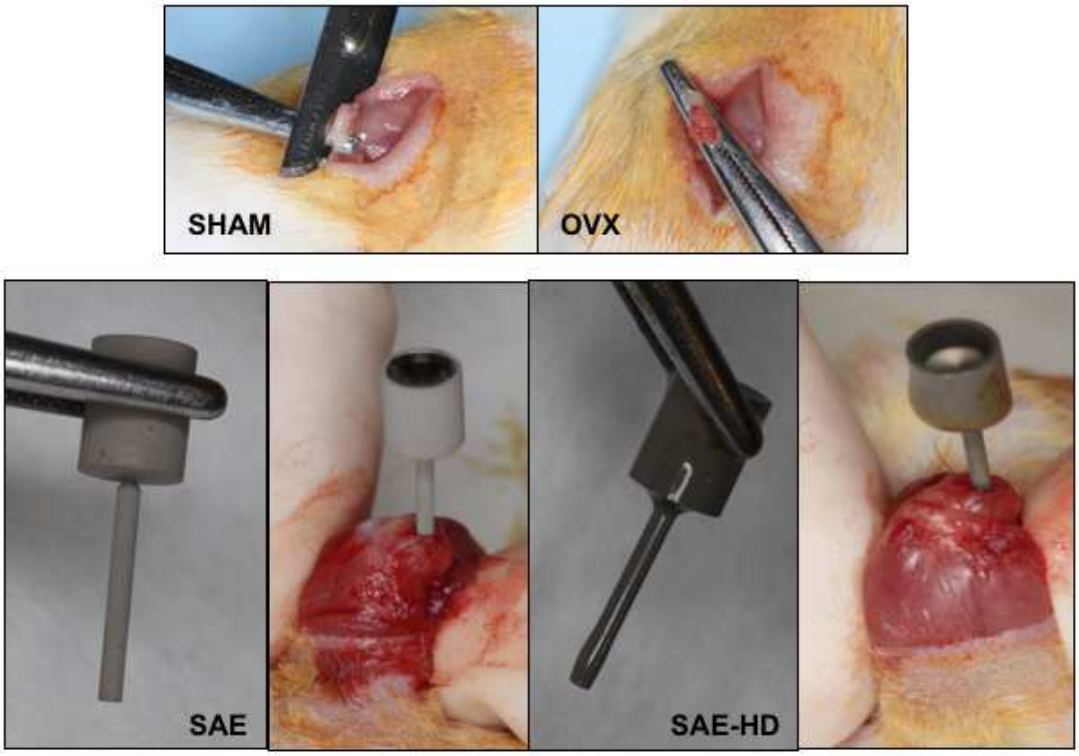

Figure 1.Upper Representative images of false ovariectomy (SHAM) and ovariectomy (OVX) in mice for osteoporosis induction. **Figure 1. Lower** One pair of cpTi grade IV wire (diameter 0.7 mm and length 8mm) prepared with a hydrophobic (SAE) (left) and hydrophilic (SAE-HD) (right) surface was placed in each femur.

Figure 2

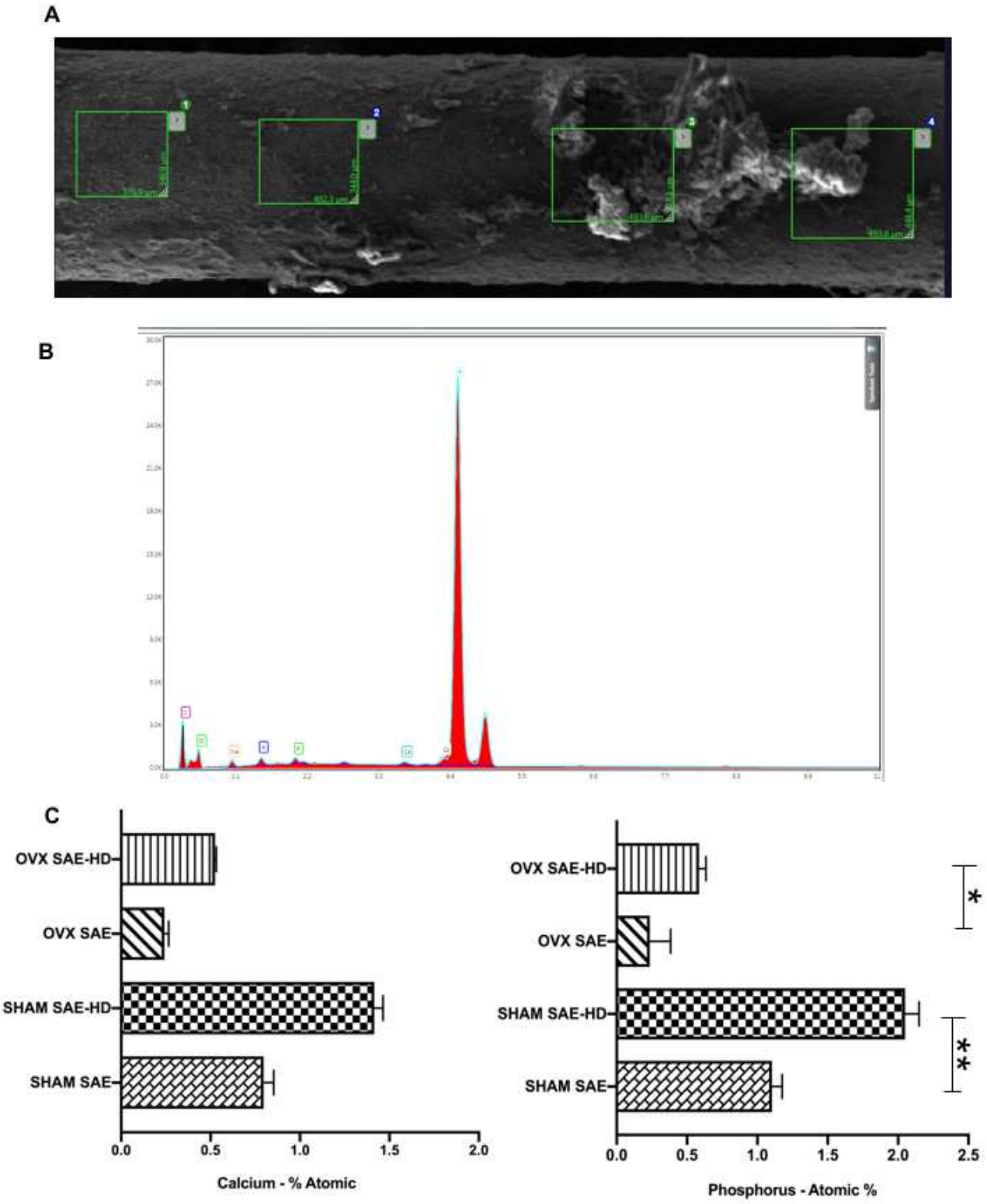

Figure 2.A and B Scanning electron microscopy and Energy Dispersive X-Ray spectrum representative of selected area on the implants surface 7 days post–implantation. **Figure 2.C** Calcium and Phosphorus % Atomic content measured by EDS on the surface of the implant (n=4 and 6 measurements/sample). The results are expressed as the mean±SD; * represents a signifcant diference (P<0.05)

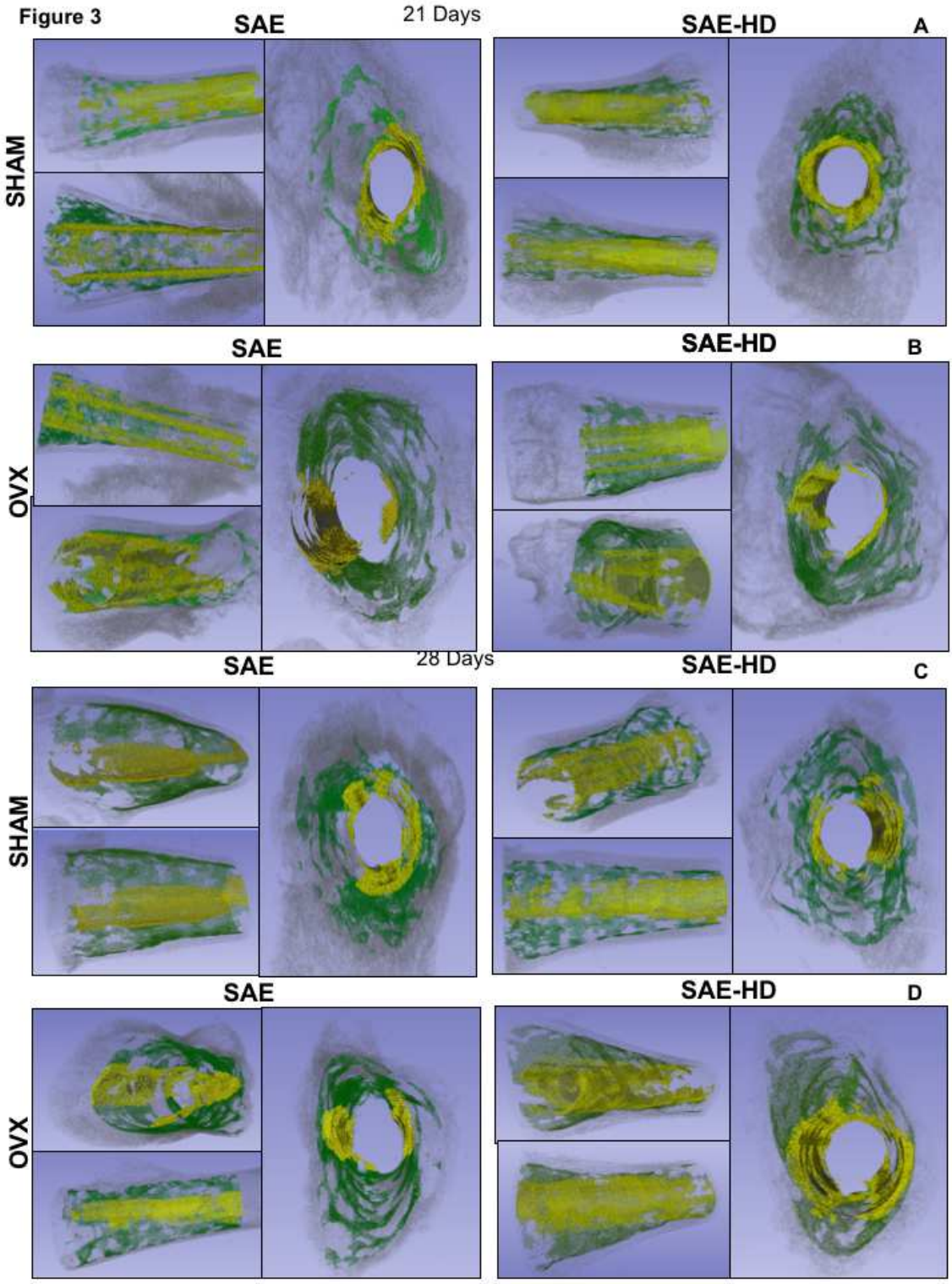

Figure 3. Representative Micro-CT 3D Reconstruction of new bone tissue present and the entire trabecular bone around implant are represented by yellow and green, respectively. Hydrophilic SAE-HD and etched SAE implants at 21 days (A and B) and 28 days (C and D) post-implantation.

A

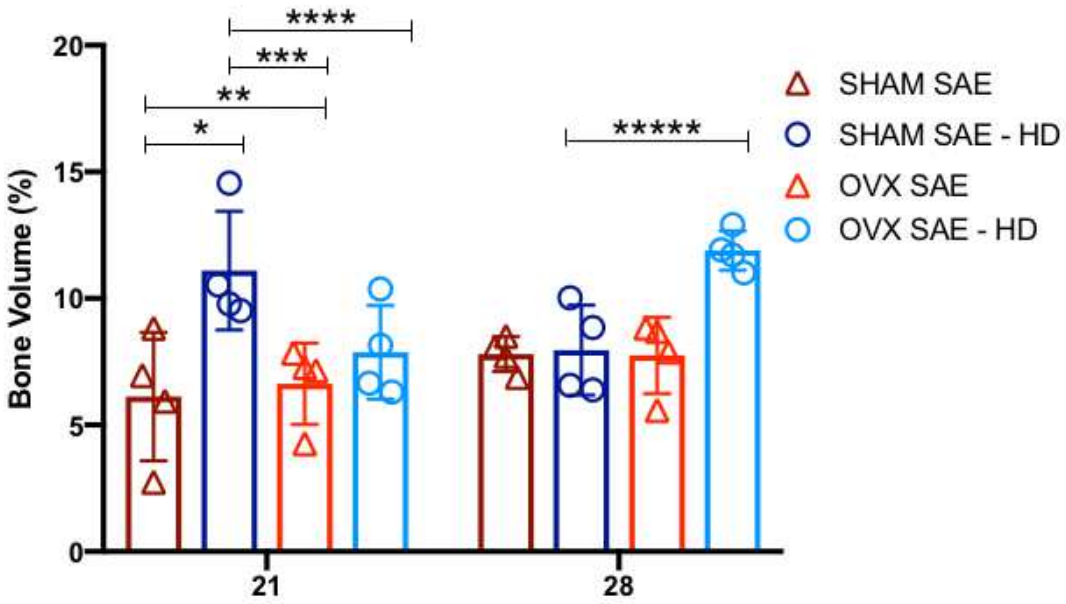

Figure 4.A Bone volume fraction (BV) of micro-computed tomography analyses calculated as a percentage of the total implant perimeter. Results are shown as mean percentages ± standard deviation in the SAE and SAE-HD groups, 21 and 28 days post-implantation. Statistically significant differences are indicated by an asterisk - 21 days :* p< 0.0001, ** p= 0.0120, ***p< 0.0001, **** p< 0.0001; 28 days: ***** p< 0.0001.

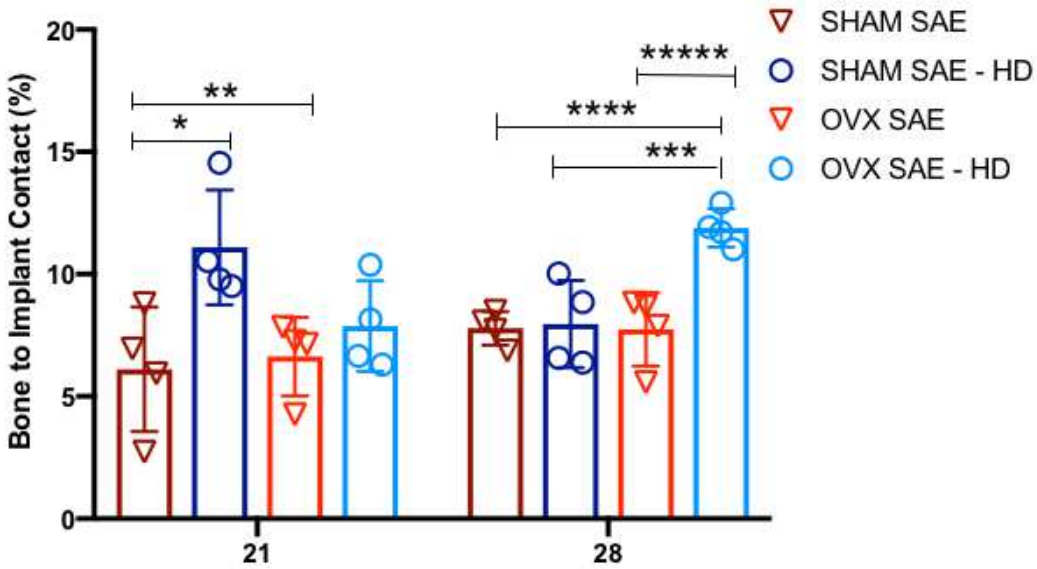

Figure 4.B Bone-implant contact (BIC) of micro-computed tomography analyses calculated as a percentage of the total implant perimeter. Results are shown as mean percentages ± standard deviation in the SAE and SAE-HD groups, 21 and 28 days post-implantation. Statistically significant differences are indicated by an asterisk - 21 days: * p=0.0026; BIC: ** p=0.0071; 28 days: p***< 0.0143, **** p< 0.0196, ***** p< 0.0132.

Figure 5

A

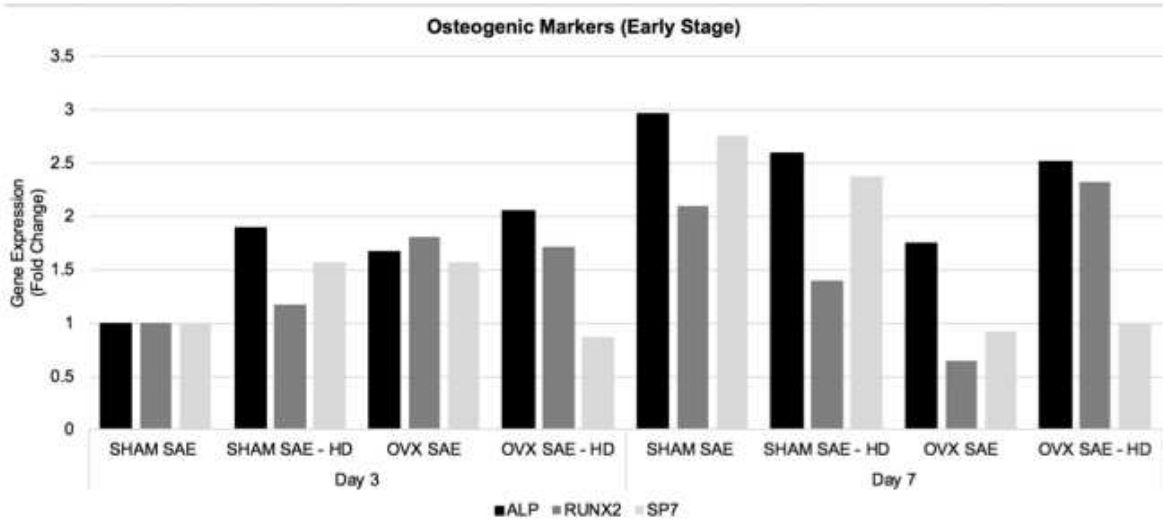

Figure 5.A Relative gene expression level for early osteogenic genes. Total RNA was isolated on days 3 and 7 days. The results are shown in the relative expression for the SAE Day 1 (Method 2-ΔΔCt) n = 5 control group. Statistical differences P<0.05).

B

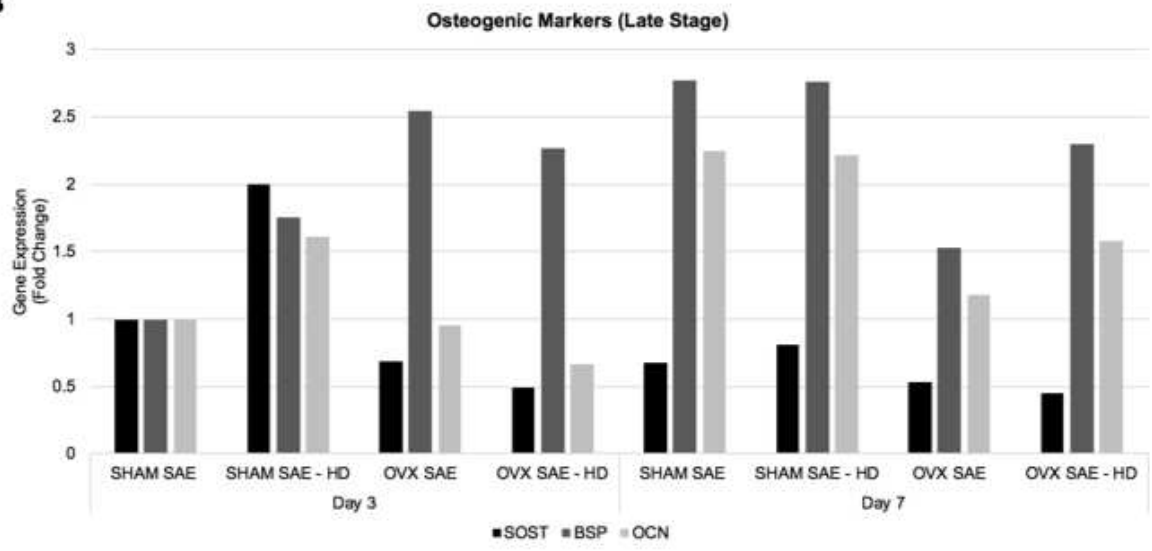

Figure 5.B Relative gene expression level for late osteogenic genes. Total RNA was isolated on days 3 and 7 days. The results are shown in the relative expression for the SAE Day 1 (Method 2-ΔΔCt) n = 5 control group. Statistical differences P <0.05).

C

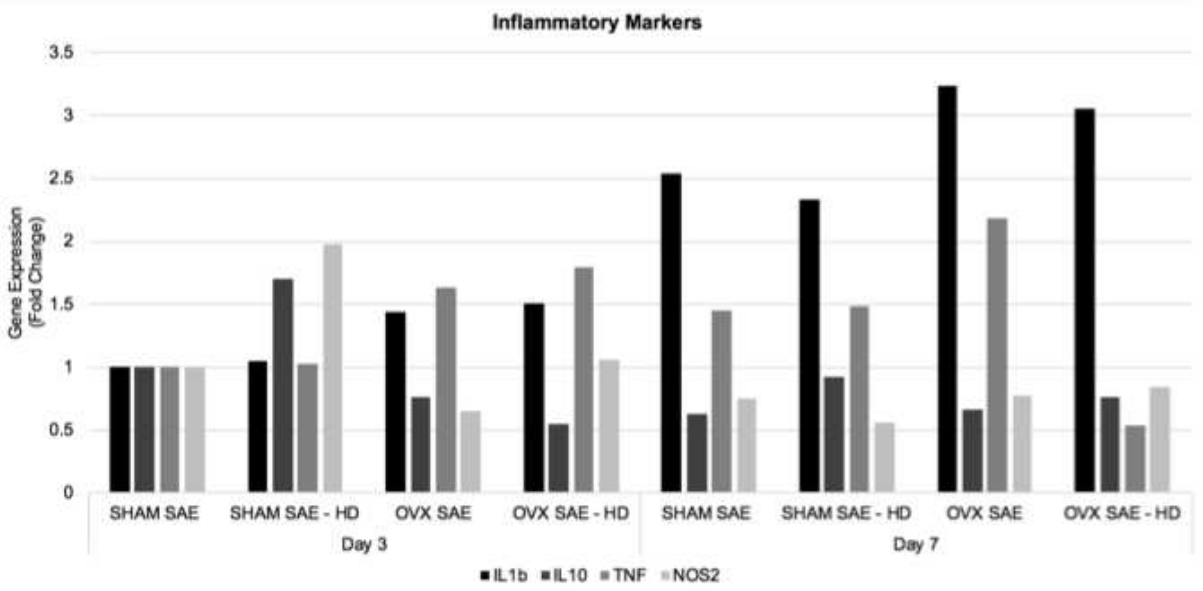

Figure 5.C. Relative gene expression level for pro-inflammatory and anti-inflammatory genes. Total RNA was isolated on days 3 and 7 days. The results are shown in the relative expression for the SAE Day 3 (Method 2-ΔΔCt) n = 5 control group. Statistical differences $p < 0.05$ when compared to the SAE day 1.

CAPÍTULOS

3.3. CAPÍTULO 3

Artigo a ser enviado ao periódico Plos One

Hypoacetylation of acetyl-histone H3 (H3K9ac) as marker of bone modulation in titanium implants with nanoscale surface

Jessica Afonso Ferreira[1,2], MSc.
Liana Preto Webber[3], MSc., PhD.
Lais Morandini Carvalho[4], MSc., PhD.
Daniela Baccelli Silveira Mendonça[1], MSc., PhD.,
Denildo de Magalhães[2], PhD.
Cristiane H. Squarize[3,5], MSc., PhD.
Rogerio Moraes de Castilho[3,5], MSc., PhD.
Gustavo Mendonça[1*], MSc., PhD.

[1]Department of Biological and Material Sciences, Division of Prosthodontics, University of Michigan, School of Dentistry, Ann Arbor, MI, USA
[2]Department of Periodontology and Implant Dentistry, School of Dentistry, Federal University of Uberlandia, Uberlândia, MG, Brazil
[3]Laboratory of Epithelial Biology, Department of Periodontics and Oral Medicine, University of Michigan School of Dentistry, Ann Arbor, MI, USA
[4]Department of Biosciences and Oral Diagnosis, São Paulo State University, Institute of Science and Technology, São José dos Campos, SP, Brazil
[5]Comprehensive Cancer Center, University of Michigan Ann Arbor, MI, USA

***Correspondence to:** Gustavo Mendonça
Clinical Associate Professor
Biologic & Materials Sciences, Division of Prosthodontics
1011 N University Ave, Rm 1027
Email mgustavo@umich.edu

ABSTRACT

Implant-based treatment has been widely used in the fields of orthopedics and dentistry with high success rates. Epigenetic regulation has been found to be a key modulator of stem cells differentiation and an important factor in osteoblast differentiation related to implant topography. In this study we propose to investigate the global chromatin modifications mediate by titanium Nano surface compared to smooth surface and how pharmacological induction of histone acetylation induces MSC differentiation, especially for conditions such as osteoporosis and impaired bone healing, using an experimental mouse model.

We found that titanium implants presenting nanotopography were able to induce a strong histone acetylation response compared to a smooth titanium implant surface at days 7 and 14. Analyzing the amount of positive cells for H3K9 ac. in both surfaces and control group without any surface stimulation, nano surface showed better results at both time points. The results also show the relative expression levels in relation to the smooth day 1 as baseline group for gene (SP7) had high expression on nano surface and represents the expression pattern of osteogenic early genes (OSX). Bsp and ALP also increased compared with the control. We further observed that platting fresh collected MSC from ovariectomized (OVX) mice present reduced ALP activity and compromised ability to undergo osteogenic differentiation of cells to osteoblasts.

Our findings suggest that Ti implants presenting nanotopography are capable of inducing global chromatin modifications in bone marrow cells as demonstrated by the accumulation of H3K9. The clinical importance of research efforts to identify and validate novel epigenetic modifications associated with osteoporosis cannot be underestimated. In these studies, nanoscale surface and Vorinostat, mediated by histone, can play a key role in MSC differentiation, especially in osteoporosis conditions.

Key words: epigenetics; histone modifications; dental implants; osteoporosis; titanium surface; gene expression; histone H3.

INTRODUCTION

Implant-based treatment has been widely used in the fields of orthopedics and dentistry with high success rates. The survival rate of dental implants over a 10-year note has been reported to be higher than 90% in totally edentulous jaws (Lekholm U et al., 1999), although dental implants do fail in some patients. There are some patient conditions that may affect the osseointegration process and resulted the implant loss as osteoporosis. Bone regeneration can be a challenge in compromised bone conditions as are frequently present in elderly patients. Osteoporosis is defined as a skeletal disease, characterized by a low density of bone tissues (Temmerman A et al., 2018). Although osteoporosis is not considered as a risk factor for dental implant failure (Giro G et al., 2015; de Medeiros F et al., 2018), initial implant stability can be influenced by both local and skeletal bone densities. (Merheb J et al., 2016; Aro HT et al., 2012).

Experimental studies manly with Mesenchymal Stem Cells (MSC) provide evidence that bone formation could be promoted by implant surface modifications, dependent on the alterations of surface topography and roughness (Palmquist A et al., 2010) although the biological process is not well understood. Cellular differentiation is influenced by changes in cell shape (Mosser DM et al., 2008) thus implicating a role for different topographies in affecting osseointegration. Nanotopography can contribute to the mimicry of natural cellular environments which promote rapid bone accrual (Stanford CM et al., 2010). Nanoscale topography has direct and indirect effects on cell behavior. It mimics the cell environment favoring protein adsorption, modulating cell/surface interactions and cell fate (Masuda T et al., 1997; Stanford CM et al., 2010).

Epigenetic regulation has been found to be a key modulator of stem cells differentiation and an important factor in osteoblast differentiation related to implant topography (Ezhkova E et al. 2009; Lian JB et al. 2006). The histone acetylation plays a role in DNA transcription even without modification of DNA sequence. Histones are proteins that assist in the packaging of DNA and may undergo post-translational modifications, such as acetylation or deacetylation. These modifications result in gene transcription through the uncoiling of

chromatin or gene silencing through compacting DNA (Warburton G et al., 2005; Cooper LF et al., 1998, Dike LE et al., 1999; Mendonca G, et al., 2009). In general, histone modifications modulate a diverse array of biological processes, including gene regulation, DNA repair, differentiation via chromosome remodeling (Mendonca G, et al., 2009).

Post-translational modification of histones dynamically influences gene expression independent of alterations to the DNA sequence. These mechanisms are often mediated by histone linkers, proteins associated with the recruitment of DNA-binding proteins, HDAC I and II interacting proteins and transcriptional activators, coactivators or corepressors. Therefore, histones are molecular markers of epigenetic changes (Yang J et al., 2014). Early evidence suggested that histones and their modifiers are involved in sophisticated processes that modulate normal tissues and tumor behavior along with cellular phenotype. Despite all the research being conducted in this field there is still a lack of knowledge on how nanoscale topography signals are integrated inside the cell and control cell fate.

The important roles between implant and cell interactions need to be investigated. One important mechanism of action related to osseointegration could be related to post-translational modification of histones. In this study we propose to investigate the global chromatin modifications mediate by titanium Nano surface and how pharmacological induction of histone acetylation induces MSC differentiation, especially for conditions such as osteoporosis and impaired bone healing.

MATERIALS AND METHODS

Induction of osteoporosis-like conditions

Experimental osteoporosis was induced by ovariectomy (OVX) and calcium and phosphorus deficient diet using a method previously described (Shimizu M. 2010) In all the animals, the ovaries were identified and displayed bilaterally, following a longitudinal incision in the region below the last rib and next to the kidney. In 5 animals (OVX group), hemostasis was secured by suturing the top of the fallopian tube (Vicryl 4-0; Ethicon, Somerville, NJ, USA) and the ovaries

together with the oviduct and a small portion of the uterus were excised. Another 5 control mice were sham operated (Sham group) by only having their ovaries identified and surgically exposed, and free access to regular food and water. The muscles and skin were then sutured in layers in all animals (Vicryl 4-0; Ethicon) and wound clips were used to final closure.

The ovariectomized mice were fed with calcium and phosphorus deficient diet (0.1% calcium and phosphorus 0.77%; Lab diet, St. Louis, MO, USA) and water ad libitum throughout the whole experimental period.

Cell Culture

Bone marrow cells collected by flushing from osteoporotic and healthy CD-1 mice (Charles River Laboratories) femurs and tibiae were used to characterize the osteoblast colony forming units and ALP activity. The project was approved by the University of Michigan Committee on Use and Care of Animals (UCUCA, protocol PRO00006203). The femurs and tibiae were dissected away from attached muscle and connective tissue, the ends of the bones were removed, and marrow was extruded with a 21-gauge needle into the shaft of the bone and flushed with 1mL of PBS pH 7.4 (1X) (Phospharte Buffered Saline) with red blood cells were collected in 1.5-mL tubes and centrifuged at 10,000 rpm for 3 minutes, the supernatant was removed, and cell pellets were suspended in the fresh medium MesenCult™ Medium (Mouse) (Stem Cell Technologies, Vancouver, BC, Canada) described earlier. Cells were treated every another day with 1μM Vorinostat (Cayman Chemical Company Ann Arbor, MI, USA) for 14 days.

ALP Activity

ALP activity was measured at 14 days with bone marrow cells collected by flushing from OVX and SHAM CD-1 mice (Charles River Laboratories) femurs and tibiae. Five hundred thousand bone marrow cells were plated on the 24-well plate in triplicate. The wells with cells were washed two times with cold PBS (Gibco) and lysed using 1% Triton X-100 (Sigma). The lysate was collected into 1.5-mL tubes and centrifuged at 14,000 rpm for 10 minutes. Only the supernatant collected was used for analysis. To measure ALP activity, 40uL of each sample

was loaded into a 96-well plate, 200uL of p-nitrophenol phosphate (p-NPP) (BluePhos Microwell Phosphatase Substrate System, KPL) was added, and a spectrophotometer (PowerWave HT, BioTek Instruments) was used for the measurement at 630 nm. ALP activity (units/mL) was normalized with protein measurements for each sample. Measurements of total proteins were performed using a protein assay kit (Precision Red Advanced Protein Assay, Cytoskeleton) and read in the spectrophotometer (PowerWave HT, BioTek Instruments).

Analysis of Colony Forming Units–Osteoblasts

The staining analysis was performed at 14 days with bone marrow cells collected by flushing from OVX and SHAM CD-1 mice (Charles River Laboratories) femurs and tibiae. Two million bone marrow cells were plated on the 24-well plate in triplicate. The non- adherent cell population was removed after 3 days, and fresh media was added to the cultures. For colony forming units–osteoblasts (CFU-Ob) assay, each well was rinsed two times with cold PBS, cells were fixed with 4% paraformaldehyde at room temperature for 10 minutes, and samples were rinsed two times with PBS. The staining solution (Alkaline Phosphatase Staining Kit, Sigma) was prepared according to the manufacturer's instructions. One milliliter of the prepared staining solution was added per well. The plates were covered with aluminum foil and stored in the dark for approximately 1 hour. The staining solution was removed by aspiration, and wells were washed with ddH2O. Pictures were taken using a digital camera (Canon A640 PowerShot).

Samples preparation

The project was submitted and approved by the Ethics Committee on Animal Research at the University of Michigan - UMICH in Ann Arbor - Michigan (UCUCA - protocol PRO00006203).

Commercially pure grade IV titanium implants (8mm x 0.9mm corresponding to the long axis of the femur of the mice) were prepared. The implants nanoscale group were grit-blasted with 100-µm aluminum oxide particles and sonicated three times in water MilliQ for 15 min each to clean, followed by immersion in 1:1

v/v % solution of 30% H_2O_2 and 2N H_2SO_4 (Fisher Scientific, Pittsburgh, PA) overnight. Following treatment with H_2SO_4/H_2O_2 solution, the implants were sonicated three times in ultrapure deionized (DI) water (resistivity 1/4 8.2MO, pH1/4 6.82; Millipore), and then three times in 70% ethanol, before drying under the hood (samples prepared in this manner are hereafter referred to as ‘‘Nano’’). Smooth samples didn't receive any surface treatment, just the cleaning sequence and sterilization in UV light on hood.

Experimental implant surgical procedure

Fifteen mice *Osx*-mCherry were used for implants surgery. These were developed by Dr. Peter Maye (University of Connecticut). The *Osx*-mcherry mouse express fluorescent protein concomitant with gene osterix expression. Each animal presented the average weight of 30 grams and the implants were placed in the femur through of a medial parapatellar arthrotomy. The mice were anesthetized by isoflurane inhalation 2% and medicated before the surgery with Carprofen® base (5mg / kg) subcutaneously. The surgery region was submitted tricotomy and iodine asepsis and the incision was made in the medial parapatelar region with displacement and remoteness of the muscle complex. After the location of the femoral intercondylar fossa, the intramedullary canal was perforated manually and gradually with 25, 23 and 20 gauge needles. For standardization, rights femurs received smooth implants and lefts nano implants. The tissues were repositioned through 5-0 Vicryl® wire suture (Ethicon, San Angelo, TX, USA). The animals were medicated with Carprofen® (5mg / kg) subcutaneously 24 hours post-surgery. Ration and water were given ad libitum after the mice recovery. The mice were kept in cages in groups of five, housed at 21ºC ambient temperature and maintained in a light / dark cycle of 12 / 12h. Euthanasia occurred through the inhalation of carbon dioxide.

Immunohistochemistry

Euthanasia for histological examination was performed at day 14 and 21 after surgery, with n=5 animals for each time point. Muscle tissue and epiphyses was removed, and the set bone/implant was fixed with paraformaldehyde (Z Fix)

and decalcified with EDTA for 7 days in refrigerator (4°C) and shaking all the time. Samples were sectioned into 3-µm sections and placed on silanized slides. The slides were deparaffinized in xylene and hydrated in descending grades of ethanol. Antigen retrieval was performed prior to primary antibody incubation with citrate buffer in a microwave. Tissue samples were blocked with 0.5% (v/v) Triton X-100 in PBS and 1% (w/v) bovine serum albumin (BSA), and incubated with anti-H3K9ac (C5B11 9649, Cell Signaling Danvers, MA, 1:500 overnight). Samples were washed three times with 1x PBS and incubated with biotinylated secondary antibody (Vector Laboratories, Burlingame, CA, USA) followed by incubation with diaminobenzidine tetrahydrochloride (Sigma-Aldrich, St. Louis, MO, USA) and stained with Mayer´s hematoxylin. Immunohistochemistry images were taken using a QImaging ExiAqua monochrome digital camera attached to a Nikon Eclipse 80i Microscope (Nikon, Melville, NY), visualized with QCapturePro software, and quantified with ImageJ (NIH, Bethesda, MD, USA). Ten fields were taken in each sample and nuclear brown labelling was considered positive staining. The total number of cells and positive cells were counted, and the results were expressed as the percentage of positive cells.

RNA isolation and analysis

Implants were removed from femur and placed in 1ml Trizol lysis reagent (Invitrogen, Carlsbad, CA, USA). The samples were kept frozen at -80 °C for at least 24 hours. Total RNA in the cell lysates was isolated according to the manufacturer's protocol and collected by ethanol precipitation. Total RNA concentration was quantified using a NanoDrop 2000 spectrophotometer (NanoDrop products, Wilmington, DE, USA). The extracted RNA was reverse transcribed following a conventional protocol to synthesize complementary DNA (cDNA). cDNA synthesis was performed using 500ng of RNA following the manufacturer's recommendations (SuperScript VILO cDNA Synthesis, Invitrogen). The cDNA was used as a template in real-time PCR. All primers for quantitative PCR (qPCR) were obtained from Qiagen (Qiagen Sciences, Germantown, MD, USA). The reactions were prepared using SYBR Green Real-Time PCR Master Mix (Qiagen) according to the manufacturer's protocol.

Thermal cycling was performed on an ABI 7900HT (Applied Biosystems, Foster City, CA, USA) according to recommended protocol. The relative mRNA expression was determined by 2-ΔΔCt method and reported as fold induction.

Samples of smooth group at day 1 were set as control; 1.0-fold expression level. All cDNAs were subjected to polymerase chain reaction (PCR) for Glyceraldehyde-3-phosphate dehydrogenase (GAPDH) as a test of RNA integrity and cDNA synthesis. Subsequently, equal volumes of cDNA were used to program real-time PCR reactions specific for mRNAs encoding the early osteogenic markers: *SP7*; late osteogenic marker: *Bsp*; osteoblast differentiation marker: *ALP*. The data points were analyzed at 1 and 7 days, n=5 for each time point.

Statistical analysis

Real time PCR results were shown as Fold Change by the 2-ΔΔC method, in baseline 2, with smooth day 1 being used as the control. The test-t was used as statistical test for comparison between the day 1 smooth control and the other groups. For the other tests, two-way ANOVA was used followed by the Tukey test when necessary. The software used for statistical analysis was Prism 6 (Graphpad Software INC, La Jolla, CA, USA). For all statistical analyzes, the level of significance was set at $p < 0.05$.

RESULTS

Global chromatin modifications mediate by titanium nanosurface

Nanoscale topography of titanium plays an important role on the process of osseointegration by inducing differentiation of MSC into osteoblasts. Osseointegration is dependent upon the adhesion and population of the implant surface by HC (Hematopoietic Cells) and MSC orchestrated in a manner that result in osteoid formation and its subsequent mineralization (Masuda T et al., 1997). In this study, we investigate the impact of different titanium surfaces on transcriptional activity and osteogenic potential of MSC. Histone modifications are epigenetic markers associated with gene expression. This is particularly thrust for histones H3 lysine 9 (H3K9) and H3 lysine 27 (H3K27) (Bogliotti YS,. 2012) in

which increased transcription is often associated with cellular differentiation. Here we placed titanium posts presenting either a smooth surface or a surface characterized by a nanotopography into the bone marrow of mice femur and looked into changes on histone acetylation. We found that titanium post presenting nanotopography were able to induce a strong histone acetylation response compared to titanium posts presenting a smooth surface at days 7 and 14 (Fig. 1A and 1B) (* $p<0.05$; *** $p<0.001$).

Analyzing the amount of positive cells for H3K9 ac. in both surfaces and control group without any surface stimulation, mean H3K9ac labelling was 46.5% in cases of any stimulation, 46.2% in cases of smooth surface 7 days post-implant, 60.9% in cases of nano surface 7 days post-implant, 31.21% for smooth surface 14 days post-implant and 62.2% for nano surface 14 days post-implant. Interestingly, when comparing bone marrow exposed to Ti posts with unstimulated bone marrow it becomes clear that the nanotopography nature of the posts result in increased acetylation of histone H3K9 at day 7 and 14, while histone levels from Ti posts presenting a smooth surface present no differences between the unstimulated control (Fig. 1C). Moreover, no difference between unstimulated and smooth surface at day 7 and 14 was found ($P > 0.06$) (Fig. 1B and 1C).

Independently, the levels of H3K9 are higher from nanotopography Ti posts compared with smooth surface Ti posts (Fig. 1D) (* $p<0.05$; ** $p<0.01$). Smooth surface was hypoacetylated in comparison to nano surface in both experimental periods (Anova followed by Mann-Whitney test, 7 days: $P = 0.02$ and 14 days: $P=0.0008$) (Fig. 1D and 1E). Looking into early genetic markers of MSC differentiation we decided to explore the expression levels of SP7 (Osterix), BSP, and ALP levels at days 1 and 7 post Ti implantation. The results also show the relative expression levels (fold change) in relation to the smooth day 1 as baseline group (n=5/group)(Method 2-ΔΔCt) Early gene (SP7) had high expression on nano surface and represents the expression pattern of osteogenic early genes (Osterix) also an osteoblast key transcription factor for differentiation, showed overexpression at day 1 on the nanoscale surface reaching maximum peak at day 1, presenting expression almost 3 times higher than the baseline, showing

on this day statistical differences in relation to the control group. At day 5, the smooth surface also presented the expression with values lower to the nano surface. The expression of the osteogenic late gene is represented by Bsp, showed values slightly above of the baseline for nano surface, presented 1.5-fold upregulated at day 1 for the nano surface and in the same period for smooth surface, presented 1-fold regulated. At day 5 there is an increase in this gene expression for smooth surface, showing fold change in 2 and for nano surface, Bsp did not change significantly after day 1. Alp as a marker that indicates osteoblast differentiation in osteogenesis early stage, showed 3-fold upregulated on the nanoscale surface at day 1 presented, while smooth presented only 1-fold regulated, however, similar genic expression was observed at day 5 on both surfaces, displaying 2-fold change (Fig. 1F). Overall our findings suggest that Ti posts presenting nanotopography are capable of inducing global chromatin modifications in bone marrow cells as demonstrated by the accumulation of H3K9 (Fig. 1G).

Osteoporotic mice are characterized by poor osteoblasts differentiation

The effects of osteoporosis on osseointegration have been demonstrated to be deleterious to the implant long-term success. Several authors have already demonstrated differences in bone density related to osteoporosis (Chambrone L, 2016), and that higher osteoblastic activity led to differences in bone formation rate (Kouzarides T, 2007). Here we demonstrate that two-dimensional images and three-dimensional reconstructed images of the SHAM (healthy) and osteoporotic (OVX) mice model 7 weeks post ovariectomy are characterized by the reduced trabecular bone, disorganized trabecular architecture, and expanded marrow cavities compared to the sham-operated animals (Fig. 2A). We further observed that platting fresh collected bone marrow cells from OVX mice present reduced ALP activity and compromised ability to undergo osteogenic differentiation of cells to osteoblasts (Fig. 2B).

Pharmacological induction of histone acetylation induces MSC differentiation

Histones can be post-translationally modified at the amino-terminal ends

by acetylation, methylation, phosphorylation, sumoylation, ubiquitination, and ADP-ribosylation (Kouzarides T. 2007). These modifications result in gene transcription through the uncoiling of chromatin or gene silencing through compacting DNA. Histone-mediated gene transcription is often observed during tissue differentiation. Despite all the research being conducted in this field there is still a lack of knowledge on how nanoscale topography signals are integrated in different stages of MSC differentiation and osseointegration. Here we decide to explore the potential clinical application of pharmacological manipulation of histone acetylation aiming at the activation of MSC differentiation into osteoblast. This approach holds the potential to improve implant osteointegration in subpar clinical conditions as osteoporotic bones. On this, our data show that 14 days of MSC culture under osteogenic medium supplemented with Vorinostat (HDACi), we observed an increased differentiation of MSC followed by the formation of osteoblast colonies (ALP-positive colonies) in SHAM and OVX groups compared to groups receiving only osteogenic medium (Fig. 3A). Excitingly, MSC growing in osteogenic medium containing Vorinostat presented higher count of colonies than observed in normal MSC control group growing in osteogenic medium (Fig. 3B) (*$p<0.0001$, ** $p=0.0028$).

Alkaline Phosphatase activity was also found upregulated in OVX samples receiving Vorinostat (Fig. 3B-right graphic). In fact, the accumulation of differentiated MSC upon administration of Vorinostat resulted in the rescue of the OVX MSC phenotype observed during the administration of osteogenic medium alone (* $p=0.0053$). Overall, we shown that epigenetic modifications of histone acetylation and consequently increase gene transcription result in MSC differentiation as demonstrated by colony formation and increased ALP activity (Fig. 3C).

DISCUSSION

In recent years, in vitro studies have been published showing the beneficial effects of nanostructured surfaces on osseointegration. In this study, controlled nanotopographic surface were fabricated to examine microscale-topographical effects on osteoblast behavior. Furthermore, we found that Vorinostat, mediated

by histone, plays a key role in MSC differentiation, especially in osteoporosis conditions.

Nanoscale surface on Ticp implants were produced by sandblasting with 100μm Al_2O_3 particles and treatment with immersion in 30% H_2O_2 and 2N H_2SO_4 (Mendonça et al. 2010). The mixture H_2SO_4 / H_2O_2 has been used for deoxidation and controlled reoxidation of metals and creates new amorphous titanium oxide nanostructures on implant surface (de Oliveira and Nanci, 2004). Moreover, according to Mendonça et al. (2010) treatment with the peroxide and acid mixture helps to remove the particles from the aluminum hydroxide blasting, trim edges left by blasting and results in nanoscale topography. Our data shows the effects of nanoscale topography in enhancing the differentiation of MSCs to osteoblasts (Yang J et al. 2014; Mendonca G et al., 2010; Bryington M, et al., 2014; Kato RB et al., 2014). Figure 1 is one example of the nanoscale topography effect on the increase of global histone acetylation around implants with nanotopography compared with smooth (control surfaces in our mouse model of osseointegration) (Figure 1). Our data also shows that the nanotopography is linked to increased gene expression and is indicative of faster osteoblastic differentiation. However, few studies question the nanostructures influence on cellular behavior and the exact role of the surface in the osseointegration molecular events in vivo (Thalji et al. 2013).

The effects of osteoporosis on osseointegration have been demonstrated to be deleterious for implant long-term success. Several authors have already demonstrated differences in bone density related to osteoporosis (Chambrone L et al., 2016), and that higher osteoblastic activity led to differences in bone formation rate (Sheng MH et al., 2004). Moreover, our data show a significant beneficial effects of titanium surface topography to enhance osseointegration in the osteoporotic mouse model. These results indicate a possible mechanism by translational repression or gene silencing in the MSCs differentiation into osteoblasts affected by nanoscale topography.

Due to the epigenetic capacity of histone, it has been suggested to evaluate the influence of this marker on bone differentiation in healthy and osteoporosis conditions. Thus, histone acetyltransferases (HAT), histone methyltransferases

(HMT), and histone deacetylases (HDAC) are key co-factors that modify histones and produce the epigenetic changes observed in diseases including cancer. Histone acetylation, deacetylation and methylation are the major marks associated with transcriptional activity. Histone acetylation results in chromatin decondensation, promotion of transcription, and inhibition of DNA methylation, and it is often correlated with formation of euchromatin. In contrast, histone deacetylation is the predominant epigenetic influence in transcriptional gene silencing (Warburton G et al., 2005; Cooper LF et al., 1998, Dike LE et al., 1999).

Inflammatory, early and late osteogenic genes are related to each stage of differentiation of the bone cell line, and the intensity of each marker can indicate how active is the cell, which ideally could determine the ability of these cells to form bone at implant surface (Meirelles, 2010), so we evaluated different genes involved in osseointegration. *SP7 (OSX*) is a very important gene involved in the differentiation and function of osteoblasts, because is an important transcription factor that is essential in the osteoblasts differentiation into functional osteoblasts (Baek et al. 2009; Tang et al. 2011). Our results showed that on nano surface *SP7* was overexpressed and higher than smooth surface, indicating that nano surface is better to induce the differentiation of mMSCs into pre osteoblasts. There is a consensus among the studies that evaluate surface with alterations in their topography at micro/nano level, in which they positively influence the expression of *OSX*, considering these gene as key osteoinductive transcription factors (Guo et al. 2007; Mendonça et al. 2010, Thalji and Cooper. 2014).

The potential of the surface to promote osseointegration is dependent on ability to induce differentiation of pluripotent mesenchymal stem cells along osteoblast lineage and to stimulate matrix secretion by osteoblasts. This is orchestrated by the aforementioned transcription factors (*RUNX2, OSX* and *SATB2)* that regulate the expression of various bone genes (Cooper, 1998) such as *ALP and BSP* (Harada et al. 1999; Webster et al.2000; Harada and Rodan, 2003, Tang et al. 2011). ALP is one of the early proteins that regulates bone mineralization and tests that evaluate alkaline phosphatase activity are considered a primary parameter indicative of cell differentiation in osteoblasts (Bryington et al. 2014). This gene showed overexpression only on nano surface

at day 1, however, both surfaces showed similar results at day 7. *BSP* (bone sialoprotein) is the largest structural protein in the bone matrix and fully differentiated osteoblasts express this gene, being the first to be detected in differentiated osteoblasts forming bone (Tang et al. 2011). The results allowed us to affirm that the nanoscale surface participates more effectively in the osseointegration process, inducing faster bone mineralization than the smooth surface. Once implanted, surgical implants adsorb proteins and simultaneously incite an inflammatory foreign body response that begins with an acute response and develops as a chronic fibrotic response representing the first step in tissue repair (Anderson et al. 2008; Ma et al. 2014). Collectively, our gene expression results suggest that these three genes alone would allow us to conclude that the nanoscale surface is more active in the initial processes of osteogenesis acting more effectively in the mineralization of the bone matrix.

CONCLUSION

Within the limitation of this study, it was concluded that nanotopography surfaces affected MSC differentiation to osteoblasts. Our findings also suggest that Ti implants presenting nanotopography are capable of inducing global chromatin modifications in bone marrow cells as demonstrated by the accumulation of H3K9. The clinical importance of research efforts to identify and validate novel epigenetic modifications associated with osteoporosis cannot be underestimated. In these studies, nanoscale surface and Vorinostat, mediated by histone, can play a key role in MSC differentiation, especially in osteoporosis conditions, due to good osteoconductive properties and possibility to improve the biological events that occur at the bone / implant interface, it may also help control and understand the osseointegration process.

CONFLICT OF INTEREST

No conflict of interest.

ACKNOWLEDGMENTS

CAPES by scholarship concession for PhD.

REFERENCES

1. Lekholm U., Gunne J., Henry P., Higuchi K., Lindén U., Bergstrom C., van Steenberghe D. Survival of the Brånemark implant in partially edentulous jaws: A 10-year prospective multicenter study. Int. J. Oral Maxillofac. Implants. 1999;14:639–645.

2. Temmerman A, Rasmusson L, Kübler A, Thor A, Merheb J, Quirynen M. A Prospective, Controlled, Multicenter Study to Evaluate the Clinical Outcome of Implant Treatment in Women with Osteoporosis/Osteopenia: 5-Year Results. J Dent Res. 2018.1-7.

3. Giro G, Chambrone L, Goldstein A, Rodrigues JA, Zenobio E, Feres M, Figueiredo LC, Cassoni A, Shibli JA. Impact of osteoporosis in dental implants: a systematic review. World J Orthop. 2015;6(2):311–5.

4. de Medeiros F, Kudo GAH, Leme BG, Saraiva PP, Verri FR, Honorio HM, Pellizzer EP, Santiago Junior JF. Dental implants in patients with osteoporosis: a systematic review with meta-analysis. Int J Oral Maxillofac Surg. 2018;47(4):480–91.

5. Merheb J, Temmerman A, Rasmusson L, Kubler A, Thor A, Quirynen M. Influence of skeletal and local bone density on dental implant stability in patients with osteoporosis. Clin Implant Dent Relat Res. 2016;18(2):253–60.

6. Aro HT, Alm JJ, Moritz N, Makinen TJ, Lankinen P. Low BMD affects initial stability and delays stem osseointegration in cementless total hip arthroplasty in women: a 2-year RSA study of 39 patients. Acta Orthop. 2012;83(2):107–14.

7. Palmquist A, Omar OM, Esposito M, Lausmaa J, Thomsen P. Titanium oral implants: surface characteristics, interface biology and clinical outcome. J R Soc Interface. 2010 Oct 6;7 Suppl 5: S515-27.

8. Mosser DM, Zhang X. Activation of murine macrophages. Curr Protoc Immunol 2008;Chapter 14:Unit 14-12.

9. Stanford CM. Surface modification of biomedical and dental implants and the processes of inflammation, wound healing and bone formation. Int J Mol Sci 2010; 11:354-369.

10. Masuda T, Salvi GE, Offenbacher S, Felton DA, Cooper LF. Cell and matrix reactions at titanium implants in surgically prepared rat tibiae. The International journal of oral & maxillofacial implants 1997;12:472-485.

11. Ezhkova E, Pasolli HA, Parker JS, Stokes N, Su IH, Hannon G et al. Ezh2 orchestrates gene expression for the stepwise differentiation of tissue-specific stem cells. Cell 2009; 136:1122–1135. 10. Lian JB, Stein GS, Javed A, van Wijnen AJ, Stein JL, Montecino M et al.)

12. Lian JB, Stein GS, Javed A, Van Wijnen AJ, Stein JL, Montecino M, Hassan MQ, Gaur T, Lengner CJ, Young DW. Networks and hubs for the transcriptional control of osteoblastogenesis. Rev Endocr Metab Disord. 2006 Jun;7(1-2):1-16.

13. Warburton G, Nares S, Angelov N, Brahim JS, Dionne RA, Wahl SM. Transcriptional events in a clinical model of oral mucosal tissue injury and repair. Wound Repair Regen 2005;13:19-26.

14. Cooper LF. Biologic determinants of bone formation for osseointegration: clues for future clinical improvements. J Prosthet Dent 1998;80:439-449.

15. Dike LE, Chen CS, Mrksich M, Tien J, Whitesides GM, Ingber DE. Geometric control of switching between growth, apoptosis, and differentiation during angiogenesis using micropatterned substrates. In Vitro Cell Dev Biol Anim 1999;35:441-448.

16. Mendonca G, Mendonca DB, Simoes LG, Araujo AL, Leite ER, Duarte WR, et al. Nanostructured alumina-coated implant surface: effect on osteoblast-related gene expression and bone-to-implant contact in vivo. The International journal of oral & maxillofacial implants 2009;24:205-215.

17. Yang J, McNamara LE, Gadegaard N, Alakpa EV, Burgess KV, Meek RM, et al. Nanotopographical Induction of Osteogenesis through Adhesion, Bone Morphogenic Protein Cosignaling, and Regulation of MicroRNAs. ACS nano 2014;8:9941-9953.

18. Shimizu M, Furuyam R, Kawawam T, Sasaki T.Bone wound healing after maxillary molar extraction in ovariectomized aged rats: quantitative backscattered electron image analysis. Anatomical Records 2000;259: 76–85.
19. Masuda T, Salvi GE, Offenbacher S, Felton DA, Cooper LF. Cell and matrix reactions at titanium implants in surgically prepared rat tibiae. The International journal of oral & maxillofacial implants 1997; 12:472-485.
20. Bogliotti YS, Ross PJ. Mechanisms of histone H3 lysine 27 trimethylation remodeling during early mammalian development. Epigenetics. 2012 Sep 1; 7(9): 976–981.
21. Chambrone L. Current status of the influence of osteoporosis on periodontology and implant dentistry. Curr Opin Endocrinol Diabetes Obes 2016; 23:435-439.
22. Kouzarides T. Chromatin modifications and their function. Cell 2007; 128:693-705.
23. Mendonca G, Mendonca DB, Aragao FJ, Cooper LF. The combination of micron and nanotopography by H(2)SO(4)/H(2)O(2) treatment and its effects on osteoblast-specific gene expression of hMSCs. Journal of biomedical materials research Part A 2010;94:169-179.
24. Yang J, McNamara LE, Gadegaard N, Alakpa EV, Burgess KV, Meek RM, et al. Nanotopographical Induction of Osteogenesis through Adhesion, Bone Morphogenic Protein Cosignaling, and Regulation of MicroRNAs. ACS nano 2014;8:9941-9953.
25. Mendonca G, Mendonca DB, Aragao FJ, Cooper LF. The combination of micron and nanotopography by H(2)SO(4)/H(2)O(2) treatment and its effects on osteoblast-specific gene expression of hMSCs. Journal of biomedical materials research Part A 2010;94:169-179.
26. Bryington M, Mendonca G, Nares S, Cooper LF. Osteoblastic and cytokine gene expression of implant-adherent cells in humans. Clinical oral implants research 2014;25:52-58.
27. Kato RB, Roy B, De Oliveira FS, Ferraz EP, De Oliveira PT, Kemper AG, et al. Nanotopography directs mesenchymal stem cells to osteoblast lineage through regulation of microRNA-SMAD-BMP-2 circuit. Journal of cellular physiology 2014;229:1690-1696.

28. Sheng MH, Lau KH, Beamer WG, Baylink DJ, Wergedal JE. In vivo and in vitro evidence that the high osteoblastic activity in C3H/HeJ mice compared to C57BL/6J mice is intrinsic to bone cells. Bone 2004; 35:711-719.
29. Meirelles L. Nanoestruturas e a resposta óssea.Uma alternativa segura para a reabilitação com implantes osseointegráveis. 2010.Revista Implant News. 7(2): 169-72.
30. Baek WY, Lee MA, Jun JW, Kim SY, Akiyama H, de Crombrugghe B, Kim JE. 2009. Positive regulation of adult bone formation by osteoblast-specific transcription factor osterix J Bone Miner Res.24(6):1055-65.
31. Tang W, Li Y, Osimiri L, Zhang C.2011. Osteoblast-specific transcription factor Osterix (Osx) is an upstream regulator of Satb2 during bone formation. J Biol Chem. 286(38):32995- 3002.
32. Guo J, Padilla RJ, Ambrose W, De Kok IJ, Cooper LF. 2007. The effect of hydrofluoric acid treatment of TiO2 grit blasted titanium implants on adherent osteoblast gene expression in vitro and in vivo. Biomaterials. 28(36):5418-25.
33. Mendonça G, Mendonça DB, Aragão FJ, Cooper LF.2010. The combination of micron and nanotopography by H2SO4/H2O2 treatment and its effects on osteoblast-specific gene expression of hMSCs. J Biomed Mater Res A. 94(1):169-79.
34. Thalji G, Cooper LF. 2014.Molecular assessment of osseointegration in vitro: a review of current literature. Int J Oral Maxillofac Implants. 29(2):e171-99.
35. Harada H, Tagashira S, Fujiwara M, Ogawa S, Katsumata T, Yamaguchi A. 1999. Cbfa1 isoforms exert functional differences in osteoblast differentiation. J Biol Chem. 274(11):6972-8.
36. Webster TJ, Ergun C, Doremus RH, Siegel RW, Bizios R. 2000. Enhanced functions of osteoblasts on nanophase ceramics. Biomaterials. 21(17):1803-10.
37. Bryington M, Mendonça G, Nares S, Cooper LF. 2014. Osteoblastic and cytokine gene expression of implant-adherent cells in humans. Clin Oral Implants Res. 25(1):52-8.
38. Anderson JM, Rodriguez A, Chang DT.2008. Foreign body reaction to biomaterials. Semin Immunol .20(2):86-100.

39. Ma QL, Zhao LZ, Liu RR, Jin BQ, Song W, Wang Y. 2014 Improved implant osseointegration of a nanostructured titanium surface via mediation of macrophage polarization. Biomaterials. 35(37):9853-9867.

FIGURES AND LEGEND

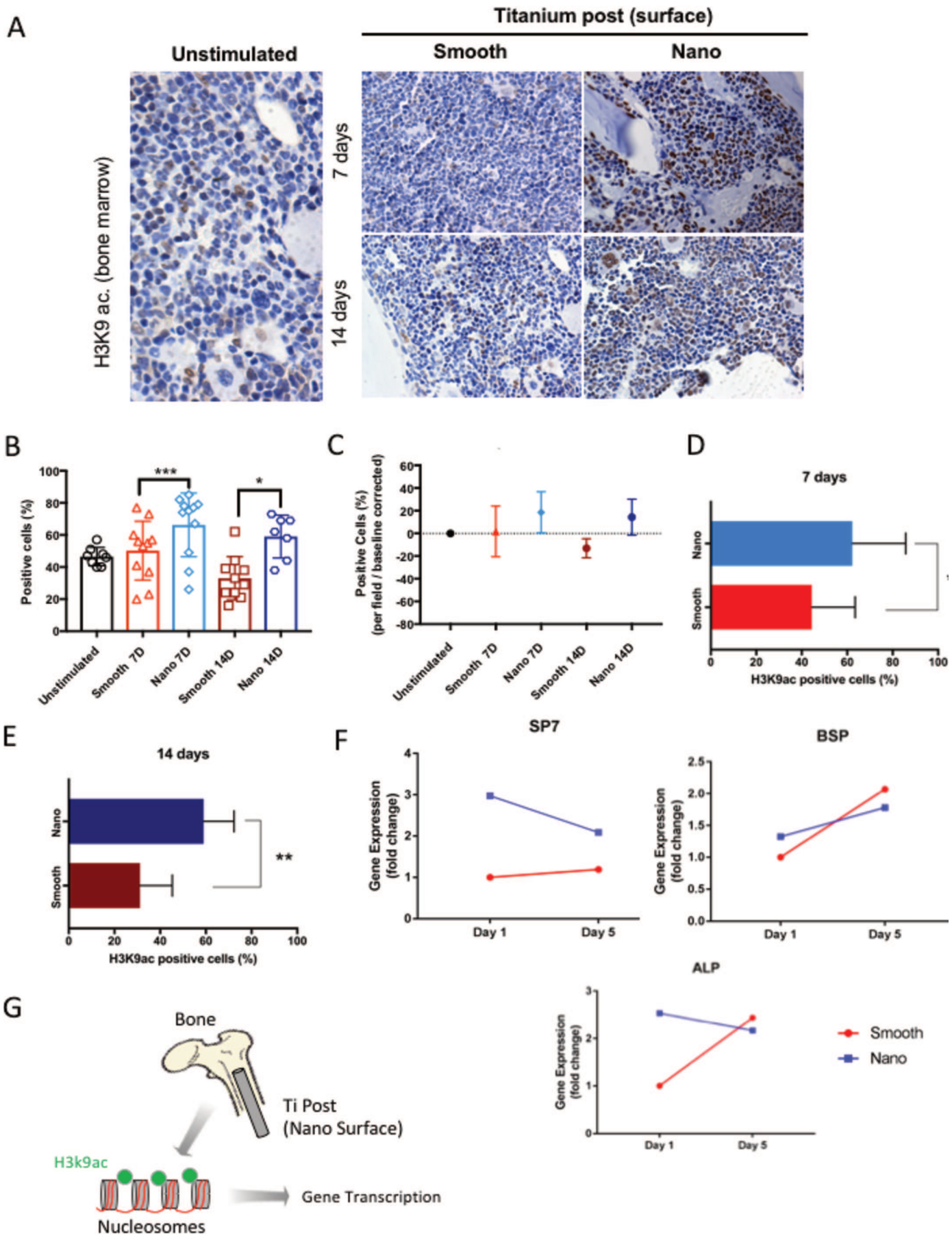

Fig. 1. Global chromatin modifications mediate by titanium nanosurface.

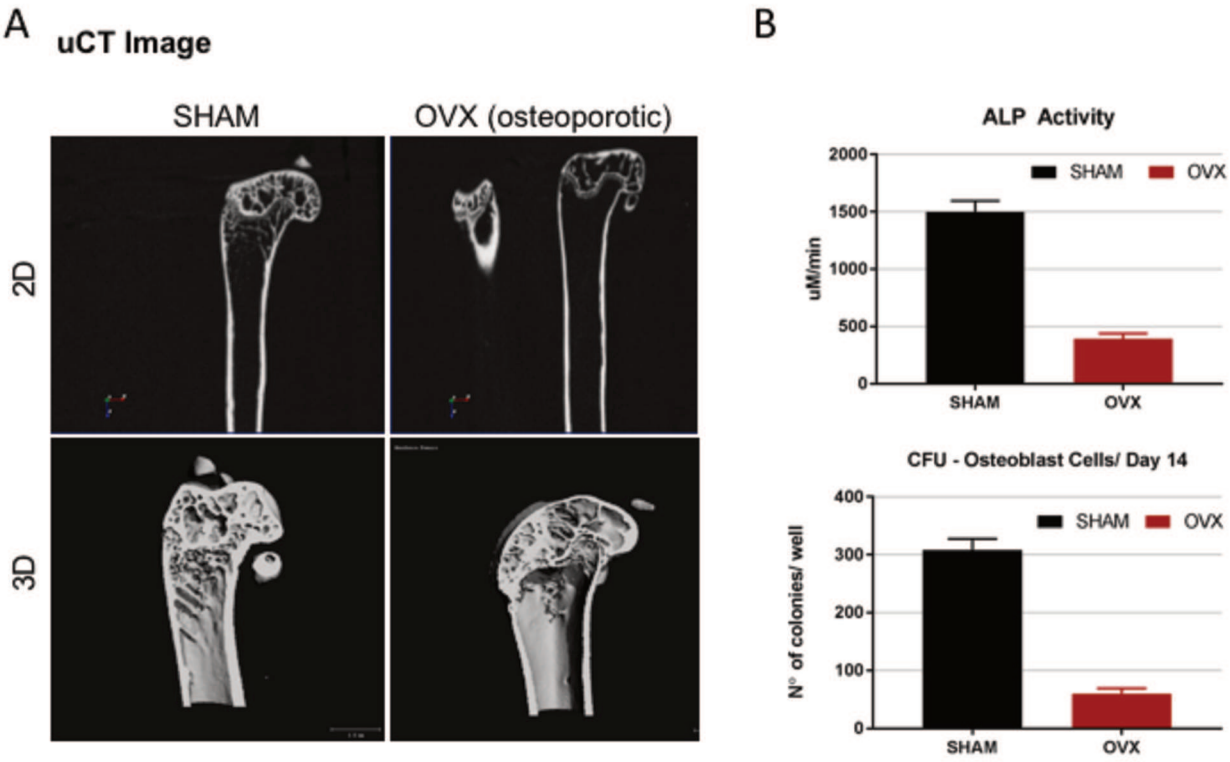

Fig. 2. Osteoporotic mice are characterized by poor osteoblasts differentiation.

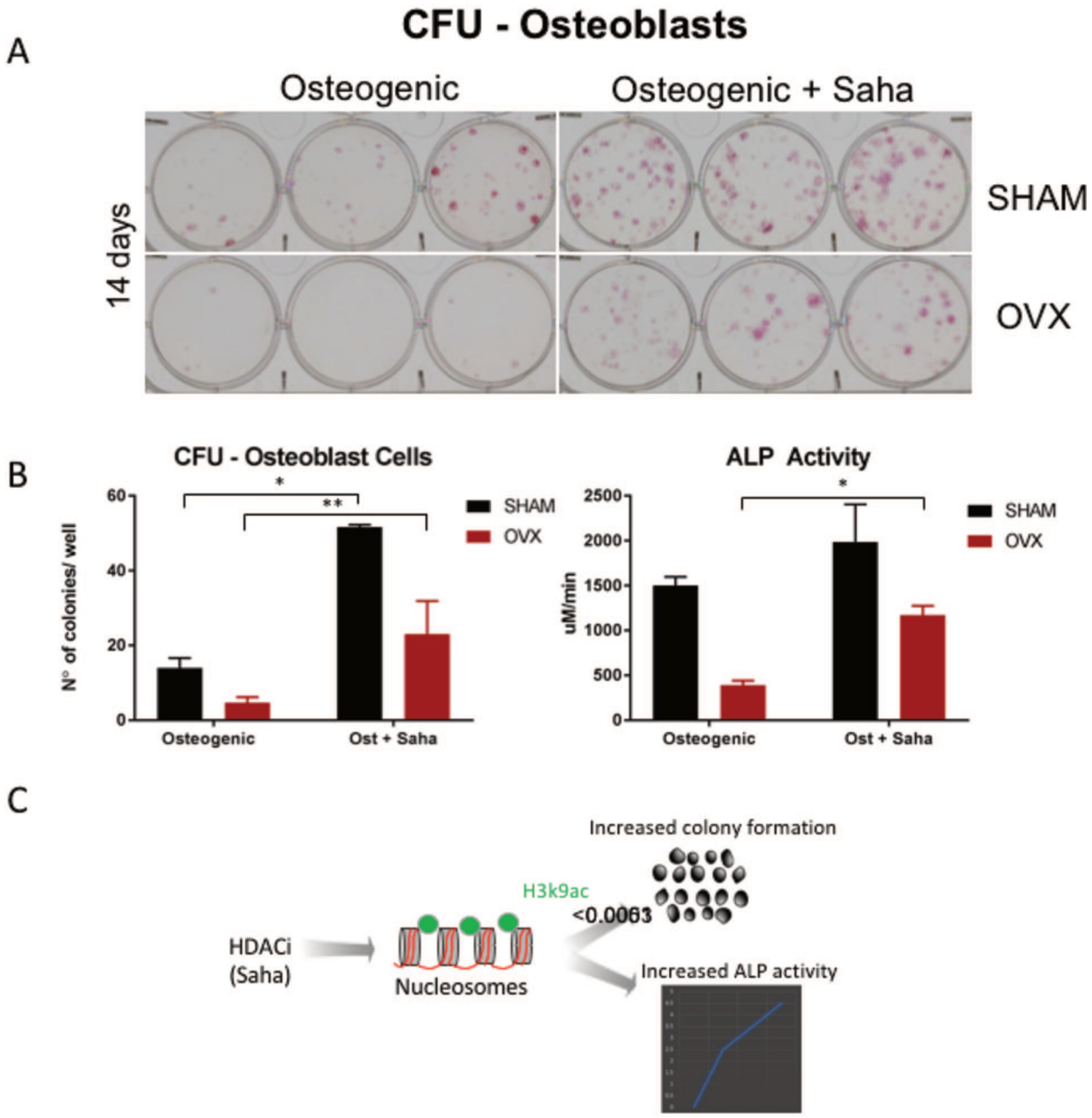

Fig. 3. Pharmacological induction of histone acetylation induces MSC differentiation.

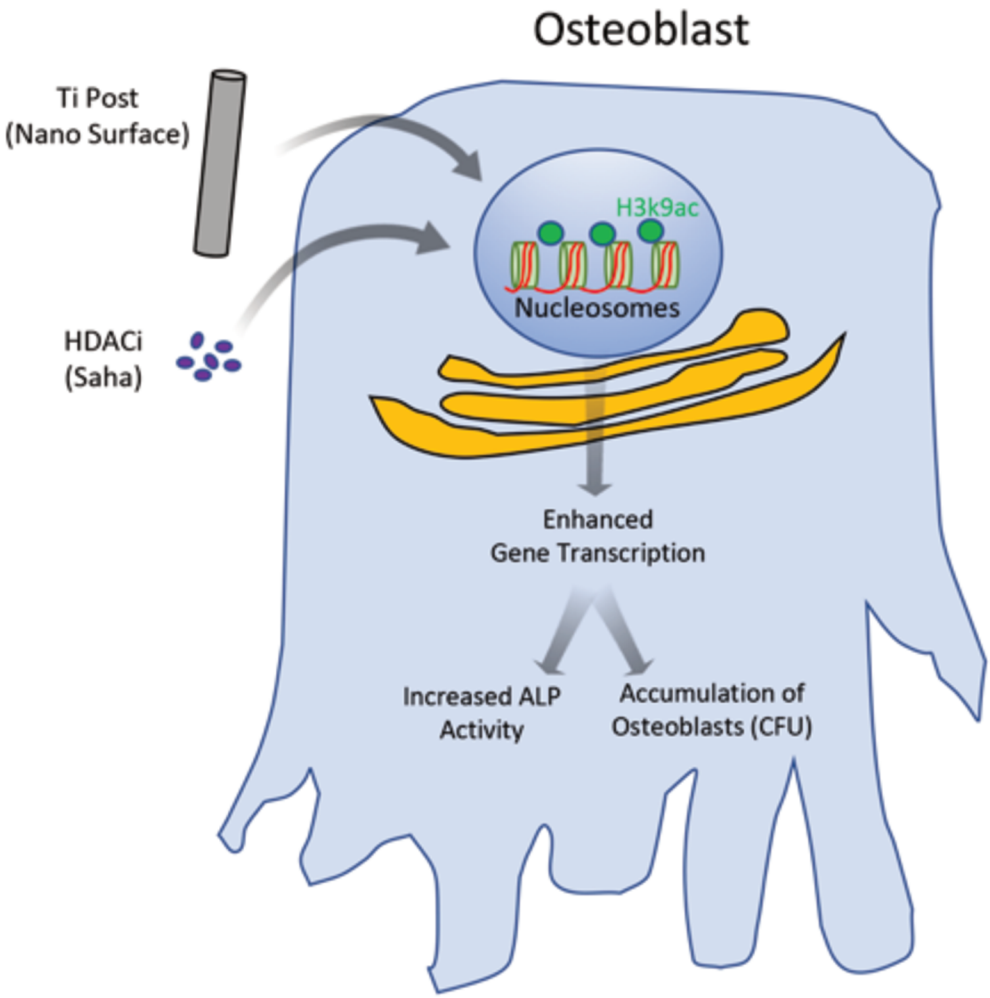

Fig. 4. Schematic representation of Hypoacetylation of acetyl-histone H3 (H3K9ac) as marker of bone modulation in titanium implants with nanoscale surface.

CONCLUSÕES

4- CONCLUSÕES

Dentro das limitações metodológicas impostas pelo delineamento experimental destes 3 estudos *in vivo* em modelo animal, pode-se concluir-se que:

- Superfície hidrofóbica e superfície hidrofílica contribuíram para resposta biológica favorável. No entanto, comportamento hidrofílico da superfície SAE-HD desencadeou melhores resultados na fase inicial de osseointegração. Diante disso, nossos dados *in vivo* em sugerem que a superfície hidrofílica analisada pode permitir uma redução considerável no período de cicatrização devido maior formação óssea em relação a superfície mais hidrofóbica.

- Devido ao aumento da expressão de genes relacionados à diferenciação osteogênica e à quantidade significativa de cálcio e volume ósseo formado diretamente sobre a superfície de implantes dentários SAE-HD, a escolha da superfície hidrofílica em situações de osteoporose pode ser significativamente considerada a fim de melhorar processo de osseointegração.

- Superfícies de nanotopografia afetaram a diferenciação das células-tronco mesenquimais em osteoblastos. Além disso, implantes de Ti que apresentam nanotopografia são capazes de induzir modificações globais da cromatina de núcleos celulares, devido acúmulo de H3K9.

- Superfícies hidrofílicas e em nanoescala, assim como Vorinostat mediados pela histona, podem desempenhar um papel fundamental na diferenciação das células-tronco mesenquimais em osteoblastos, especialmente nas condições de osteoporose. Isso ocorre devido propriedades osteocondutoras e possibilidade de melhorar eventos biológicos que ocorrem na interface osso/implante.

RERERÊNCIAS

REFERÊNCIAS

1. Gaetti-Jardim EC, Santiago-Junior JF, Goiato MC, Pellizer EP, Magro-Filho O, Jardim Junior EG. Dental implants in patients with osteoporosis: a clinical reality? J Craniofac Surg. 2011;22(3):1111-3. https://doi.org/10.1097/SCS.0b013e3182108ec9
PMid:21586959

2. Giro G, Chambrone L, Goldstein A, Rodrigues JA, Zenóbio E, Feres M, Figueiredo LC, Cassoni A, Shibli JÁ. Impact of osteoporosis in dental implants: A systematic review. World J Orthop. 2015;18:6(2):311-315.
https://doi.org/10.5312/wjo.v6.i2.311
PMid:25793172 PMCid:PMC4363814

3. NIH consensus development panel on osteoporosis prevention, diagnosis, and therapy, March 7-29, 2000: Highlights of the conference. South Med J. 2001;94: 569-573.
https://doi.org/10.1097/00007611-200194060-00004

4. Sanfilippo F, Bianchi AE. Osteoporosis: the effect on maxillary bone resorption and therapeutic possibilities by means of implant prostheses: a literature review and clinical considerations. Int J Periodont Rest Dent 2003;23:447e57.

5. Fini M, Giavaresi G, Greggi T, et al. Biological assessment of the bone-screw interface after insertion of uncoated and hydroxyapatite-coated pedicular screws in the osteopenic sheep. J Biomed Mater Res Part A. 2004;66:176-183.
https://doi.org/10.1002/jbm.a.10605
PMid:12833444

6. Erdogan O, Shafer DM, Taxel P, Freilich MA. A review of the association between osteoporosis and alveolar ridge augmentation. Oral Surg Oral Med Oral Pathol Oral Radiol Endod. 2007;104(6):738.e1-13.
https://doi.org/10.1016/j.tripleo.2007.04.008
PMid:17656117

7. Tsolaki IN, Madianos PN, Vrotsos JA. Outcomes of dental implants in osteoporotic patients. A literature review. Journal of Prosthodontics 2009;18:309-323.
https://doi.org/10.1111/j.1532-849X.2008.00433.x
PMid:19210307

8. Lemus, LM.; Almagro, Z.; León, C. Origen y evolución de los implantes dentales. Rev. Hab. Cienc. Méd., v.8, n.4, out-nov, 2009.

9. Melo, MD.; Shafle, H.; Obeid, G. Implant survival rates for oral and maxillofacial surgery residents: a retrospective clinical review with analysis of resident level of training on implant survival. J. Oral Maxillofac. Surg., v.64, n.8, p.1185-1189, ago, 2006.
https://doi.org/10.1016/j.joms.2006.04.014
PMid:16860207

10. Adell, R.; Lekholm, U.; Rockler, B.; Brånemark, PI. A 15-year study of osseointegrated implants in the treatment of the edentulous jaw. Int. J. Oral Surg., v.10, n.6, p.387-416, Dez, 1981.
https://doi.org/10.1016/S0300-9785(81)80077-4

11. Noack, N.; Willer, J.; Hoffmann, J. Long-term results after placement of dental implants: Longitudinal study of 1,964 implants over 16 years. Int. J. Oral Maxillofac. Implants, v.14, n.5, p.784-755, set-oct, 1999.

12. Saab, XE.; Griggs, JA.; Powers, JM.; Engelmeier, RL. Effect of abutment angulation on the strain on the bone around an implant in the anterior maxilla: a finite element study. J. Prosthet. Dent., v.97, n.2, p.85-92, fev, 2007.
https://doi.org/10.1016/j.prosdent.2006.12.002
PMid:17341376

13. Capelli, M; Zuffeti, F.; Del Fabbro, M.; Testori, T. Immediate rehabilitation of the completely edentulous jaw with fixed prostheses supported by either upright or tilted implants: a multicenter clinical study. Int. J. Oral Maxillofac. Implants, v.22, n.4, p.639-644, jul-ago, 2007.

14. Danza, M.; Quaranta, A.; Carinci, F.; Paracchini, L.; Pompa, G.; Vozza, I. Biomechanical evaluation of dental implants in D1 and D4 bone by Finite Element Analysis. Minerva Stomatol., v.59, n.6, p.305-313, jun, 2010.

15. Hasan, I.; Bourauel, C.; Keilig, L.; Reimann, S.; Heinemann, F. The influence of implant number and abutment design on the biomechanical behavior of bone for an implant-supported fixed prosthesis: a finite element study in the upper anterior region. Comput. Methods Biomech. Biomed. Engin., v.14, n.12, p.1113-1116, dez, 2011.
https://doi.org/10.1080/10255842.2010.515212
PMid:20924861

16. Sahin, S.; Cehreli, M.C.; Yalçin, E. The influence of functional forces on the biomechanics of implant-supported prostheses--a review. J. Dent., v.30, n.7- 8, p.271-282, set-nov, 2002.
https://doi.org/10.1016/S0300-5712(02)00065-9

17. Bidez, M.W.; Misch, C.E. Force transfer in implant dentistry: basic concepts and principles. J. Oral Implantol., v.18, n.3, p.264-274, 1992.

18. Wang, J.; Meng, F.; Song, W.; Jin, J.; Ma, Q.; Fei, D.; Fang, L; et al. Nanostructured titanium regulates osseointegration via influencing macrophage polarization in the osteogenic environment. Int. J. of Nanomedicine, v.13, p.4029-4043, 2018.
https://doi.org/10.2147/IJN.S163956
PMid:30022825 PMCid:PMC6045901

19. Hotchkiss, K.M.; Reddy, G.B.; Hyzy, S.L.; Boyan, B.D.; Olivares-Navarrete R. Titanium surface characteristics, including topography and wettability, alter macrophage activation. Acta Biomater., v.31, p.425-434, 2016.
https://doi.org/10.1016/j.actbio.2015.12.003
PMid:26675126 PMCid:PMC4728000

20. Kapoor, R. et al. Comparative assessment of structural and biological properties of biomimetically coated hydroxyapatite on alumina (alpha-Al2O3) and titanium (Ti-6Al- 4V) alloy substrates. J. Biomed. Mater. Res. A., v.94, n.3, p.913-26, Sep. 2010.
https://doi.org/10.1002/jbm.a.32767
PMid:20730928

21. Ahn SJ; Leesungbok, R; Lee, SW. Histomorphometric Analysis and Removal Torque of Small Diameter Implants With Alternative Surface Treatments and Different Designs. J. O. Impl., v. 16, n. 4, p.263-272. 2010.
https://doi.org/10.1563/AAID-JOI-D-09-00052
PMid:20735263

22. Buser D, Broggini N, Wieland M, Schenk RK, Denzer AJ, Cochran DL, et al. Enhanced bone apposition to a chemically modified SLA titanium surface. J. Dent. Res., v.83, p.529-33, 2004.

https://doi.org/10.1177/154405910408300704
PMid:15218041

23. Bosshardt DD, Salvi Ge, Huynh-Ba G, Ivanovski S, Donos N, Lang NP. The role of bone debris in early healing adjacent to hydrophilic and hydrophobic implant surfaces in man. Clin. Oral Implants Res., v.22, p.357-64, 2011.
https://doi.org/10.1111/j.1600-0501.2010.02107.x
PMid:21561477

24. Wennerberg A, Albrektsson T. Effects of titanium surface topography on bone integration: a systematic review. Clinical Oral Implants Research, v.20 (Suppl 4):172-84, 2009.
https://doi.org/10.1111/j.1600-0501.2009.01775.x
PMid:19663964

25. Namkung-Matthai, H, Appleyard R, Jansen J, Hao Lin J, Maastricht S, Swain M, Mason RS, Murrell GA, Diwan AD, Diamond T. Osteoporosis influences the early period of fracture healing in a rat osteoporotic model. Bone 2001;28: 80-86.
https://doi.org/10.1016/S8756-3282(00)00414-2

26. Shimizu M, Furuyam R, Kawawam T, Sasaki T.Bone wound healing after maxillary molar extraction in ovariectomized aged rats: quantitative backscattered electron image analysis. Anatomical Records 2000;259: 76-85.
https://doi.org/10.1002/(SICI)1097-0185(20000501)259:1<76::AID-AR9>3.0.CO;2-0

27. Teofilo JM, Brentegani LG, Lamano-Carvalho TL. Bone healing in osteoporotic female rats following intra-alveolar grafting of bioactive glass. Archives of Oral Biology 2004;49: 755-762.
https://doi.org/10.1016/j.archoralbio.2004.02.013
PMid:15275863

28. Gao Y, Zou S, Liu X, Bao C, Hu J. The effect of surface immobilized bisphosphonates on the fixation of hydroxyapatite-coated titanium implants in ovariectomized rats. Biomaterials 2009;30:1790e6.
https://doi.org/10.1016/j.biomaterials.2008.12.025
PMid:19135249

29. Vidigal Jr GM, Groisman M, Gregorio LH, Soares Gde A. Osseointegration of titanium alloy and HA-coated implants in healthy and ovariectomized animals: a histomorphometric study. Clin Oral Impl Res 2009;20:1272e7.
https://doi.org/10.1111/j.1600-0501.2009.01739.x
PMid:19832768

30. Mardas N, Schwarz F, Petrie A, Hakimi A-R, Donos N. The effect of SLActive surface in guided bone formation in osteoporotic-like conditions. Clin Oral Impl Res 22, 2011; 406-415.
https://doi.org/10.1111/j.1600-0501.2010.02094.x
PMid:21303420

31. Qi M, Hu J, Li J, et al. Effect of zoledronate acid treatment on osseointegration and fixation of implants in autologous iliac bone grafts in ovariectomized rabbits. Bone. 2012;50: 119-127.
https://doi.org/10.1016/j.bone.2011.10.011
PMid:22023930

32. Yang G, Song L, Guo C, Zhao S, Liu L, He F. Bone Responses to Simvastatin-Loaded Porous Implant Surfaces in an Ovariectomized Model. Int J Oral Maxillofac Implants 2012;27:369-374.

33. Alghamdi HS,Bosco R, van den Beucken JJJP, Walboomers XF, Jansenet JA. Osteogenicity of titanium implants coated with calcium phosphate or collagen type-I in osteoporotic rats. Biomaterials 2013;34:3747-3757.
https://doi.org/10.1016/j.biomaterials.2013.02.033
PMid:23465489

34. Ghanem A, Kellesarian SV, Abduljabbar T, Al-Hamoudi N, Vohra F, Javed F. Role of Osteogenic Coatings on Implant Surfaces in Promoting Bone-To-Implant Contact in Experimental Osteoporosis: A Systematic Review and Meta-Analysis. Implant Dent 2017;26:770-777.
https://doi.org/10.1097/ID.0000000000000634
PMid:28767464

35. Palmquist A, Omar OM, Esposito M, Lausmaa J, Thomsen P. Titanium oral implants: surface characteristics, interface biology and clinical outcome. J R Soc Interface. 2010 Oct 6;7 Suppl 5: S515-27.
https://doi.org/10.1098/rsif.2010.0118.focus
PMid:20591849

36. Mosser DM, Zhang X. Activation of murine macrophages. Curr Protoc Immunol 2008;Chapter 14:Unit 14-12.
https://doi.org/10.1002/0471142735.im1402s83

37. Stanford CM. Surface modification of biomedical and dental implants and the processes of inflammation, wound healing and bone formation. Int J Mol Sci 2010; 11:354-369.
https://doi.org/10.3390/ijms11010354
PMid:20162020 PMCid:PMC2821008

38. Masuda T, Salvi GE, Offenbacher S, Felton DA, Cooper LF. Cell and matrix reactions at titanium implants in surgically prepared rat tibiae. The International journal of oral & maxillofacial implants 1997;12:472-485.

39. Ezhkova E, Pasolli HA, Parker JS, Stokes N, Su IH, Hannon G et al. Ezh2 orchestrates gene expression for the stepwise differentiation of tissue-specific stem cells. Cell 2009; 136:1122-1135.
10. Lian JB, Stein GS, Javed A, van Wijnen AJ, Stein JL, Montecino M et al.)
https://doi.org/10.1016/j.cell.2008.12.043
PMid:19303854 PMCid:PMC2716120

40. Lian JB, Stein GS, Javed A, Van Wijnen AJ, Stein JL, Montecino M, Hassan MQ, Gaur T, Lengner CJ, Young DW. Networks and hubs for the transcriptional control of osteoblastogenesis. Rev Endocr Metab Disord. 2006 Jun;7(1-2):1-16.
https://doi.org/10.1007/s11154-006-9001-5
PMid:17051438

41. Warburton G, Nares S, Angelov N, Brahim JS, Dionne RA, Wahl SM. Transcriptional events in a clinical model of oral mucosal tissue injury and repair. Wound Repair Regen 2005;13:19-26.
https://doi.org/10.1111/j.1067-1927.2005.130104.x
PMid:15659033

42. Cooper LF. Biologic determinants of bone formation for osseointegration: clues for future clinical improvements. J Prosthet Dent 1998;80:439-449.
https://doi.org/10.1016/S0022-3913(98)70009-5

43. Dike LE, Chen CS, Mrksich M, Tien J, Whitesides GM, Ingber DE. Geometric control of switching between growth, apoptosis, and differentiation during angiogenesis using micropatterned substrates. In Vitro Cell Dev Biol Anim 1999;35:441-448.

https://doi.org/10.1007/s11626-999-0050-4
PMid:10501083

44. Mendonca G, Mendonca DB, Simoes LG, Araujo AL, Leite ER, Duarte WR, et al. Nanostructured alumina-coated implant surface: effect on osteoblast-related gene expression and bone-to-implant contact in vivo. The International journal of oral & maxillofacial implants 2009;24:205-215.

45. Yang J, McNamara LE, Gadegaard N, Alakpa EV, Burgess KV, Meek RM, et al. Nanotopographical Induction of Osteogenesis through Adhesion, Bone Morphogenic Protein Cosignaling, and Regulation of MicroRNAs. ACS nano 2014;8:9941-9953.
https://doi.org/10.1021/nn504767g
PMid:25227207

ANEXOS

ANEXOS

Parecer do Comitê de ética

Principal Investigator: Gustavo Mendonca
Protocol: PRO00006203
Protocol Title: miRNA Modulation of Osteoblast Differentiation on Nanoscale Titanium Surfaces
Approval Period: 5/11/2015 - 5/11/2018

The University Committee on Use and Care of Animals (UCUCA) has reviewed your application to use vertebrate animals referenced below. This project has been approved. The proposed animal use procedures are in compliance with University guidelines, State and Federal regulations, and the standards of the "Guide for the Care and Use of Laboratory Animals."

There may be additional issues that need to be addressed prior to initiation of the associated research. It is your responsibility, as Principal Investigator, to secure all the necessary requirements and recommendations (e.g., IBC approval, Animal Use training, accepting OSEH Findings and Recommendations).

When communicating with the UCUCA Office please refer to protocol PRO00006203 .

The approval date is 5/11/2015 . The approval period is for three years from this date. However, the United States Department of Agriculture (USDA) requires an annual review of protocols to use animals. Therefore, each year of this protocol prior to the anniversary of its approval date, you will be notified via email to submit a short annual review. Your continued animal use approval is contingent upon the completion and return of this annual review.

You will also be notified prior to expiration so that your renewal application can be prepared, submitted and reviewed in a timely manner to avoid noncompliance. For any change to the study, an amendment must be submitted to the UCUCA for review and approval prior to the implementation of the proposed change.

The University's Animal Welfare Assurance Number with the NIH Office Of Laboratory Animal Welfare (OLAW) is A3114-01, and most recent date of accreditation by the Association For The Assessment And Accreditation Of Laboratory Animal Care International (AAALAC, Intl.) is November 6, 2009.

If you receive news media inquiries concerning any aspect of animal care or use in this project, please contact James Erickson, News and Information Services, 647-1842. If you have security concerns regarding the animals or animal facilities, contact Bill Bess, Director of Public Safety, 763-3434.

A formal approval letter will follow for each funding source listed on the protocol.

Sincerely,

Dr. Daniel D. Myers, DVM, MPH
Associate Professor and Chairperson
University Committee on Use and Care of Animals